

“Groundwater mean transit times, mixing and recharge in faulted–hydraulic drop alluvium aquifers using chlorofluorocarbons (CFCs) and tritium isotope ( $^3\text{H}$ )” by Ma, B., Jin, M., Liang, X., Li, J., *Hydrol. Earth Syst. Sci.*, doi:10.5194/hess-2018-143.

We appreciate the many valuable suggestions and helpful comments of **Anonymous Referee #1**. We have seriously considered all of the suggestions and comments and have attempted to address each of the comments point-by-point. Detail explanations are as follows.

Author’s response – Line numbers referring to the old and revised version manuscripts are preceded by L and RL, respectively.

## **Anonymous Referee #1**

### **General Comments**

The paper reports CFC, tritium, carbon-14 and stable isotope measurements for groundwater in the Manas River Basin in China and uses them to estimate mean transit times for the complex mixtures of groundwaters in the area resulting from the complicated geology.

The complications of the subject combined with English that is not quite right make this a difficult read. However, the paper addresses relevant scientific questions suitable for publication in HESS, with novel concepts and ideas. Substantial conclusions are reached.

The methods are valid and described satisfactorily, and title and references are well done. There is a problem with the abstract (see below) and consequently the overall structure needs improvement. Some of the figures are complex and could be explained better.

Response: We would like to thank you very much for taking the time to review our manuscript and for your generally positive feedback. We have asked Chris Law (Wallace Academic Editing) to modify the language to help improve readability. We have reorganized the structure and tried our best to present a clear roadmap to readers. We also agree with you that some of the figures are complex which have also been pointed out by Ref #2. Some figures have been redrawn.

The outline of the manuscript have been reorganized as follows:

Title: Application of environmental tracers for investigation of groundwater mean residence time and aquifer recharge in faulted–hydraulic drop alluvium aquifers

1. Introduction
2. Geological and hydrogeological setting
3. Materials and methods
  - 3.1 Water sampling
  - 3.2 Analytical techniques
  - 3.3 Groundwater dating
    - 3.3.1 CFCs indicating modern water recharge
    - 3.3.2 The apparent  $^{14}\text{C}$  ages
    - 3.3.3 Groundwater mean residence time estimation
4. Results and discussion

- 4.1 Stable isotope and major ion hydrochemistry
- 4.2 Modern and paleo–meteoric recharge features
  - 4.2.1 Stable isotope indications
  - 4.2.2 CFCs indications
  - 4.2.3  $^3\text{H}$  and  $^{14}\text{C}$  indications
- 4.3 Groundwater mean residence time
  - 4.3.1  $^3\text{H}$  and CFCs
  - 4.3.2 Hydrochemistry evolution

5. Conclusions

Figures 6, 8 and 9 have been redrawn as follows:

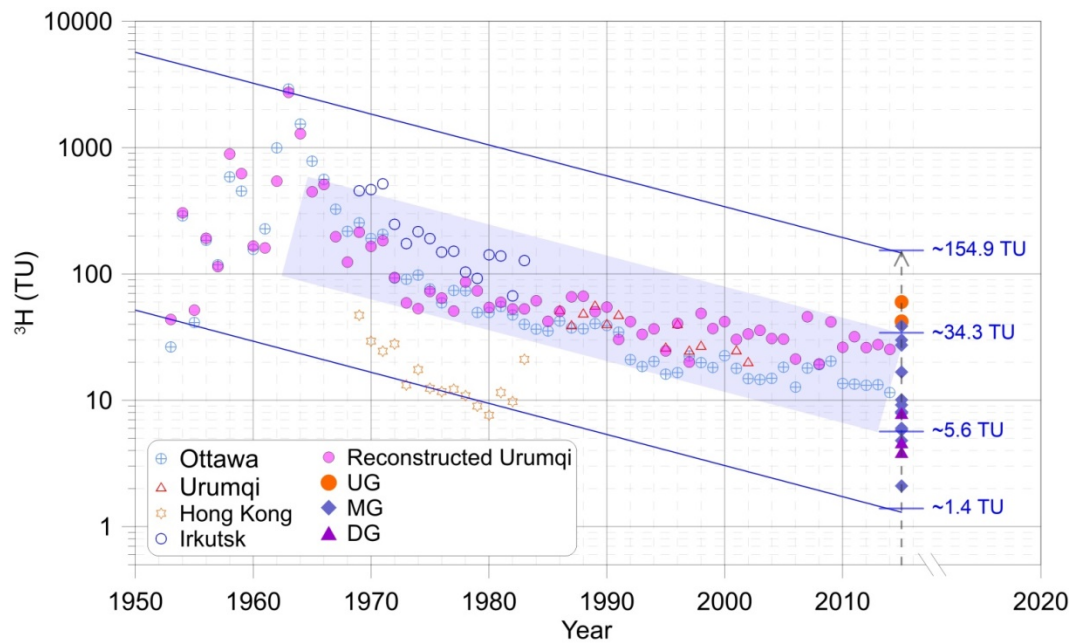
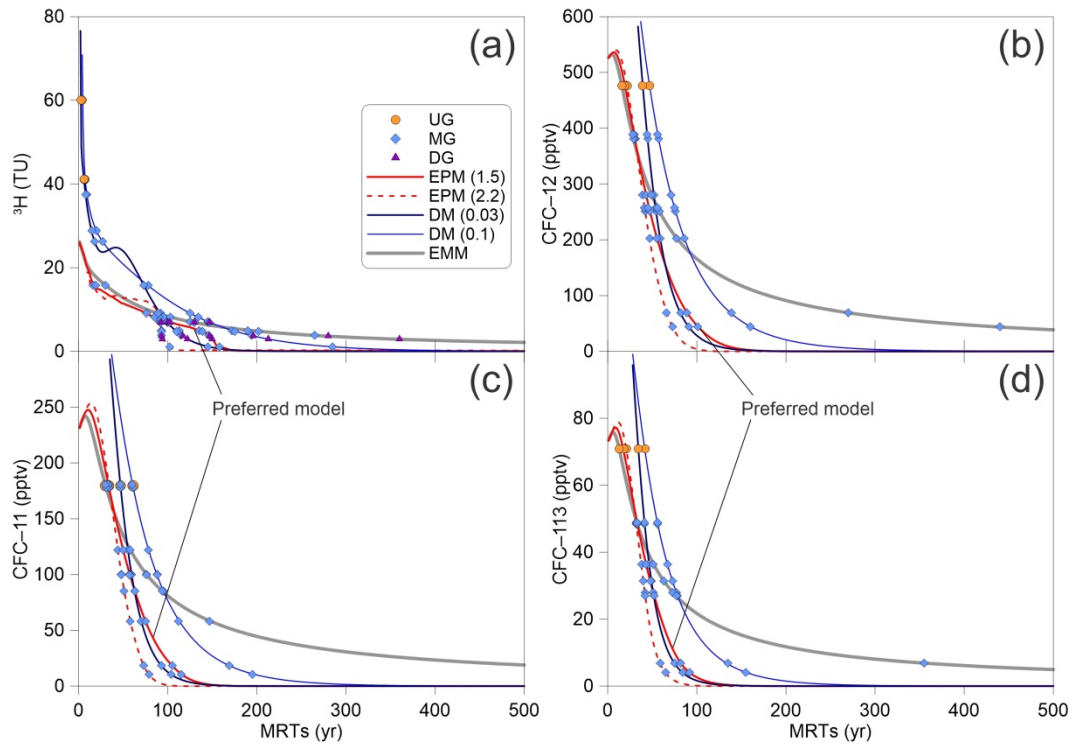
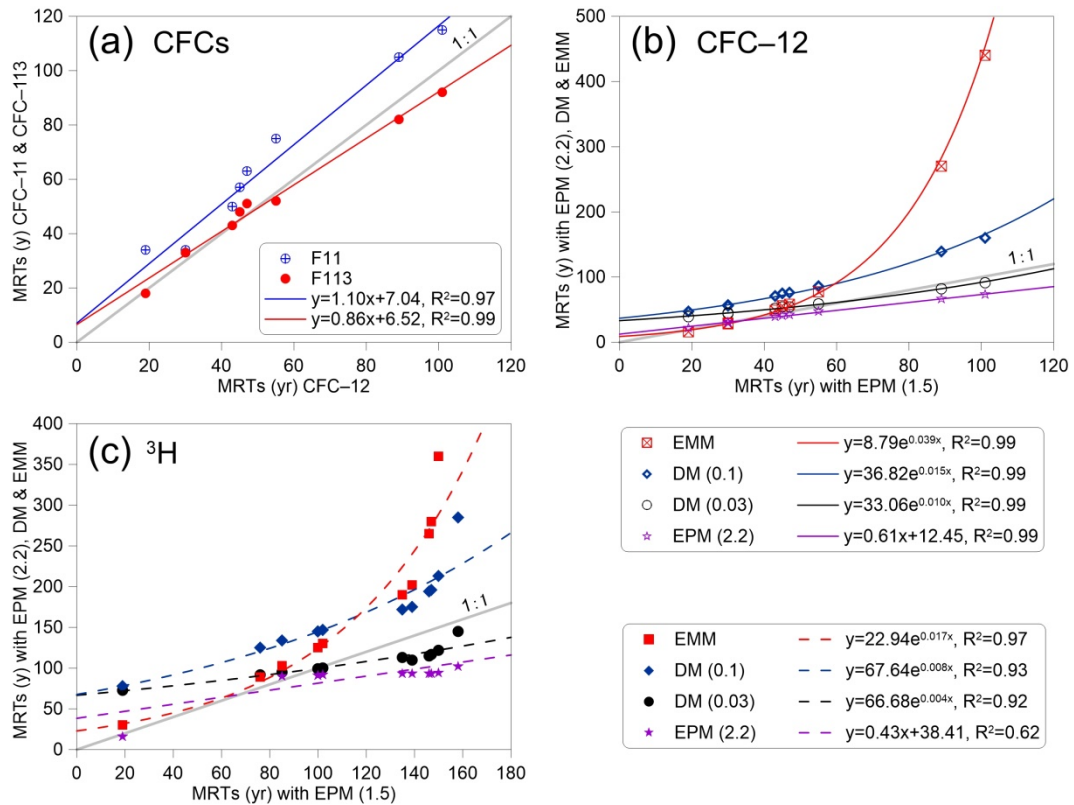


Figure 6. Tritium concentration (TU) of groundwater water samples of upstream groundwater (UG), midstream groundwater (MG), and downstream groundwater (DG). Time series of tritium concentration in precipitation at Ottawa, Urumqi, Hong Kong, and Irkutsk were obtained by GNIP in IAEA (<https://www.iaea.org/>). The blue solid lines and shaded field were drawn using the half–life (12.32 yrs) of tritium decayed to 2014. (It is Fig. 4 in the revised manuscript)



**Figure 8.** Tritium and CFCs (CFC-11, CFC-12 and CFC-113) output vs. mean residence times for different lumped-parameter models estimated using Eqs. (2) to (5). The input  $^3\text{H}$  activity and CFCs concentration are using the estimated  $^3\text{H}$  activities in precipitation in Urumqi station (Fig. 4) and the Northern Hemisphere atmospheric mixing ratio (Fig. 3), respectively. (It is Fig. 10 in the revised manuscript)



**Figure 9.** (a) MRTs with EPM (1.5) of CFC-12 vs. CFC-11 & CFC-113, (b) CFC-12 MRTs with EPM

(1.5) vs. EPM (2.2), DM & EMM, and (c) 3H MRTs with EPM (1.5) vs. EPM (2.2), DM & EMM. (It is Fig. 11 in the revised manuscript)

### Specific Comments

1) A major problem is that there appears to be a disconnect between the abstract/conclusions and the rest of the paper. The following sentence from the abstract/conclusions:

“The thrust faults were found to play a paramount role on groundwater flow paths and MTTs due to their block water features, where the relatively long MTTs were found near the Manas City with shorter distance and smaller hydraulic gradients.”

is not supported by any discussion in the paper. Yes, it may be supported by implication from the results, but such support needs to be made explicit (possibly in its own subsection since this is an important conclusion).

Response: This sentence has been deleted. To make the abstract and conclusions to be more clear and well-founded, we have revised the abstract/conclusions and delete some incorrect statements. Yes, this conclusion is important in the paper. Indeed, there are some results that show large differences on both sides of the thrust fault. For example, there is a level difference of 130 m hydraulic drop (Fig. 1c) in the south margin in Shihezi (SHZ),  $^3\text{H}$  activities of groundwater decrease rapidly along the Manas River motion in the north of the fault but show relatively the highest values in the south of the fault (Fig. 8). These results still cannot support the conclusion explicitly “The thrust fault were found to play a paramount role on groundwater flow paths ...”.

The revised abstract is as follows (RL12–26):

“Documenting groundwater residence time and the recharge source is crucial for water resource management in the alluvium aquifers of arid basins. Environmental tracers (CFCs,  $^3\text{H}$ ,  $^{14}\text{C}$ ,  $\delta^2\text{H}$ ,  $\delta^{18}\text{O}$ ) and groundwater hydrochemical components are used for assessing groundwater mean residence times (MRTs) and aquifer recharge in faulted–hydraulic drop alluvium aquifers in the Manas River Basin (China). The very high  $^3\text{H}$  activity (41.1–60 TU) in the groundwater in the Manas River upstream (south of the fault) indicates rainfall recharge during the nuclear bomb tests (since the 1960s). Carbon–14 groundwater age increases with distance (3000–5000 yrs in the midstream to > 7000 yrs in the downstream) and depth, as well as with decreasing  $^3\text{H}$  activity (1.1 TU) and  $\delta^{18}\text{O}$  values, confirming that the deeper groundwater is derived from paleometeoric recharge in the semi–confined groundwater system. MRTs estimated using an exponential–piston flow model vary from 19 to 101 yrs for CFCs and from 19 to 158 yrs for  $^3\text{H}$ ; MRTs for  $^3\text{H}$  are much longer than those for CFCs probably due to the time lag (liquid vs. gas phase) through the thick unsaturated zone. The remarkable correlations between CFCs rather than  $^3\text{H}$  MRTs and pH,  $\text{SiO}_2$ , and  $\text{SO}_4^{2-}$  concentrations allow estimating first–order proxies of MRTs for groundwater at different times. Relatively modern recharge is found in the south of the fault with young (post–1940) water fractions of 87–100 %, whereas in the north of the fault in the midstream area the young, water fractions vary from 12 to 91 % based on the CFC binary mixing method. This study shows that the combination of CFCs and  $^3\text{H}$  residence time tracers can help analyze groundwater MRTs and identify the recharge sources for the different mixing end–members.”

The revised conclusions are as follows (RL542–554):

“In this study, we used environmental tracers and hydrochemistry to identify the modern and paleo-meteoric recharge sources, to constrain the different end-members mixing rates, and study the mixed groundwater MRTs in faulted-hydraulic drop alluvium aquifer systems. The paleo-meteoric recharge in a cooler climate was distinguished from the lateral flow from the higher elevation precipitation in the Manas River downstream area. The relatively modern groundwater with young (post-1940) water fractions of 87–100 % was obtained, indicating a small extent of mixing south of the fault. The short MRTs (19 yrs) along with the higher-than-natural  $\text{NO}_3^-$  concentration ( $7.86 \text{ mg L}^{-1}$ ) south of the fault (headwater area) indicated the invasion of modern contaminants. This finding warrants particular attention. High mixing rate amplitudes varying from 12 to 91 % were widespread in north of the fault due to the varying depths of long-screened boreholes as well as within the aquifer itself. Furthermore, the mixing diversity was highlighted by the substantial water table fluctuations during groundwater pumping, vertical recharge through the thick unsaturated zone, and young water mixtures in different decades. The strong correlations between groundwater MRTs and hydrochemical concentrations enable a first-order proxy at different times to be used. In addition, this study has revealed that MRTs estimated by CFCs were more appropriate than those using  $^3\text{H}$  in the arid MRB with a thick unsaturated zone.”

2) The meaning of the phrase “block water features” is not clear, possibly it means areas where there are strong (semi-vertical) contrasts in hydraulic conductivity (due to the thrust faults).

Response: Yes, the phrase “block water features” is not a very appropriate statement in this paper. What we want to tell the reader is that there are strong contrasts in hydraulic conductivity due to the thrust fault. The variant hydraulic conductivity also can be reflected by the geological and hydrogeological settings. Previous studies (Wu, 2007; Zhao, 2010) and other geological survey works in the Manas River Basin have indicated that the thrust faults shown in Fig. 1b are compressional faults and thus of water-blocking feature, which can explain the “a level difference of 130 m hydraulic drop is observed due to the thrust fault in the alluvium aquifer (Fig. 1c)”.

A recent study by Bresciani et al (2018) has distinguished the mountain-front recharge (MFR) and mountain-block recharge (MBR) by using hydraulic head, chloride and electrical conductivity data in the arid basin. MFR predominantly consists of stream infiltration in the mountain-front zone, and MBR consists of subsurface flow from the mountain towards the basin. Manas River Basin aquifers may receive the recharge from the south mountain through the MFR mechanism, and more specific analysis will be carried out in the future work.

3) Use of “apparent” ages in the preliminary discussion (Section 4.2.1) is defensible as described.

Response: We find that the phrase “apparent CFC ages” has been widely used in many other literatures (e.g. Darling et al., 2012; Hagedorn et al., 2011; Han et al., 2012; Happell et al., 2006; Koh et al., 2012; Plummer et al., 2006; Qin et al., 2011, 2012). However, a review paper by Suckow (2014) pointed out that the “apparent age” is “only well defined if the formula is given and if the tracer is stated”. There are appropriate formulas for different tracers, such as  $^{14}\text{C}$ ,  $^{36}\text{Cl}$ ,  $^{81}\text{Kr}$ ,  $^3\text{H}/^3\text{He}$ , and so on, but not for the CFCs, for  $\text{SF}_6$  and for  $^{85}\text{Kr}$ . Therefore, Suckow (2014) thinks that, strictly speaking, the term “apparent age”, should not be used for CFCs. This erroneous term “apparent age” for CFCs is also pointed out by Ref #2 (“L277: The paragraph on “apparent age” makes no sense for ... and sampling”).

We agree that the term “apparent age” for CFCs will not be used anywhere in our paper. As we know that the CFCs are synthetic organic compounds and largely released to the air since 1930s, and thus

they have been regarded as very good tracers for dating young water recharge time (post-1940 recharge). Therefore, we would like to use CFCs to explain the modern water recharge features.

The revised contents can be seen in Section 3.3.1 (RL172–191) and in Section 4.2.2 (RL340–406):

Section 3.3.1 (RL172–191):

“Knowledge of the history of the local atmospheric mixing ratios of CFCs in precipitation is first required for indicating modern water recharge. The difference between the local and global background atmospheric mixing ratios of CFCs in the Northern Hemisphere – *CFC excess* – varies substantially based on the industrial development. Elevated CFC concentrations (10–15 % higher than those of the Northern Hemisphere) have been reported in the air of urban environments such as Las Vegas, Tucson, Vienna, and Beijing (Barletta et al., 2006; Carlson et al., 2011; Han et al., 2007; Qin et al., 2007), whereas in Lanzhou and Yinchuan (Northwest China) they were approximately 10 % lower (Barletta et al., 2006). The MRB is located in Northwest China (Fig. 1a), has a very low population density, and is far from industrial cities. To evaluate CFC ages, the time series trend of Northern Hemisphere atmospheric mixing ratio (Fig. 3; 1940–2014, <http://water.usgs.gov/lab/software/air/cure/>) was adopted in this study.

Measured CFC concentrations (in  $\text{pmol L}^{-1}$ ) can be interpreted in terms of partial pressures of CFCs (in pptv) in solubility equilibrium with the water sample based on Henry's law. Concrete computational process was conducted following Plummer et al. (2006a). In arid Northwest China, estimating the local shallow groundwater temperature as recharge temperature is more suitable than the annual mean surface air temperature (Qin et al., 2011) because the local low precipitation usually cannot reach the groundwater. Studies On the MRB (Ji, 2016; Wu, 2007) have also indicated much less vertical recharge water from the local precipitation compared with abundant groundwater lateral flow recharge and river leakage from the mountain to the piedmont areas. In this study, the measured groundwater temperature, which varied from 11.5 to 15.7 °C between wells (Table 1), was used as the recharge temperature to estimate the groundwater input CFC concentrations. Surface elevations of the recharge area vary from 316 to 755 m. The modern water recharge was then determined by comparing the calculated partial pressures of CFCs in solubility equilibrium with the water samples with historical CFC concentrations in the air (Fig. 3).”

Section 4.2.2 (RL340–406):

“Table 1 shows that groundwater with well depths of 13–150 m contained detectable CFC concentrations (0.17–3.77  $\text{pmol L}^{-1}$  for CFC–11, 0.19–2.18  $\text{pmol L}^{-1}$  for CFC–12, and 0.02–0.38  $\text{pmol L}^{-1}$  for CFC–113) in both the upstream and midstream areas, indicating at least a small fraction of young groundwater components (post-1940). The highest concentration was observed in the UG (G3), south of the fault. The median and the lowest were observed in the west and east banks, respectively, of the East Main Canal in the MG, north of the fault. In the midstream area (Fig. 2), CFC concentrations generally decreased with well depth south of the reservoirs (G25, G8, and G9), and increased with well depth north of the reservoirs (G15 and G16), which might indicate different groundwater flow paths (e.g., downward or upward flow directions).

The groundwater aerobic environment (Table 1, DO values vary from 0.7 to 9.8  $\text{mg L}^{-1}$ ) makes CFC degradation under anoxic conditions unlikely. Nevertheless, CFC–11 has shown a greater propensity for degradation and contamination than CFC–12 (Plummer et al., 2006b). Therefore, we use CFC–12 to interpret the modern groundwater recharge in the following discussions. The estimated CFC partial

pressure and possible recharge year are shown in Table 2 and Fig. 3. The UG (G3) CFC-113 and CFC-12 both indicate the 1990 precipitation recharge (Table 2), probably a piston flow recharge in the upstream area. The MG CFC-11-based modern precipitation recharge was in agreement with that based on CFC-12 concentrations within 2–8 yrs, whereas the CFC-113-based recharge was as much as 4–11 yrs later than that the other two, signifying recharge of a mixture of young and old groundwater components in the midstream area. The most recent groundwater recharge was in the upstream area (G3 with 1990 rainfall recharge), which was most likely because the flow paths from recharge sources here were shorter than those of the piedmont groundwater samples in the midstream area.

G5 and G7 were located in the east bank of the East Main Canal in the midstream area and were closer than G15 and G16 north of the reservoir, showing that the modern recharge was much earlier than that of G15 and G16 (Table 2). This could be explained by the lower groundwater velocities in the east bank of the East Main Canal, where the hydraulic gradient (Fig. 2) was much smaller than that in the west. Furthermore, groundwater recharge became earlier with increasing well depth from 48 to 100 m south of the reservoir (G25, G8 and G9), whereas that north of the reservoir became later with increasing well depth from 23 to 56 m (G15 and G16; Table 2, Fig. 2). The different trends for the relationship between groundwater recharge year and well depth might be due to the different flow paths between the two sites (e.g., reservoir south and north).

Comparing CFC concentrations helps to indicate samples containing young (post-1940) and old (CFC-free) water (Han et al., 2007; Han et al., 2012; Koh et al., 2012) or exhibiting contamination or degradation (Plummer et al., 2006b). The cross-plot of the concentrations for CFC-113 and CFC-12 (Fig. 7a) demonstrates that all of the groundwater can be characterised as binary mixtures between young and older components, though there is still room for some ambiguity around the crossover in the late 1980s (Darling et al., 2012). As shown in Fig. 7a, all of the MG samples are located in the shaded region, representing no post-1989 water recharge. The UG (G3) sample is clearly relatively modern and seems to have been recharged in 1990 through piston flow or mixed with old water and post-1995 water. Using the method described by Plummer et al. (2006b) with the binary mixing model, the fractions of young water were found to vary from 12 to 91 % (Table 2) for the MG samples with the relatively low young fractions of 12 and 18 % in the MG samples (G5 and G7) from east bank of the East Main Canal. These two well water table were deeper than 40 m, probably indicating a relatively slow and deep circulated groundwater flow. This hypothesis is also suggested by the lower DO ( $3.7\text{--}4.6\text{ mg L}^{-1}$ ; Table 1) and nitrate concentrations ( $8.6\text{--}9.5\text{ mg L}^{-1}$  from Ma et al., 2018) and considerably smaller hydraulic gradient (Fig. 2). Furthermore, a fraction of young water as high as 100 % was obtained for G3 sample with the recharge water from 1990, and a 87 % fraction was obtained by from the binary mixture of post-1989 water and old water (Table 2). The relatively modern recharge for the G3 sample was likewise explained by its high DO ( $9.8\text{ mg L}^{-1}$ ; Table 1) and relatively low nitrate concentration ( $7.9\text{ mg L}^{-1}$  from Ma et al., 2018), which represented the contribution of high-altitude recharge rather than the old water.

CFC contamination and sorption in the unsaturated zone during recharge considerably influenced the interpretation of groundwater recharge. Points off the curves in the cross-plot of CFC concentrations may indicate contamination from the urban air with CFCs during sampling (Carlson et al., 2011; Cook et al., 2006; Mahlknecht et al., 2017) or the degradation or sorption of CFC-11 or CFC-113 (Plummer et al., 2006b). Figure 7 demonstrates that the urban air with CFC contaminations, which generally increased CFC concentrations above the global background atmospheric CFC concentrations for the Northern Hemisphere, are unlikely. Elevated CFC concentrations have been reported in

the air of urban environments such as Las Vegas, Tucson, Vienna and Beijing (Barletta et al., 2006; Carlson et al., 2011; Han et al., 2007; Qin et al., 2007) rather than in the arid regions of Northwest China (Barletta et al., 2006). Hence, the anomalous ratios of CFC-11/CFC-12 (Fig. 7b) off the model lines might be attributed to sorption in the unsaturated zone during recharge rather than the degradation of CFC-11 (Cook et al., 2006; Plummer et al., 2006b) under anoxic conditions (Table 1, DO values vary from 0.7 to 9.8 mg L<sup>-1</sup>). Nevertheless, the small deviations (Fig. 7b) indicate a low sorption rate. A higher CFC sorption rate occurs with high clay fraction and high organic matter in soils (Russell and Thompson, 1983), and vice versa (Carlson et al., 2011). Therefore, the hypothesis of a low sorption rate due to the low clay fraction and low organic matter content in the intermountain depression and the piedmont plain (Fig. 1c) seems reasonable.

The time lag for CFC transport through the thick unsaturated zone (Cook and Solomon, 1995), as well as degradation, especially for CFC-11 being common in anaerobic groundwater (Horneman et al., 2008; Plummer et al., 2006b), are both important considerations when interpreting groundwater recharge using CFC concentrations. The time lag for CFC diffusions through the deep unsaturated zone in simple porous aquifers, a function of the tracer solubility in water, tracer diffusion coefficients, and soil water content (Cook and Solomon, 1995), have been widely proved (Darling et al., 2012; Qin et al., 2011). The small differences in CFC-11 and CFC-12 recharge years (Table 2) demonstrate that the time lag should be short in the faulted-hydraulic drop alluvium aquifers with the deep unsaturated zone (Fig. 1c). Studies on the MRB (Ma et al., 2018; Wang, 2007; Zhou, 1992) have shown that groundwater mainly recharged by the river fast leakage in the upstream area and piedmont plain, where the soil texture consists of pebbles and sandy gravel (Fig. 1c); this suggests that the unsaturated zone air CFC closely follows that of the atmosphere, so the recharge time lag through the unsaturated zone is not considered.”

4) Strictly, groundwater has “residence time” or “mean residence time”/“MRT” (being the time water takes to travel through a groundwater system to where it is sampled by a bore), rather than “transit time” or “mean transit time”/“MTT” which is generally reserved for streamflow (being the time for water to transit through the catchment and into the stream). Consequently, the word “residence” should be substituted for the word “transit” wherever “transit” appears. And also “MRT” for “MTT”.

Response: Agree and changes made. The term “transit” was changed to “residence” and term “MTT” was changed to “MRT”, and we insisted on the “residence” and “MRT” throughout the manuscript.

We re-read the literatures and found that term “transit time” was numerously used to indicate the time for water to transit through the catchment and into the stream (Cartwright et al., 2018; Cartwright and Morgenstern, 2015, 2016; Hrachowitz et al., 2009, 2010; Morgenstern et al., 2010; Stewart and Morgenstern, 2016). Stewart et al. (2010) pointed out that “Residence time is the time spent in the catchment since arriving as rainfall. Transit time is the time taken to pass through the catchment and into the stream.” Leray et al. (2016) have adopted a general but robust definition for the residence time “the amount of time a moving element has spent in a hydrologic system”, and considered the terms residence time, transit time, travel time, age, and exposure time as equivalent in their discussions. Custodio et al. (2018) used both residence times and transit times for groundwater samples collected from springs and deep wells. In our study, all of the groundwater samples were collected from the wells/artesian wells. Thus, we tend to use the term “residence” instead of “transit” in our manuscript.

5) A selection of comments on the English are given below, to help the clarity of the writing. There



are many other very small infelicities in the English.

Response: We thank you very much for modifying the expressions of the manuscript. We have asked Chris Law (Wallace Academic Editing) to modify the language to help improve readability.

### Technical Corrections

1) P1 L24-25 Change to “Quite ‘modern’ recharge is found in the south of the fault with young (post–1940) water fractions of 87–100 %, ...” from “The quite ‘modern’ recharge in the south of the fault with young (post–1940) water fractions of 87–100 % is obtained, ...”

Response: Agree and changes made. The sentence was changed to (RL23–25): “Relatively modern recharge is found in the south of the fault with young (post–1940) water fractions of 87–100 %, whereas in the north of the fault in the midstream area the young, water fractions vary from 12 to 91 % based on the CFC binary mixing method.”

2) P2 L51 “Instead of” not “over for”

Response: Changes made (RL52). “over” was replaced by “than”.

3) P2 L53 “closed” not “close”

Response: Agree and changes made (RL54). “close” was replaced by “closed”.

4) P3 L89 “common” not “true”

Response: Agree and changes made (RL87). “true” was replaced by “common”.

5) P3 L90-91 “Pumping from long-screened wells (of which there are over 10,000, Ma et al., 2018) ...” not “Pumping from the long–screened over 10 000 boreholes (Ma et al., 2018) ...”

Response: Agree and changes made. The sentence was changed to (RL88–90): “In particular, pumping from long–screened wells (of which there are over 10 000 boreholes, Ma et al., 2018) makes groundwater mixing mostly likely.” Number “10 000” (not “10,000”) is divided in groups of three using a thin space, complying with the “manuscript preparation guidelines for authors”.

6) P3 L93 “result from” not “impacted by”

Response: Agree and changes made (RL90). “impacted by” was replaced by “result from”.

7) P3 L94 “insufficiently recognised” not “insufficient recognition”

Response: Agree and changes made (RL91). “insufficient recognition” was replaced by “insufficiently recognised”.

8) P4 L106 “total” not “totally”

Response: Agree and changes made (RL104). “totally” was replaced by “total”.

9) P4 L107 “intermittently active” not “intermittent activity”

Response: Agree and changes made (RL105). “intermittent activity” was replaced by “intermittently active”.

10) P4 L117 “depth” not “buried depth”

Response: Agree and changes made (RL115). Word “buried” was deleted.

11) P6 L177 “Manas River Basin” not “MRB”

Response: Agree and changes made (RL177). “MRB” was replaced by “Manas River Basin”.

12) P9 L259 & 264 “slope” not “slop”

Response: Agree and changes made (RL277 and 282). Erroneous “slop” was changed to “slope”.

13) P10 L300 “we use” not “one assign”

Response: Agree and changes made (RL350). “one assign” was replaced by “we use”.

14) P10 L304 “increasing” not “elevated”

Response: Changes made. The sentence was deleted.

15) P11 L323 “indicates a larger fraction of 1960s precipitation recharge for G4 ...” not “indicate that more fractions of the 1960s precipitation recharge was occurred for G4 ...”

Response: Agree and changes made. The sentence was changed to (RL417–419): “First, increase in <sup>3</sup>H activity in groundwater in the upstream area from 41.1 (G1 and G2) to 60 TU (G4) with distance indicated a larger fraction of 1960s precipitation for G4 than for G1 and G2; indeed, as seen in Fig. 2, near G4 samples exhibited the highest hydraulic gradient values.”.

16) P12 L370 “generally” not “totally” and “overlap” not “overlapping”

Response: Agree and changes made (RL321). “totally” was deleted, and “overlapping” was replaced by “overlap”.

17) P13 L397 delete “far”

Response: Agree and changes made (RL241). “far” was deleted.

18) P14 L413 “series” not “serious”

Response: Agree and changes made (RL468). “serious” was replaced by “series”.

19) P14 L423 “Overall” not “Totally”

Response: Agree and changes made (RL477). “Totally” was replaced by “Overall”.

20) P15 L448 “permit” not “permitting”

Response: Agree and changes made (RL502). “permitting” was replaced by “permit”.

21) P15 L465 “other sources” not “either source” (?)

Response: Changes made. “, and giving more accurate prediction of the contaminants like nitrate than either source of information” was deleted.

22) P15 L466 “decreases” not “decrease”

Response: Agree and changes made (RL518). Erroneous “decrease” was changed to “decreases”.

23) P16 L488 “which did not contribute groundwater recharge” not “which had non–contributes to groundwater recharge”

Response: Agree and changes made. The sentence was changed to (RL539–540): “..., which did not contribute to groundwater recharge in the arid regions of the Northwest China”.

24) P17 L520 delete “have occurred”

Response: Agree and changes made. “have occurred” was deleted.

25) P19 L578 “... area) imply invasion of modern contaminants, ...” not “... area), implying the modern contaminants invading, ...”

Response: Agree and changes made. The sentence was changed to (RL547–548): “... area) indicated the invasion of modern contaminants.”

“Groundwater mean transit times, mixing and recharge in faulted–hydraulic drop alluvium aquifers using chlorofluorocarbons (CFCs) and tritium isotope ( $^3\text{H}$ )” by Ma, B., Jin, M., Liang, X., Li, J., *Hydrol. Earth Syst. Sci.*, doi:10.5194/hess-2018-143.

We appreciate the many valuable suggestions and helpful comments of **Anonymous Referee #2**. We have seriously considered all of the suggestions and comments and have attempted to address each of the comments point-by-point. Detail explanations are as follows.

Author’s response – Line numbers referring to the old and revised version manuscripts are preceded by L and RL, respectively.

## **Anonymous Referee #2**

1) As indicated by the title, this manuscript presents the results of a groundwater dating and mixing study conducted using two different atmospheric tracers (CFCs and tritium). The two aims of the study were to (i) relate “ages” to local and general hydrogeological conditions and (ii) explore the possibility to use mineralisation as proxy for environmental tracers. I agree with referee #1 concerning the style, which is a huge disservice to the manuscript by its approximate use of technical terms and the general turn of phrase. I disagree however with the novelty (I do not see any) and the “substantial conclusions” (very unsubstantial and too dependent on mean transit time calculations that at present look extremely weak). As far as comment 4 of referee #1 is concerned, I think it is simply a matter of opinion and taste to use “transit time” instead of “residence time” (I prefer transit time because my work is related to solute transport problems, and “transit time” conveys this very idea of transport). One can argue over that, but it is really a hair splitting exercise.

Response: We would like to thank you very much for taking the time to review our manuscript. We think that the many valuable suggestions and helpful comments will help to improve our manuscript quality greatly.

We agree with you about the aims of the study and the opinion on the terms “transit time” and “residence time”. We re-read the literatures and found that term “transit time” was numerously used to indicate the time for water to transit through the catchment and into the stream (Cartwright et al., 2018; Cartwright and Morgenstern, 2015, 2016; Hrachowitz et al., 2009, 2010; Morgenstern et al., 2010; Stewart and Morgenstern, 2016). Stewart et al. (2010) pointed out that “Residence time is the time spent in the catchment since arriving as rainfall. Transit time is the time taken to pass through the catchment and into the stream.” Leray et al. (2016) have adopted a general but robust definition for the residence time “the amount of time a moving element has spent in a hydrologic system”, and considered the terms residence time, transit time, travel time, age, and exposure time as equivalent in their discussions. Custodio et al. (2018) used both residence times and transit times for groundwater samples that collected from springs and deep wells. In our study, all of the groundwater samples were collected from the wells/artesian wells. Thus, we tend to use the term “residence time” instead of “transit time” in our manuscript.

In addition, we have reorganized the structure and tried our best to present a clear roadmap to readers. Some incorrect phrase or expressions, for example the “apparent CFC ages” (L277) and “The apparent ages (Table 2 and Fig. 5) estimated from the PFM ...” (L509), which mislead the study and thus

have been revised and rewritten. In the revised manuscript, we tried to discuss the mean residence times and hydrochemistry evolution clearly and reasonably.

2) Overall, the authors seem to have read sufficiently thoroughly the existing literature on the subject as well as the most recent developments (such as Kirchner's analysis of the effect of heterogeneity on mean transit time estimation using amplitude damping) and understood the different problems and pitfalls relevant for their study. However, the phrasing is sometimes very awkward and tends to obfuscate what the authors mean (see specific comments below).

Response: We have checked the manuscript carefully and have tried our best to modify some erroneous words and phrases that you and Ref #1 pointed out. Some ambiguous statements and sentences have also been rewritten. We have asked Chris Law (Wallace Academic Editing) to modify the language to help improve readability.

3) But above all, I am missing a strong reason for this study to be published at all. As case study, it does not go beyond the classical scheme of sampling a few boreholes, analyse the groundwater samples for one or more tracers, calculate some kind of "age" and correlate it to depth or water chemistry. Doing so however, the authors try to apply different methods (lumped-parameter modelling, binary mixing) without presenting a clear roadmap.

Response: Manas River with the longest channel length and the largest river flow is representative among the hundreds of inland rivers in the Junggar Basin in the arid northwest China (Fig. 1a). There are more than 1 million people in the Manas River Basin. Groundwater is the very important and even the only water resources for the local residents. However, the paucity of research on groundwater mean residence time, mixing and recharge features have hampered the rational development and utilization of water resources in the Junggar Basin. We think that the case study of our manuscript is very essential and can be a good proxy for other analogous areas in the Junggar Basin.

Yes, we tried to estimate the mean residence time using lumped-parameter models. In addition, we also have tried to recognize the modern and paleo-meteoric recharge features. However, it is a pity that there are many deficiencies for the initial manuscript. We have reorganized the structure and tried our best to present a clear roadmap to readers. The outline of the manuscript have been reorganized as follows:

Title: Application of environmental tracers for investigation of groundwater mean residence time and aquifer recharge in faulted-hydraulic drop alluvium aquifers

1. Introduction
2. Geological and hydrogeological setting
3. Materials and methods
  - 3.1 Water sampling
  - 3.2 Analytical techniques
  - 3.3 Groundwater dating
    - 3.3.1 CFCs indicating modern water recharge
    - 3.3.2 The apparent  $^{14}\text{C}$  ages
    - 3.3.3 Groundwater mean residence time estimation
4. Results and discussion
  - 4.1 Stable isotope and major ion hydrochemistry

## 4.2 Modern and paleo–meteoric recharge features

### 4.2.1 Stable isotope indications

### 4.2.2 CFCs indications

### 4.2.3 $^3\text{H}$ and $^{14}\text{C}$ indications

## 4.3 Groundwater mean residence time

### 4.3.1 $^3\text{H}$ and CFCs

### 4.3.2 Hydrochemistry evolution

## 5. Conclusions

4) Model choice in particular is strangely presented: first, “apparent age” is presented as “based on the hypothesis of pistonflow”. Then that very piston-flow model is used although mixing is supposed to be “most likely” either within the aquifer or at the sampling point. This is completely contradictory and there is no reason not to apply another model to the CFC data (and for that matter, to the  $^{14}\text{C}$  data as well. See Custodio et al., 2018).

Response: We have deleted “apparent CFC ages” and rewritten the content of the model choice for mean residence time estimation (Section 3.3.3 (RL219–268)):

“Groundwater mixing may occur both within the aquifer and in the long–screened wells (Cook et al., 2017; Custodio et al., 2018; Visser et al., 2013). The groundwater residence times (ages) often display a wide range because recharge occurs under various climate conditions (Custodio et al., 2018). With the aid of gaseous tracers (e.g.  $^3\text{H}$ , CFCs,  $\text{SF}_6$  and  $^{85}\text{Kr}$ ) one can describe the mixing distribution using a mixing model (Stewart et al., 2017; Zuber et al., 2005) to obtain the groundwater MRTs. LPMs is an alternative approach to interpret MRTs for water flow through the subsurface systems to the output. For the steady–state subsurface hydrologic system,  $^3\text{H}$  and CFCs tracers entering groundwater with precipitation are injected proportionally to the volumetric flow rates by natural processes; the output concentration in water at the time of sampling relating to the input  $^3\text{H}$  and CFCs can be described by the following convolution integrals (Małozzewski and Zuber, 1982):

$$C_{\text{out}}(t) = \int_0^{\infty} C_{\text{in}}(t-\tau) g(\tau) e^{-\lambda_{^3\text{H}}\tau} d\tau \quad \text{for } ^3\text{H} \text{ tracer} \quad (2a)$$

$$C_{\text{out}}(t) = \int_0^{\infty} C_{\text{in}}(t-\tau) g(\tau) d\tau \quad \text{for CFCs tracer,} \quad (2b)$$

where  $C_{\text{out}}$  is the tracer output concentration,  $C_{\text{in}}$  is the tracer input concentration,  $\tau$  is the residence time,  $t-\tau$  is the time when water entered the catchment,  $\lambda_{^3\text{H}}$  is the  $^3\text{H}$  decay constant ( $\lambda_{^3\text{H}} = \ln 2/12.32$ ), and  $g(\tau)$  is the system response function that describes the residence time distributions (RTDs) in the subsurface hydrologic system.

In this study, the CFC concentrations from the time series trend of the Northern Hemisphere atmospheric mixing ratio (Fig. 3) and  $^3\text{H}$  concentrations in precipitation in Urumqi (Fig. 4) are treated as proxies for CFC and  $^3\text{H}$  recharge concentrations ( $C_{\text{in}}$ ), respectively. The historical precipitation  $^3\text{H}$  activity in the Urumqi station (Fig. 4) is reconstructed with the data available from the International Atomic Energy Agency (IAEA) using a logarithmic interpolation method. The precipitation  $^3\text{H}$  activity between 1969 and 1983 at Hong Kong and Irkutsk with different latitudes are used (data is available at <<https://www.iaea.org/>>). The time series of  $^3\text{H}$  activity (Fig. 4) was used as the input data are based on the following considerations. First, the MRB is located in the Northern Hemisphere, where the bomb–pulse  $^3\text{H}$  activity is several orders of magnitude higher than in the Southern Hemisphere (Clark

and Fritz, 1997; Tadros et al., 2014) and was superimposed with the China atmospheric nuclear tests from 1964 to 1974 in the arid regions of Northwest China; thus, the remnant  $^3\text{H}$  activity remains affected by the tail–end of the bomb pulse. Second, the study area is more than 3500 km away from the western Pacific, where the atmospheric  $^3\text{H}$  activity is much higher than that at coastal sites due to the continental effect (Tadros et al., 2014). Furthermore, although the atmospheric  $^3\text{H}$  activity varies between seasons (Cartwright and Morgenstern, 2016; Morgenstern et al., 2010; Tadros et al., 2014), the mean annual values (Fig. 4) were considered in this study.

Several RTDs have been described (Małozzewski and Zuber, 1982; Jurgens et al., 2012) and have been widely used in studies of variable timescales and catchment areas (Cartwright and Morgenstern, 2015, 2016; Cartwright et al., 2018; Hrachowitz et al., 2009; Morgenstern et al., 2010, 2015; McGuire et al., 2005). The selection of each model depends on the hydrogeological situations in the hydrologic system to which it is applicable. The exponential–piston flow model (EPM) describes an aquifer that contain a segment of the exponential flow followed by a segment of piston flow. The piston flow model assumes minimal water mixing from different flow lines and little or no recharge in the confined aquifer; the exponential flow model assumes a full mixing of water in the unconfined aquifer and the receipt of areally distributed recharge (Jurgens et al., 2012; Małozzewski and Zuber, 1982). The weighting function of this model is given by

$$g(\tau) = 0 \quad \text{for } \tau < \tau_m(1-1/\eta) \quad (3a)$$

$$g(\tau) = \frac{\eta}{\tau_m} e^{(-\eta\tau/\tau_m + \eta - 1)} \quad \text{for } \tau \geq \tau_m(1-1/\eta) \quad (3b)$$

The dispersion model (DM) mainly measures the relative importance of dispersion to advection, and is applicable for confined or partially confined aquifers (Małozzewski, 2000). Its RTD is given by

$$g(\tau) = \frac{1}{\tau \sqrt{4\pi D_p \tau / \tau_m}} e^{-\left(\frac{(1-\tau/\tau_m)^2}{4\pi D_p \tau / \tau_m}\right)} \quad (4)$$

The weighting function of the exponential mixing model (EMM) is

$$g(\tau) = \frac{1}{\tau_m} e^{(-\tau/\tau_m)}, \quad (5)$$

where  $\tau_m$  is the mean residence time,  $\eta$  is the ratio defined as  $\eta = (l_p + l_E)/l_E = l_p/l_E + 1$ , where  $l_E$  (or  $l_p$ ) is the length of area at the water table (or not) receiving recharge,  $D_p$  is the dispersion parameter, which is the reciprocal of the Peclet number ( $Pe$ ) and defined as  $D_p = D/(vx)$ , where  $D$  is the dispersion coefficient ( $\text{m}^2 \text{day}^{-1}$ ),  $v$  is velocity ( $\text{m day}^{-1}$ ), and  $x$  is distance (m).

Each RTD has one or two parameters, MRT ( $\tau_m$ ) is determined by convoluting the input (the time series  $^3\text{H}$  and CFCs input in rainfall) to each model to match the output (the measured  $^3\text{H}$  and CFC concentrations in groundwater), and other parameters ( $\eta$  and  $D_p$ ) are determined depending on the hydrogeological conditions. To interpret the ages of the MRB data set, EPM ( $\eta=1.5$  and  $2.2$ ), DM ( $D_p=0.03$  and  $0.1$ ), and EMM models were used, after which MRTs with different RTDs were cross-referenced.”

We read the literature carefully and think that both the method and idea are very innovative by Custodio et al. (2018), who related chloride (Cl) and  $^{14}\text{C}$  activity changes in recharge for aquifers in the arid area to indicate the effect of variations in recharge rate during the previous wetter–than–present period.

We think that it would be also good applications in other arid areas around the world because the climatic change is global. In our manuscript, the apparent  $^{14}\text{C}$  ages estimation was adopted. The changes in groundwater reserves and  $^{14}\text{C}$  content will be conducted in the future in the Manas River Basin.

5) I know it is customary to interpret CFC data assuming piston-flow, but it is nonetheless a priori wrong. Model choice must be substantiated from knowledge of the hydrogeological situation and the sampling scheme (Maloszewski and Zuber, 1982; Leray et al., 2016). Later on in the manuscript however different models are used in the binary mixing plots, and model choice is discussed briefly. Why use the “apparent age” concept at all, then ? This is confusing and reads like the two authors have written separately different parts of the manuscript and then pasted the two parts together.

Response: Sorry, we have realized that the apparent CFC ages are not appropriate. As we know that the CFCs are synthetic organic compounds and largely released to the air since 1930s, and thus they have been treated as good tracers for dating young water recharge time (post–1940 recharge).

We totally agree with you that “Model choice must be substantiated from knowledge of the hydrogeological situation and the sampling scheme”. Therefore, in the revised manuscript, we have rewritten the content and have discussed the model choice in detail in Section 3.3.3 (See Response 4).

The mean residence times estimated by the lumped–parameter models have been deleted in the binary mixing plots (Fig. 7). However, the binary plots of CFC vs. CFC and CFCs vs.  $^3\text{H}$  are widely used in the literatures and can provide useful information on the co–existence of young water with old water (Cook et al., 2017; Han et al., 2007; Han et al., 2012; Koh et al., 2012; Qin et al., 2011), as well as can provide a powerful tool to recognize contamination, degradation and irrigation infiltration and so on (Cook et al., 2017; Han et al., 2015; Mahlknecht et al., 2017; Qin et al., 2012). However, these information mentioned above have not been clarified clearly before in the Manas River Basin, and even not in the Junggar Basin (Fig. 1a). Therefore, we think that the binary mixing plots are essential in the manuscript in order to tell the reader more information about groundwater mixing or recharge features.

6) I also have my doubts concerning the calculations of the mean transit times as they are presented.

Response: Take the CFC–12 and exponential–piston flow model (1.5) for example, the calculation process of the mean residence times is as follows: First, we chose the Eq. (2b) as the convolution integral, and chose the exponential–piston flow model (Eq. (3a, 3b)) as the system response function. Second, we used the time series CFC–12 trend of Northern Hemisphere atmospheric mixing ratio (1940–2014, <http://water.usgs.gov/lab/software/air/cure/>) as input concentrations. We treated the calendar year 2015 (groundwater sampling time) as age=0 yrs by convoluting the input (times series of CFC–12 input) to the EPM (1.5), and increased the mean residence time  $\tau_m$  from 1 to 500 yrs with the time step of 1 yr within 100 yrs and with the time step of 5 yrs between 101 to 500 yrs. Then we can get a sequence of results of output CFC–12 concentrations and mean residence times (vary from 1 to 500 yrs). Third, we plotted the output CFC–12 concentrations vs. mean residence times and then compared the measured groundwater CFC–12 concentrations to get the groundwater mean residence times. The computational procedures were conducted by using MATLAB (version R2014a). The output CFC–12 concentrations decreased from 526.4 pptv with  $\tau_m$  of 1 yr to 3.0 pptv with  $\tau_m$  of 155 yrs. As



the detection limit for each CFC is about 0.01 pmol<sup>-1</sup> of water (be equal to 3.54 pptv with the laboratory temperature of 25°C), the output CFC–12 concentrations lower than 3.54 pptv can be neglected.

7) The method with which the tritium input has been reconstructed is not documented properly (which stations were used, and how long were the available time series?) and the estimated modern value (31 TU) seems extremely high compared to Western Europe for instance (about 6 TU). Is that because of the Chinese nuclear tests of the 60s and 70s that are being referred to in the introduction, or the result of some kind of regional effect?

Response: Agree and changes made. The input tritium (<sup>3</sup>H) activity in Urumqi station was reconstructed as follows: First, as we know that there is a proportionality between the logarithmic precipitation <sup>3</sup>H activity and the latitude in the Northern Hemisphere, we can reconstruct the Urumqi precipitation <sup>3</sup>H activity according to the following equation:

$$\lg C_U = \lg C_H + \frac{\lg C_I - \lg C_H}{X_I - X_H} * (X_U - X_H) \quad (S1)$$

where  $C_U$  is Urumqi precipitation <sup>3</sup>H activity,  $C_H$  is Hong Kong precipitation <sup>3</sup>H activity,  $C_I$  is Irkutsk (in Russia) precipitation <sup>3</sup>H activity,  $X_U$  is Urumqi latitude,  $X_H$  is Hong Kong latitude, and  $X_I$  is Irkutsk latitude. The precipitation <sup>3</sup>H activity are available in the International Atomic Energy Agency (IAEA). The results based on Eq (S1) are show in Table S1.

Table S1. The reconstructed Urumqi precipitation <sup>3</sup>H activity between 1969 and 1983.

Date	$C_H$ (TU)	$C_I$ (TU)	$C_U$ (TU)	Ottawa precipitation (TU)
1969	46.93	454.79	248.63	253.66
1970	29.38	464.15	222.82	190.77
1971	24.38	516.61	229.38	206.1
1972	27.86	247.23	138.36	92.34
1973	13.22	173.34	87.44	90.41
1974	17.47	216.58	110.90	98.07
1975	12.42	190.93	92.33	75.86
1976	11.71	148.8	75.69	58.91
1977	12.24	150.72	77.31	73.93
1978	10.89	103.11	56.72	73.63
1979	8.96	92.06	49.55	49.62
1980	7.63	141.8	65.20	49.54
1981	11.53	138.3	71.44	55.09
1982	9.73	66.92	40.08	47.29
1983	21.14	127.26	78.96	40

Second, a good linear regression between the  $C_U$  and Ottawa precipitation <sup>3</sup>H activity can be obtained as follows:

$$C_{Ui} = 1.0102C_{Ottawa} + 11.647 \quad (R^2 = 0.933, n = 15) \quad (S2)$$

where  $C_{Ottawa}$  is Ottawa precipitation <sup>3</sup>H activity,  $C_{Ui}$  is the Urumqi annual precipitation <sup>3</sup>H activity.

Third, considering the precipitation amount effect, the reconstructed Urumqi precipitation <sup>3</sup>H activity

can be obtained as follows:

$$C_{RU} = C_{Ui} * \frac{P_i}{P_m} \quad (S3)$$

where  $C_{RU}$  is the reconstructed Urumqi precipitation  $^3\text{H}$  activity shown in Fig. 6 (estimated  $^3\text{H}$ ),  $P_i$  is the annual precipitation amount (1953–2015),  $P_m$  is the annual mean precipitation amount in Urumqi between 1953 and 2015.

Yes, the estimated modern precipitation  $^3\text{H}$  activity are indeed extremely high (mean value of 31.55 TU between 2000 and 2015). We speculate that the very high precipitation  $^3\text{H}$  activity may be ascribed to both the Chinese atmospheric nuclear tests (around 350 km away to Manas River Basin) from 1964 to 1974 (Zhou, 1992) and the continental effect (Tadros et al., 2014), where the Manas River Basin is more than 3500 km away from the western pacific. The high precipitation  $^3\text{H}$  activity was also shown in Fig. S1 (Cauquoin et al., 2015).

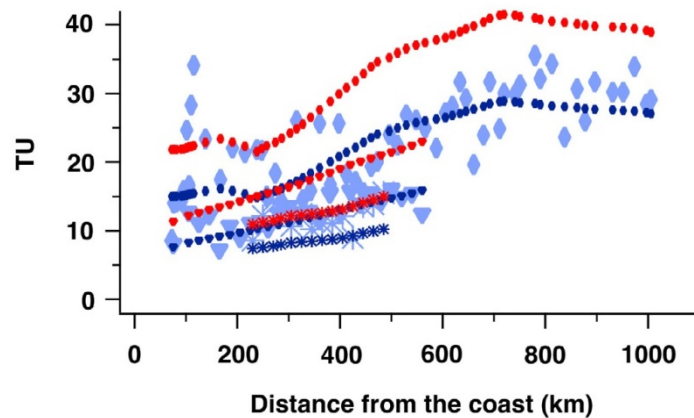


Figure S1. Comparison of modelled tritium in precipitation with surface snow samples from two ITASE Antarctic traverses (Proposito et al., 2002; Becagli et al., 2004) and some pre-bomb measurements. (The figure is from Cauquoin et al., 2015, Fig. 10d)

8) Furthermore, the authors do address the non-uniqueness problems that are bound to arise when calibrating an exponential piston-flow or a dispersion model (2 free parameters each) using a single tritium measurement in aquifers that still retain some of the “bomb tritium” (see Stewart et al., 2010 for details), but in a terribly confusing way and without first explaining the rationale and the approach taken.

Response: Sorry. We should have given more details about the two free parameters each for the exponential–piston flow and the dispersion model. These parameters are substantial based on the geological/hydrogeological conditions. We have added some more detailed explanations concerning the rationale and the approach taken in Section 3.3.3 (Response 4). The revised version can be seen in the “Response 4”.

9) I suppose figure 8 was meant to show the range of parameters that match the measured tracer concentrations. That’s commendable, but badly explained.

Response: Yes, thanks. We have redrawn the figure 8 to show the most useful information to the readers (see the “Specific Comments Response 55”).

10) In the final step relating mineralisation to transit time, the authors finally select the EPM calibrated with the CFC12 measurements, but this is once again presented in a unclear fashion.

Response: There are some reasons that we select the EPM (1.5) calibrated with the CFC–12 to relate hydrochemistry evolution. First, groundwater CFCs results show that the urban air with CFC compounds contaminations, which generally cause elevated CFC than the global background atmospheric CFC concentrations (Northern Hemisphere), are unlikely (Fig. 7) in the Manas River Basin. Second, CFC–12 has much less propensity for degradation and/or contamination than CFC–11 and CFC–113. Third, the exponential–piston flow model is one of the mostly commonly used system response functions. The choice of exponential–piston flow model is suitable for the aquifer that has two segments, in which a segment of exponential flow followed by a segment of piston flow. As shown in Fig. 1c and relative hydrogeological discussions, exponential–piston flow model is a good choice to be chose as the system response function. In addition, the mean residence times mathematic relation between EPM (1.5) and other system response functions are obtained (Fig. 11). We can relate mineralization to mean residence time based on these mathematic relations.

11) The discussion is too long, relies too much on untested and untestable hypotheses, and presents so many singular and unfocused results that it is difficult for the reader to grasp a clear picture of their meaning and significance. The paragraph on “apparent age” should be scraped altogether and the different estimates of “age” (i.e. mean transit time of the respective model) and mixing ratios organised in a clear and synthetic manner.

Response: To avoid misleading, we have deleted some irrelevant content, such as the incorrect statement of “apparent age” for the CFCs, and the incorrect hypothesis of piston flow as mixing is supposed to be “most likely” either within the aquifer or at the sampling point. We also tried to present a clear roadmap to readers, including modern and paleo-meteoric recharge features, mean residence time estimated by LPMs, and mixing features as well as irrigation infiltration indications.

12) All in all, the manuscript must be seriously reorganised and streamlined. The calculation of mean transit times of the different tracers must be redone, removing entirely the “apparent age” nonsense and explaining clearly the different steps taken by the authors to (I) select a model (II) explore model parameter range and (III) compare the different results obtained from tritium, the CFCs and carbon 14. Interpretation of the obtained “ages” in terms of hydrogeology and its correlation to hydrochemistry must then be presented in a clear and synthetic fashion. Only when this is done might the manuscript rise above an unoriginal and confusing rehash of previous studies, and could be considered for publication.

Response: We reorganized the structure and tried our best to present a clear roadmap to readers. We rewrote the Section 3.3.3 in which system response functions were selected by considering the applicable hydrogeological situations. Parameter and mean residence times were recalculated and then explained in a much clearer way. Figures 8 and 9 (They are Figs. 10 and 11 in the revised manuscript) were redrawn to show much useful information to readers. The controversial “apparent CFC age” was deleted and then was shown in a more proper way to indicate the modern precipitation recharge.

## Specific Comments

- 1) Please ask the help of a proof reader to help improve readability

Response: Agree. We have asked Chris Law (Wallace Academic Editing) to modify the language to help improve readability.

- 2) L11: Why is it crucial ? Please explain or leave that out.

Response: Agree. As we know that groundwater are the very important and even the only water resources for the local residents in the Manas River Basin of arid Northwest China (It is also the same in many other arid areas around the world). Two recharge sources which, modern precipitation recharge and paleo–meteoric recharge, are known as the main sources for the groundwater in arid areas. Knowledge the recharge sources is thus can provide correct guidance for extraction of groundwater. In addition, groundwater renewability is also an important factor for guiding extracting groundwater. Groundwater residence time reveals information about water storage, mixing and transport in subsurface water systems, which has contributions to the rational development of groundwater (Cartwright et al., 2017; Custodio et al., 2018; Dreuzy and Ginn, 2016; Leray et al., 2016). Therefore, we tend to retain the sentence (L11) in consideration of the explanation mentioned above.

- 3) L15: “indicating the rainfall recharge...” You mean that the young water component is higher than in samples with lower tritium activity.

Response: The inexact expression generates misunderstanding. We mean the very high  $^3\text{H}$  activity (41.1–60 TU) of groundwater indicate rainfall recharge during the nuclear bomb.

- 4) L29: The title of this section is not very telling, and this is not really what the study is about, is it?

Response: Agree and changes made (RL27). The title was changed to “Introduction”.

- 5) L33: “may be renewable”. What do you mean ? Something about short turnover time ?

Response: Changes made. We think that “renewable” may means groundwater being recharged by other water resources after extraction (or discharge).

The sentence was changed to (RL32–34): “This is particularly crucial in alluvium aquifers where fresh groundwater renewability is generally strong (Huang et al., 2017), thus functioning as potable water resources in the arid areas; also, alluvium aquifers are more vulnerable to anthropogenic contaminants and land–use changes (Morgenstern and Daughney, 2012).”

- 6) L37-39: Rewrite the entire sentence.

Response: Agree and changes made. The entire sentence was changed to (RL35–40): “Because the residence time distribution in subsurface water systems cannot be empirically measured, a commonly used approach is parametric fitting of trial distributions to chemical concentrations (Leray et al., 2016; Suckow, 2014). The widely used lumped–parameter models (LPMs; Małoszewski and Zuber, 1982; Jurgens et al., 2012), which commonly assume that the hydrologic system is at a steady–state, have been applied to subsurface water systems containing young water with modern tracers of variable input concentrations (e.g. seasonably variable stable isotope  $^2\text{H}$  and  $^{18}\text{O}$ , tritium, and  $^{85}\text{Kr}$ ; Cartwright et al., 2018; McGuire et al., 2005; Morgenstern et al., 2015; Stewart et al., 2010).”

7) L38: “and may be inferred”. You mean “must be inferred”.

Response: Agree and changes made (RL35–40). Yes, the residence time distribution cannot be empirically measured. See “Specific Comments Response 6”.

8) L39: “at” steady-state, not “in” steady-state.

Response: Agree and changes made (RL38). “in” was replaced by “at”.

9) L40: “Three types of transit time”. You mean three time windows ?

Response: Changes made. The sentence was changed to (RL40–41): “The groundwater residence time tracers can be classified into three types depending on their time span.”

10) L46: It’s not variability, rather time span.

Response: Agree and changes made (RL41). “variabilities” was replaced by “time span”.

11) L48: “in a similar function with” should read “in a similar way to”.

Response: Agree and changes made (RL48). “in a similar function with” was replaced by “in a similar way to”.

12) L51: replace “over” with “than”.

Response: Agree and changes made (RL52). “over” was replaced by “than”.

13) L54: You mean that increasing transit time through the aquifer leads to increasing mineralisation.

Response: No change made. That “increasing transit time through the aquifer leads to increasing mineralisation” is reasonable under certain circumstance. However, groundwater mineralisation is a very complex process, which contains mineral dissolution, precipitation, hydrolysis, evaporation concentration, water–rock interaction, and so on (Ma et al., 2018). In addition, water corrosion, solubility of rocks, and groundwater runoff will also have strong impacts on mineralization (Shen et al., 1993). Thus, increasing transit time not necessarily leads to increasing mineralization. The sentence and cited literatures (L54) in the manuscript tend to show that there are some correlations between the transit time and mineralisation in some situations. Nevertheless, the correlation is still unclear in the Manas River Basin, and that is right the research objective in our manuscript.

14) L55: Please explain why tritium is “the only true age tracer”, namely because it is part of the water molecule.

Response: Agree and changes made. Yes, it is. The sentence was changed to (RL56): “The only true age for water is  $^3\text{H}$ , a component of the water molecule with a half–life of 12.32 yrs (Tadros et al., 2014).”

15) L56 (entire paragraph): Why mention the southern hemisphere at all, since the study takes place in the northern hemisphere ? This is useless information.

Response: Agree and changes made. We have deleted the statements concerning the Southern Hemisphere  $^3\text{H}$  activities and relevant references (L61–66).

16) L66: “may be used to estimate MTTs” should read “must be used to estimate MTTs”. And explain

why (non-unicity problems...).

Response: Agree and changes made. Yes, we totally agree with your opinion. As the mean annual  $^3\text{H}$  activities peaks were several hundred times natural levels in the Northern Hemisphere due to the atmospheric thermonuclear tests in the Northern Hemisphere between the 1950s and 1960s, the nowadays rainfall  $^3\text{H}$  activities are still affected by the tail-end of the bomb-pulse in the Northern Hemisphere. Groundwater residence time cannot be assigned based on measurement of a single sample  $^3\text{H}$  activity.

The sentence was changed to (RL62–64): “Thus, measurement of a single sample of  $^3\text{H}$  activity does not accurately assess the groundwater MRTs in the Northern Hemisphere (Cook et al., 2017), and time-series  $^3\text{H}$  measurements with LPMs are required (Han et al., 2007; Han et al., 2015).”

17) L69: You are confusing residence time and degradation half-life. The residence time of the CFCs in the atmosphere is no different from that of tritium or any other tracer. The difference lies in their half-lives (degradation for CFCs, decay for tritium), which are very long for the CFCs.

Response: Agree and changes made. We agree with your opinion on the “residence time” and “degradation half-lives” for the atmospheric environmental tracers (e.g. CFCs and  $^3\text{H}$ ). CFCs degrade slowly in the atmosphere and have relatively long degradation half-lives, while the decay half-life for  $^3\text{H}$  is much shorter with 12.32 yrs. The input function for CFCs is not area-specific as is the case with  $^3\text{H}$ . Therefore, the atmospheric concentrations for CFCs are uniform over large areas (Cartwright et al., 2017; Cook et al., 2017), while that for  $^3\text{H}$  often varies across latitudes and between seasons (Tadros et al., 2014).

The sentence was changed to (RL65–66): “In contrast to  $^3\text{H}$ , CFCs degrade slowly in the atmosphere and have relatively long degradation half-lives, which permits their uniform atmospheric distributions over large areas.”

18) L78-82: Please rephrase the entire sentence.

Response: Agree and changes made. The sentence was rewritten as follows (RL75–80): “However, groundwater MRTs may not always be accurate when calculated using CFCs: for example, MRTs are much lower than the actual values if CFC inputs are entrapped excess air in the unsaturated zone during recharge (Cook et al., 2006; Darling et al., 2012) or contaminated in urban and industrial environments (Carlson et al., 2011; Han et al., 2007; Mahlknecht et al., 2017; Qin et al., 2007), and are much higher if CFC inputs are degraded in anaerobic groundwater (most notably CFC-11 and CFC-113; Cook and Solomon, 1995; Horneman et al., 2008; Plummer et al., 2006b).”

19) L89: “Mixing [...] is particularly true...”. You don’t know that, it’s a probable hypothesis!

Response: Agree and changes made. Though the previous study (Ma et al., 2018) have confirmed that the groundwater lateral-flow mixing is common in the alluvium aquifers of the Manas River Basin, more work and studies should be conducted to confirm the mixtures within the aquifers and long-screened wells. On the other hand, groundwater mixing can occur within the aquifer itself (Cook et al., 2017) as well as occur during pumping from long screened wells. However, for the case study of the Manas River Basin, mixing ascribed to pumping from long-screened wells has not been demonstrated before.

The sentence was changed to (RL87–88): “The hypothesis mixing within the aquifers and pumping from the long–screened wells is common in the faulted–hydraulic drop alluvium aquifers of the Manas River Basin (MRB) in the arid regions of Northwest China (Fig. 1).”

20) L93-95: “The MTTs that impacted....”. This sentence makes no sense. Rewrite.

Response: Agree and changes made. The sentence was changed to (RL90–92): “The MRTs that result from a deep unsaturated zone (water table depth is 180 m) and contrasting geological settings (a level difference of 130 m hydraulic drop caused by the thrust fault) are still insufficiently recognised in the alluvium aquifer (Fig. 1c).”

21) L106: “with totally length” should read “with total length”.

Response: Agree and changes made (RL104). “totally” was replaced by “total”.

22) L107: “was intermittent activity” should read “was intermittently active”.

Response: Agree and changes made (RL105). “intermittent activity” was replaced by “intermittently active”.

23) L110: So the different aquifers are all fractured rock aquifers.

Response: Yes, the substantial fractures and fissures of rock aquifers in the mountain area allow groundwater migration to be possible. The literatures by Cui et al. (2007) and Zhou (1992) were cited in the relevant discussion.

24) L114: “is macroscopically similar”. What do you mean with “macroscopically” ?

Response: Changes made. The sentence was changed to (RL112): “The groundwater flow direction is consistent with the Manas River flow direction.”

25) L120: “is as large” should read “is as deep”.

Response: Agree and changes made (RL118). “large” was replaced by “deep”.

26) L124: How many samples were taken altogether ? And are there any information concerning screening depth and size (fully penetrating wells or not) ? This is important information to guide model choice.

Response: Agree and changes made. The important information concerning sample numbers as well as screening depth and size were added in the revised manuscript.

The sentences were changed to (RL122–126):

“In total, 29 groundwater (pumped from fully penetrating well, of which 3 are from spring and 3 are from the artesian well) were collected along the Manas River during June to August, 2015 (from G1 to G29 in Table 1 and Fig. 2). Groundwater were separated into three clusters including the upstream groundwater (UG, south of the Wuyi Road), midstream groundwater (MG, area between the Wuyi Road and the West Main Canal–Yisiqi), and downstream groundwater (north of the West Main Canal–Yisiqi) based on the hydrochemistry and stable isotope data.”

27) L126: What was the rationale for separating the samples into three groups ? For instance, why is G13 MG while G26 is DG ? DG seems like the downgradient boundary. Did you use the piper dia-

grams to separate the samples ?

Response: Agree and changes made. Yes, you are exactly right that the three groundwater groups are based on the result of hydrochemistry and stable isotope. Yisiqi (Fig. 2) is the dividing line where there is an obvious change for the hydrochemistry and stable isotope along the Manas River motion (Fig. S2 from Ma et al., 2018). We also use piper diagrams to separate the samples (Fig. 4).

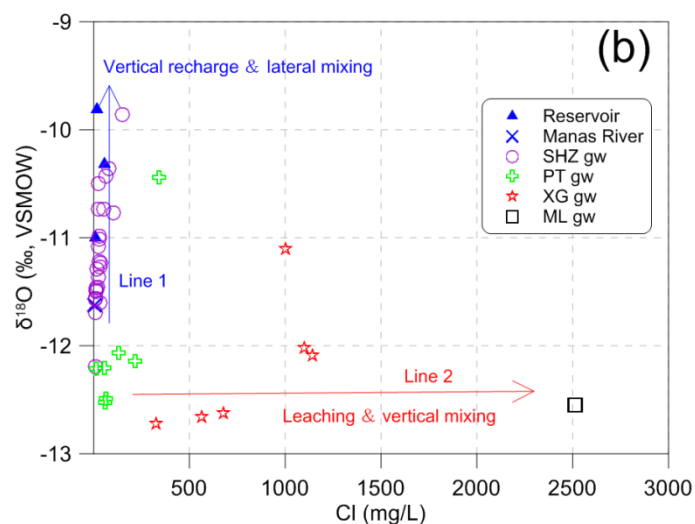


Figure S2. Relationship between  $\delta^{18}\text{O}$  and Cl concentrations for waters as a means to differentiate hydrogeological processes in the Manas River Basin. The purple circles represent the upstream and midstream groundwater, and green, red, and black legends represent downstream groundwater (from Ma et al., 2018).

28) L152: “were followed” is used multiple times but should read “after” or “following”.

Response: Agree and changes made (RL151 and 156). We have checked the manuscript carefully and seriously have corrected the erroneous words. “were followed” was changed to “were after” and we insisted on the “after” throughout the manuscript.

29) L173: “refers” is not the proper verb. Use “depends” for instance.

Response: Agree and changes made. The sentence was changed to (RL173–174): “The difference between the local and global background atmospheric mixing ratios of CFCs in the Northern Hemisphere – CFC excess – varies substantially based on the industrial development.”

30) L179: What are low latitude countries ?

Response: Changes made. The vague expression was deleted. As the atmospheric CFC concentrations are affected by the industrial development, the time series of Northern Hemisphere atmospheric CFC concentrations were widely treated as the background values for the underdeveloped areas (it is also applied to the Manas River Basin in our manuscript).

31) L189: The entire procedure is correctly explained, and also the fact that “apparent age” implies piston-flow transit time distribution, but why use apparent age in the first place ? Piston-flow is one model among many, as the authors explain later in the manuscript. Furthermore, the entire concept of “age” is problematic and should be replaced by mean transit time or mean residence time (for an in-depth discussion, see Suckow, The age of groundwater-Definitions, models and why we do not



need this term, Applied Geochemistry 50, 2014, 222-230).

Response: Agree and changes made. The erroneous “apparent CFC age” has been deleted. The concept of “age” is replaced by mean residence times and estimated by lumped-parameter models with the exponential-piston flow model, dispersion model, and exponential model, which are discussed in Section 4.3.1. In addition, the groundwater recharge sources (e.g. to distinguish the modern and paleo-meteoric recharge features) identified by the CFCs are also discussed in Section 3.3.1 and Section 4.2.2.

32) L194: What do you mean by “closed system” ? Physically bounded ?

Response: Changes made. As we know that the measured tracer output concentration in the groundwater is compared to its historical input using the convolution integral, in which the system response function is selected based on the different hydrogeological subsurface flow systems (Jurgens, et al., 2012; Małoszewski and Zuber, 1982; the details of calculation is shown in “Response 6”). The tracer output concentration can be measured from the spring, stream, well, and so on. There is no absolutely physical boundary for the subsurface flow system. Therefore, the ambiguous statements “closed system” is not rigorous and thus is deleted. See Section 3.3.3 (Response 4).

33) L208: “were given below as transit time distribution function” should read “were selected and are given below”.

Response: Agree and changes made. This sentence was deleted and more detailed interpretations were added (See Section 3.3.3 in the Response 4).

34) L219: You should also explain here how you planned to choose between these competing models.

Response: Agree and changes made. The system response function is selected based on the hydrogeological settings and the sampling position of tracer output concentration measured. We explain the basis on the choice of the models. See Section 3.3.3 (Response 4).

35) L235: Why present an equation you will not be using for lack of appropriate data ?

Response: Agree and changes made. We have deleted this equation and the accompanying description.

36) L240: This is true for the piston-flow model only ! See Custodio et al. for details.

37) L250: So the entire paragraph boils down to using literature values for the initial  $^{14}\text{C}$  activity. Make it shorter and to the point.

Response: Agree and changes made. Custodio et al. (2018) indicated that the calculated groundwater  $^{14}\text{C}$  age is really an apparent age due to the mixture of waters with different transit times, which was also indicated by other researchers (e.g. Cook et al., 2017; Suckow, 2014). Therefore, we deleted some unnecessary description and unimportant information in the text. Some sentences were reduced and revised. The revised content can be seen in Section 3.3.2 (RL193–217):

“Carbon-14 ( $^{14}\text{C}$ , half-life: 5730 yrs) activity in groundwater is often used to estimate groundwater age over time periods of approximately 200 and 30 000 yrs, and to determine the recharge from mixing water in various climate conditions (Cook, et al., 2017; Custodio et al., 2018; Huang et al., 2017).

Calculation of  $^{14}\text{C}$  groundwater age may be complicated if dissolved inorganic carbon is derived from a mixture of sources or  $^{14}\text{C}$  originating from the atmosphere or soil zone is significantly diluted by the dissolution of  $^{14}\text{C}$ -free carbonate minerals in the aquifer matrix and biochemical reactions along the groundwater flow paths (Clark and Fritz, 1997). Although only minor carbonate dissolution is likely, determination of groundwater residence times requires  $^{14}\text{C}$  correction (Atkinson et al., 2014). When the dissolution of carbonate during recharge or along the groundwater flow path may dilute the initial soil  $\text{CO}_2$ ,  $\delta^{13}\text{C}$  can be used to trace the process (Clark and Fritz, 1997). An equation for the reaction between  $\text{CO}_2$ -containing water with a carbonate mineral is commonly written as follows (modified after Pearson and Hanshaw, 1970):



where  $\delta^{13}\text{C}_{\text{carb}}$  is the dissolved carbonate  $\delta^{13}\text{C}$  value (approximately 0; Clark and Fritz, 1997), and  $\delta^{13}\text{C}_{\text{DIC}}$  is the measured  $\delta^{13}\text{C}$  value in groundwater.

Depending on knowing the measured  $^{14}\text{C}$  activity after adjustment for the geochemical and physical dilution processes in the aquifer (without radioactive decay), the groundwater apparent  $^{14}\text{C}$  ages ( $t$ ) can be calculated from the following decay equation:

$$t = -\frac{1}{\lambda_{^{14}\text{C}}} \times \ln \frac{a^{14}\text{C}}{a_0^{14}\text{C}}, \quad (1)$$

where  $\lambda_{^{14}\text{C}}$  is the  $^{14}\text{C}$  decay constant ( $\lambda_{^{14}\text{C}} = \ln 2/5730$ ), and  $a^{14}\text{C}$  is the measured  $^{14}\text{C}$  activity of the DIC in groundwater. As mentioned above, the estimated ages are really apparent ages due to the mixture of waters with wide range of ages (Custodio et al., 2018; Suckow, 2014).

Previous studies in the arid northwest China (Edmunds et al., 2006; Huang et al., 2017) have concluded that a volumetric value of 20 % “dead” carbon derived from the aquifer matrix was recognized, which is consistent with the value (10–25 %) obtained by Vogel (1970). Therefore, the initial  $^{14}\text{C}$  activity ( $a_0^{14}\text{C}$ ) of 80 pMC is used to correct groundwater  $^{14}\text{C}$  ages (results are shown in Table 1), despite this simple correction makes no attempt to correct the age of individual samples that may have experienced different water–rock interaction histories.”

38) L264: Check the discussion paper by Benettin et al. in review in HESS for the latest developments on the “evaporation slope”.

Response: Agree and changes made. We agree with the opinion on the evaporation slope that a steeper slope would be obtained due to the large source variability under different meteorological conditions in different seasons indicated by Benettin et al. (2018). As we know that water fractionation is affected by various factors, like the water surface temperature, air humidity, wind speed, and so on, but we can always obtain a linear trend from a source water with low salinity (Ma et al., 2015). However, in practice, the evaporation trend line is often obtained from various sources water, which is often not true evaporation line. In our manuscript, the evaporation line is estimated according to the surface water (ditch water, reservoir water, and Manas River water), which are all collected in summer of 2015. The ditch, reservoir and Manas River are always connected to one another (Fig. 1b), and all are recharged from the mountain areas in the same season. Though there are minor differences of the water sources for the surface water, the linear trend obtained based on these surface water may have implications for the surface water evaporation.

Therefore, we use the evaporation slope and to add some statements (as follows) for the rationality in the revised manuscript (RL282–286):

“A recent study (Benettin et al., 2018) indicated that the evaporation line obtained from various sources of water is often not the true evaporation line. All samples of surface water in the present study were collected in the summer of 2015 and were recharged from the mountain areas in the same season. Although they were collected from different areas (ditch water, reservoir water, and Manas River water), the linear trend obtained may have implications for surface water evaporation.”

39) L274: The entire paragraph is too short and should explain clearly the approach adopted to calculate “ages” from the tracer data (model and model parameter choices !). I strongly advise against using binary mixing diagrams, and encourage the authors to use a multi-tracer modelling approach trying to find a single optimum or optimal parameter regions for the different tracers.

Response: Changes made. The entire paragraph was deleted. We reorganized the structure of the Section “4. Results and discussion”, rewrote some contents and deleted some incorrect expressions, and added statements concerning the model choice in Section “3. Materials and methods”. However, we tend to retain the binary mixing diagrams (the mean residence times with different models have been deleted in the diagrams) to explain the young and old groundwater mixing features and to identify the impact of human activity on the groundwater.

40) L277: The paragraph on “apparent age” makes no sense for the reasons given above. I disagree with the proposition that “they [apparent ages] provide a good first approximation for groundwater age”. There is no reason to prefer the piston-flow model which is implied by the “apparent age” concept over other models. This argument has been for years a lazy way to skip responsibility in choosing one model based on knowledge of the hydrogeological situation and sampling.

Response: Agree and changes made. The “apparent CFC ages” has been deleted. In addition, we tend to discuss the modern precipitation recharge features and to distinguish the modern and paleo-meteoric recharge using CFCs in Section 4.2.2 (RL340–406):

“Table 1 shows that groundwater with well depths of 13–150 m contained detectable CFC concentrations (0.17–3.77 pmol L<sup>-1</sup> for CFC–11, 0.19–2.18 pmol L<sup>-1</sup> for CFC–12, and 0.02–0.38 pmol L<sup>-1</sup> for CFC–113) in both the upstream and midstream areas, indicating at least a small fraction of young groundwater components (post–1940). The highest concentration was observed in the UG (G3), south of the fault. The median and the lowest were observed in the west and east banks, respectively, of the East Main Canal in the MG, north of the fault. In the midstream area (Fig. 2), CFC concentrations generally decreased with well depth south of the reservoirs (G25, G8, and G9), and increased with well depth north of the reservoirs (G15 and G16), which might indicate different groundwater flow paths (e.g., downward or upward flow directions).

The groundwater aerobic environment (Table 1, DO values vary from 0.7 to 9.8 mg L<sup>-1</sup>) makes CFC degradation under anoxic conditions unlikely. Nevertheless, CFC–11 has shown a greater propensity for degradation and contamination than CFC–12 (Plummer et al., 2006b). Therefore, we use CFC–12 to interpret the modern groundwater recharge in the following discussions. The estimated CFC partial pressure and possible recharge year are shown in Table 2 and Fig. 3. The UG (G3) CFC–113 and CFC–12 both indicate the 1990 precipitation recharge (Table 2), probably a piston flow recharge in the upstream area. The MG CFC–11–based modern precipitation recharge was in agreement with that based on CFC–12 concentrations within 2–8 yrs, whereas the CFC–113–based recharge was as much as 4–11 yrs later than that the other two, signifying recharge of a mixture of young and old groundwater components in the midstream area. The most recent groundwater recharge was in the upstream area

(G3 with 1990 rainfall recharge), which was most likely because the flow paths from recharge sources here were shorter than those of the piedmont groundwater samples in the midstream area.

G5 and G7 were located in the east bank of the East Main Canal in the midstream area and were closer than G15 and G16 north of the reservoir, showing that the modern recharge was much earlier than that of G15 and G16 (Table 2). This could be explained by the lower groundwater velocities in the east bank of the East Main Canal, where the hydraulic gradient (Fig. 2) was much smaller than that in the west. Furthermore, groundwater recharge became earlier with increasing well depth from 48 to 100 m south of the reservoir (G25, G8 and G9), whereas that north of the reservoir became later with increasing well depth from 23 to 56 m (G15 and G16; Table 2, Fig. 2). The different trends for the relationship between groundwater recharge year and well depth might be due to the different flow paths between the two sites (e.g., reservoir south and north).

Comparing CFC concentrations helps to indicate samples containing young (post-1940) and old (CFC-free) water (Han et al., 2007; Han et al., 2012; Koh et al., 2012) or exhibiting contamination or degradation (Plummer et al., 2006b). The cross-plot of the concentrations for CFC-113 and CFC-12 (Fig. 7a) demonstrates that all of the groundwater can be characterised as binary mixtures between young and older components, though there is still room for some ambiguity around the crossover in the late 1980s (Darling et al., 2012). As shown in Fig. 7a, all of the MG samples are located in the shaded region, representing no post-1989 water recharge. The UG (G3) sample is clearly relatively modern and seems to have been recharged in 1990 through piston flow or mixed with old water and post-1995 water. Using the method described by Plummer et al. (2006b) with the binary mixing model, the fractions of young water were found to vary from 12 to 91 % (Table 2) for the MG samples with the relatively low young fractions of 12 and 18 % in the MG samples (G5 and G7) from east bank of the East Main Canal. These two well water table were deeper than 40 m, probably indicating a relatively slow and deep circulated groundwater flow. This hypothesis is also suggested by the lower DO (3.7–4.6 mg L<sup>-1</sup>; Table 1) and nitrate concentrations (8.6–9.5 mg L<sup>-1</sup> from Ma et al., 2018) and considerably smaller hydraulic gradient (Fig. 2). Furthermore, a fraction of young water as high as 100 % was obtained for G3 sample with the recharge water from 1990, and a 87 % fraction was obtained by from the binary mixture of post-1989 water and old water (Table 2). The relatively modern recharge for the G3 sample was likewise explained by its high DO (9.8 mg L<sup>-1</sup>; Table 1) and relatively low nitrate concentration (7.9 mg L<sup>-1</sup> from Ma et al., 2018), which represented the contribution of high-altitude recharge rather than the old water.

CFC contamination and sorption in the unsaturated zone during recharge considerably influenced the interpretation of groundwater recharge. Points off the curves in the cross-plot of CFC concentrations may indicate contamination from the urban air with CFCs during sampling (Carlson et al., 2011; Cook et al., 2006; Mahlkecht et al., 2017) or the degradation or sorption of CFC-11 or CFC-113 (Plummer et al., 2006b). Figure 7 demonstrates that the urban air with CFC contaminations, which generally increased CFC concentrations above the global background atmospheric CFC concentrations for the Northern Hemisphere, are unlikely. Elevated CFC concentrations have been reported in the air of urban environments such as Las Vegas, Tucson, Vienna and Beijing (Barletta et al., 2006; Carlson et al., 2011; Han et al., 2007; Qin et al., 2007) rather than in the arid regions of Northwest China (Barletta et al., 2006). Hence, the anomalous ratios of CFC-11/CFC-12 (Fig. 7b) off the model lines might be attributed to sorption in the unsaturated zone during recharge rather than the degradation of CFC-11 (Cook et al., 2006; Plummer et al., 2006b) under anoxic conditions (Table 1, DO values vary from 0.7 to 9.8 mg L<sup>-1</sup>). Nevertheless, the small deviations (Fig. 7b) indicate a low sorption rate. A

higher CFC sorption rate occurs with high clay fraction and high organic matter in soils (Russell and Thompson, 1983), and vice versa (Carlson et al., 2011). Therefore, the hypothesis of a low sorption rate due to the low clay fraction and low organic matter content in the intermountain depression and the piedmont plain (Fig. 1c) seems reasonable.

The time lag for CFC transport through the thick unsaturated zone (Cook and Solomon, 1995), as well as degradation, especially for CFC-11 being common in anaerobic groundwater (Horneman et al., 2008; Plummer et al., 2006b), are both important considerations when interpreting groundwater recharge using CFC concentrations. The time lag for CFC diffusions through the deep unsaturated zone in simple porous aquifers, a function of the tracer solubility in water, tracer diffusion coefficients, and soil water content (Cook and Solomon, 1995), have been widely proved (Darling et al., 2012; Qin et al., 2011). The small differences in CFC-11 and CFC-12 recharge years (Table 2) demonstrate that the time lag should be short in the faulted-hydraulic drop alluvium aquifers with the deep unsaturated zone (Fig. 1c). Studies on the MRB (Ma et al., 2018; Wang, 2007; Zhou, 1992) have shown that groundwater mainly recharged by the river fast leakage in the upstream area and piedmont plain, where the soil texture consists of pebbles and sandy gravel (Fig. 1c); this suggests that the unsaturated zone air CFC closely follows that of the atmosphere, so the recharge time lag through the unsaturated zone is not considered."

41) L297: "which confirms". A performative statement confirms nothing. You are supposing this is the case !

Response: Agree and changes made. We have revised this sentence (RL402-406): "Studies on the MRB (Ma et al., 2018; Wang, 2007; Zhou, 1992) have shown that groundwater mainly recharged by the river fast leakage in the upstream area and piedmont plain, where the soil texture consists of pebbles and sandy gravel (Fig. 1c); this suggests that the unsaturated zone air CFC closely follows that of the atmosphere, so the recharge time lag through the unsaturated zone is not considered."

42) L317: Shortly explain the method used to estimate the tritium input (linear regression ? And how long were the time series used ?). The reference to Han et al. is not very useful as the authors of that paper themselves refer to an IAEA publication without further explanations.

Response: Agree and changes made. The explanation is seen in "Response 7". We added short statements in the revised manuscript as follows (RL234-237):

"The historical precipitation  $^3\text{H}$  activity in Urumqi station (Fig. 4) is reconstructed with the data available from the International Atomic Energy Agency (IAEA) using a logarithmic interpolation method. Precipitation  $^3\text{H}$  activity between 1969 and 1983 at Hong Kong and Irkutsk with different latitudes are used (data is available at <<https://www.iaea.org/>>)."

We think that the reconstructed tritium ( $^3\text{H}$ ) activity in Urumqi station can be added as the supplement if necessary.

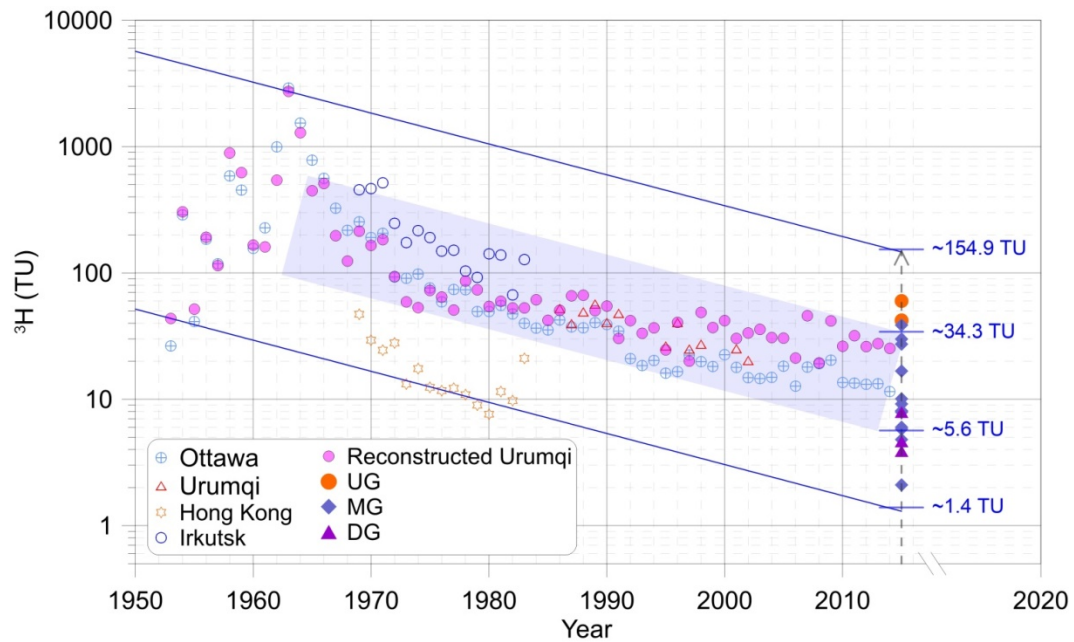


Figure 6. Tritium concentration (TU) of groundwater water samples of upstream groundwater (UG), midstream groundwater (MG), and downstream groundwater (DG). Time series of tritium concentration in precipitation at Ottawa, Urumqi, Hong Kong, and Irkutsk were obtained by GNIP in IAEA (<https://www.iaea.org/>). The blue solid lines and shaded field were drawn using the half-life (12.32 yrs) of tritium decayed to 2014. (It is Fig. 4 in the revised manuscript)

43) L318: A background of 31 TU is very high compared to Western Europe (about 6 TU). How come ?

Response: As shown in Fig. 4 and reconstructed tritium  $^3\text{H}$  activity in Urumqi, the estimated modern precipitation  $^3\text{H}$  activity are indeed extremely high (mean value of 31.55 TU between 2000 and 2015). We speculate that the very high precipitation  $^3\text{H}$  activity may be ascribed to both the Chinese atmospheric nuclear tests (around 350 km away to Manas River Basin) from 1964 to 1974 (Zhou, 1992) and the continental effect (Tadros et al., 2014), where the Manas River Basin is more than 3500 km away from the western pacific.

44) L413: What do you mean by “serious” ?

45) L414: “tend toward more discrete with their increase”. I do not understand this part of the sentence.

Response: Changes made. The spelling error “serious” was changed to “series”. The sentence was changed to (RL468–469): “Figure 11 shows that different LPMs yield different MRTs for the same time series of  $^3\text{H}$  and CFC concentrations. MRTs obtained from different LPMs tend to become more discretized by model with increasing MRTs.”

46) L448: The paragraph on hydrochemistry is not bad, but underdeveloped and bad organized. State again what you’re looking for first. A good correlation between hydrochemistry and “ages” calculated using some of the TTD models might be a way to constrain or guide model choice, but the authors do not really state that explicitly, although that would be interesting and relatively new.

Response: Yes, we agree with your opinion on the relationship between hydrochemistry and “ages”

calculated using the TTD models. Thanks very much, the suggestion of using hydrochemistry to guide model choice is definitely interesting and relatively new. We will bear in mind in the future studies in the Manas River Basin. In the present study, we tend to seek the correlations between groundwater MRTs and hydrochemical concentrations firstly.

47) L491: The entire chapter 4.5.1 makes no sense. You must first decide which model is the most appropriate, and then calculate metrics such as mean transit time, young water fraction, etc... You cannot both calculate water fractions using a binary mixing strategy (assuming piston-flow) AND later use an EPM. The same remark applied to chapter 4.5.2.

Response: We agree with your opinions that “first decide which model is the most appropriate, and then calculate metrics such as mean transit time, young water fraction, etc...”. We think that the application of mixing models (even combining two lumped-parameter models) is a good method to quantitatively analysis groundwater mixing ratios, and this method is also used more and more widespread. However, CFCs are also good tracers to distinguish groundwater mixing from the different recharge sources, like to recognize modern and paleo-meteoric recharge features, to distinguish the fraction of young groundwater. We have totally revised the entire chapter 4.5.1 and reorganized the structure of the manuscript (See “Response 3”). The erroneous phrases and expressions including apparent CFC age and groundwater ages estimated from the piston flow model have been deleted.

48) L498: “no post-1988.5”. Please round this off...

Response: Agree and changes made (RL370–371). “no post–1988.5” was changed to “no post–1989”. “1989.5” was changed to “1990”.

49) L509: Why do you treat “apparent age” as some kind of different measure of transit time than MTTs “estimated from the EPM” ? This is doing the analysis the wrong way around. First find a way to select a model, then discuss the obtained “ages” instead of hypothesizing on tons and tons of different “ages” that are meaningless because they were obtained disregarding the actual situation. This leads nowhere.

Response: Agree and changes made. The erroneous sentence and term “apparent CFC ages” been deleted. We reorganized the structure and revised the relative content to tried to present a clear roadmap to readers.

50) L541: Before engaging in complicated mixing scenarios, you should first try to find one model and one parameterisation that fits both the CFCs, tritium and carbon 14. Only if that search does not succeed should additional mixing be introduced. Please note that the binary mixture approach by Plummer et al. is only one way of doing so, and a particularly weak one at that because it assumes per default a piston-flow distribution of transit time of each component (other models can be integrated, but it becomes quickly very cumbersome). Another way to include the mixing of different reservoirs is to combine models (say two exponential models, each representing one distinct source) following Piotr Maloszewski and coworkers or Mike Stewart and Uwe Morgenstern. Binary plots such as those of figure 11 suffer from the limitation that you have to recalculate the mixing line for each parameterisation of each model, and they cannot really replace a multi-tracer lumped-parameter modelling approach, where the objective function reduces simultaneously the prediction error of all tracers.

Response: Thanks very much for the precious suggestions you offered. We believe that the modelling

approaches are commendable to interpret complicated mixing scenarios quantitatively. For example, the binary parallel lumped-parameter model (Morgenstern et al., 2015; Stewart et al., 2017), the binary mixing model that followed by two response function models (Jurgens et al., 2012), and the mathematical solutions that indicating the changes in water reserve in the relatively large systems with wide range of residence times (Custodio et al., 2018; Custodio and Custodio-Ayala, 2014). In addition, tracer-tracer binary plots are also widely used methods to determine the groundwater recharge mechanisms and to interpret the groundwater mixing (Cook et al., 2017; Darling et al., 2012; Han et al., 2015; Kagabu et al., 2017). We think that combining  $^3\text{H}$  and CFCs is a good tool to distinguish the modern precipitation recharge and to indicate the groundwater mixing properties (for example mixing old with young water, mixing irrigation infiltration water and young water) in the Manas River Basin, which has not been reported before. Recharge features (e.g. modern and paleo-meteoric recharge features, and the fractions of modern recharge water) are also the essential contents in the manuscript, which will not be all on account of the mean residence times estimated by  $^3\text{H}$  and CFCs in the revised manuscript. Further investigation work will be carried out in the Manas River Basin in the following several years (for example, time serious groundwater CFCs from some given wells will be measured). Deeper analysis concerning groundwater mixing obtained by the combination of two models using lumped-parameter models (binary mixing model) and to explore the changes in water reserve will be good choices in the next studies in the Manas River Basin.

51) L562: Solutions are obtained, explanations are devised.

Response: Thanks, no change made.

52) L572: What are mixing rates ? You mean mixing ratios ?

Response: Agree and changes made (RL544). "rates" was changed to "ratios"

53) L575: "The thrust faults were found to play a paramount role on groundwater flow path". There are not conclusions, but hypotheses very weakly suggested by the analysis of the environmental tracers, which is itself very shaky. I hardly call that evidence. Please refrain from drawing conclusions if the data necessary to test hypotheses is not available (as is the case here).

Response: Agree and changes made. This sentence has been deleted. To make the conclusions to be more clear and well-founded, we have revised the conclusions and delete some incorrect statements. Yes, this conclusion is important but not supported by strong supporting evidences in the paper. Indeed, there are some results that show large differences on both sides of the thrust fault. For example, there is a level difference of 130 m hydraulic drop (Fig. 1c) in the south margin in Shihezi (SHZ),  $^3\text{H}$  activities of groundwater decrease rapidly along the Manas River motion in the north of the fault but show relatively the highest values in the south of the fault (Fig. 8). These results still cannot support the conclusion explicitly "The thrust fault were found to play a paramount role on groundwater flow paths ...".

The revised conclusions are as follows (RL543-555):

"In this study, we used environmental tracers and hydrochemistry to identify the modern and paleo-meteoric recharge sources, to constrain the different end-members mixing rates, and study the mixed groundwater MRTs in faulted-hydraulic drop alluvium aquifer systems. The paleo-meteoric recharge in a cooler climate was distinguished from the lateral flow from the higher elevation precipitation in the



Manas River downstream area. The relatively modern groundwater with young (post-1940) water fractions of 87–100 % was obtained, indicating a small extent of mixing south of the fault. The short MRTs (19 yrs) along with the higher-than-natural  $\text{NO}_3^-$  concentration ( $7.86 \text{ mg L}^{-1}$ ) south of the fault (headwater area) indicated the invasion of modern contaminants. This finding warrants particular attention. High mixing rate amplitudes varying from 12 to 91 % were widespread in north of the fault due to the varying depths of long-screened boreholes as well as within the aquifer itself. Furthermore, the mixing diversity was highlighted by the substantial water table fluctuations during groundwater pumping, vertical recharge through the thick unsaturated zone, and young water mixtures in different decades. The strong correlations between groundwater MRTs and hydrochemical concentrations enable a first-order proxy at different times to be used. In addition, this study has revealed that MRTs estimated by CFCs were more appropriate than those using  $^3\text{H}$  in the arid MRB with a thick unsaturated zone.”

54) L585: “due to the highly complex groundwater system...”. This is no explanation at all ! Indeed, devising a conceptual model that could explain why CFC derived “ages” correlate well with mineralisation while tritium derived “ages” do not could be a useful task (but you should first redo the calculation of the “ages” as suggested above). On the one hand, the correlation between CFC12 and hydrochemistry might be an artifact, given that the area sampled is so large and hydrogeologically diverse. On the other hand, there might be some kind of systematic shift between tritium and CFC ages if differences are due to the unsaturated zone. Maybe a diffusion model using the unsaturated zone thickness might be useful. Still much work to do...

Response: The sentence has been deleted. Thanks very much for the useful suggestions. Previous studies (Ji, 2016; Wang, 2007; Zhou, 1992) have shown that the groundwater flow paths were very complicated from the mountain to the plain areas. Precipitation recharge in the ground in the mountain areas, one part groundwater discharge into spring in the south of the intermountain depression, one part groundwater discharge into stream in the mountain areas and then recharge groundwater in the intermountain depression, and one part groundwater flow in the ground through the intermountain depression. The complicated groundwater flow systems make devising a conceptual model very difficult to implement. We think that more and much detailed work should be conducted from the mountain to intermountain depression areas to find out more evidences that interpretation the conceptual flow model. In addition, the thick unsaturated zone mainly distribute in the intermountain depression and piedmont plain areas (Fig. 1c). The interpretation of CFCs in Section 4.2.2 make us to assume that the unsaturated zone air CFC closely follows that of the atmosphere and thus the recharge time lag through the unsaturated zone is not consideration. In some cases the unsaturated zone can be ignored to obtain workable solutions (Custodio et al., 2018) though the unsaturated zone is not so thick with the Manas River Basin. We think that a diffusion model using the unsaturated zone thickness is a good guide for the further studies in the arid Manas River Basin as well as in other arid basins around the world.

55) Figure 7, 8 and 9: The figures are incredibly cluttered and very difficult to read, especially figure 9 (not to mention the legend).

Response: Agree and changes made. Figures 7, 8 and 9 were redrawn as follows:

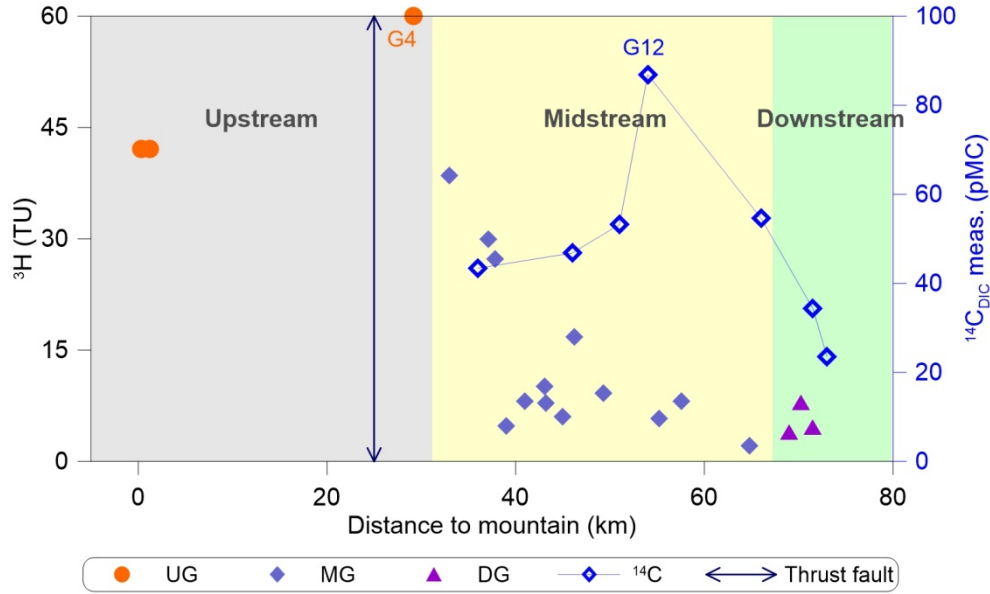


**Figure 7.** Distributions of  $^3\text{H}$  and  $^{14}\text{C}$  activities with distance to mountain. The shaded regions indicate the upstream, midstream and downstream of Manas River. (It is Fig. 8 in the revised manuscript)

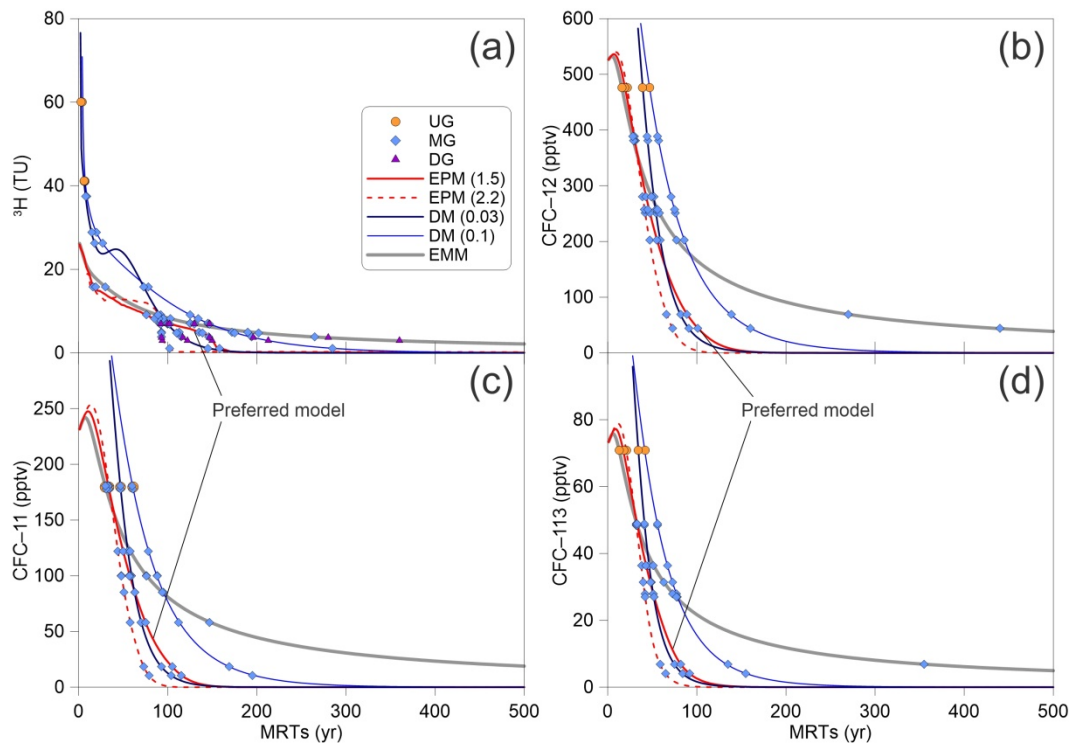


**Figure 8.** Tritium and CFCs (CFC-11, CFC-12 and CFC-113) output vs. mean residence times for different lumped-parameter models estimated using Eqs. (2) to (5). The input  $^3\text{H}$  activity and CFCs concentration are using the estimated  $^3\text{H}$  activities in precipitation in Urumqi station (Fig. 4) and the Northern Hemisphere atmospheric mixing ratio (Fig. 3), respectively. (It is Fig. 10 in the revised manuscript)

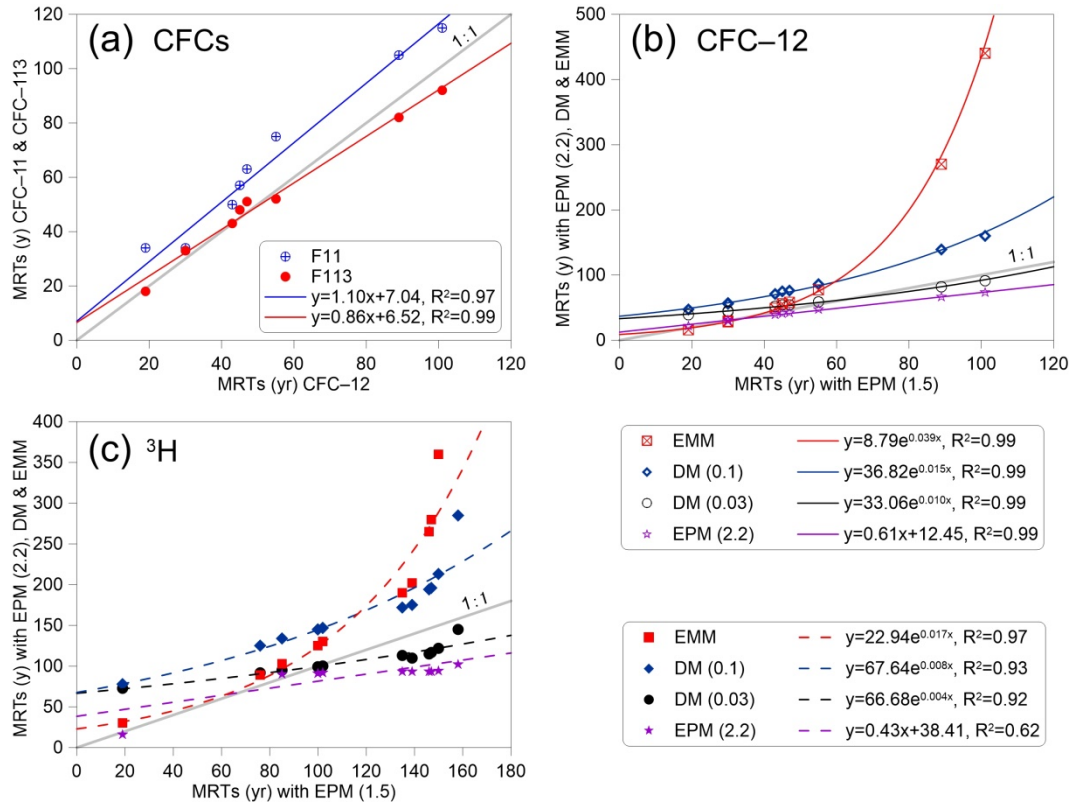


**Figure 9.** (a) MRTs with EPM (1.5) of CFC-12 vs. CFC-11 & CFC-113, (b) CFC-12 MRTs with EPM (1.5) vs. EPM (2.2), DM & EMM, and (c) 3H MRTs with EPM (1.5) vs. EPM (2.2), DM & EMM. (It is Fig. 11 in the revised manuscript)

56) Figure 10: Why are there so few points on each graph, since you sampled at 29 locations according to table 1 ?

Response: Figure 10 shows that the x-axis represents the CFC-12 mean residence times with EPM (1.5), and Table 1 shows that there are 9 groundwater CFC-12 samples. For the sample G15, the hydrochemistry show abnormal data with much higher concentrations of  $SO_4^{2-}$ ,  $HCO_3^-$ , and electrical conductivity than that of perimeter zone. Moreover, in the plot of CFC-12 mean residence times vs. hydrochemistry, G15 sample distributes abnormal. Therefore, only 8 groundwater samples are potted in Fig. 10 (It is Fig. 12 in the revised manuscript).

57) Figure 11: As I wrote above, binary mixing diagrams rapidly tend to show their limits. After two or three mixing lines for different models are drawn, reading becomes nigh impossible. Importantly, error bars are missing for the CFCs and for tritium. I suspect that with error bars, selecting a model visually will become impossible (the lack of sensitivity is another limitation of binary mixing diagrams, ).

Response: Agree and changes made. We deleted the mean residence times with different models but retain the measured CFC concentrations and <sup>3</sup>H activities of groundwater in the diagrams.

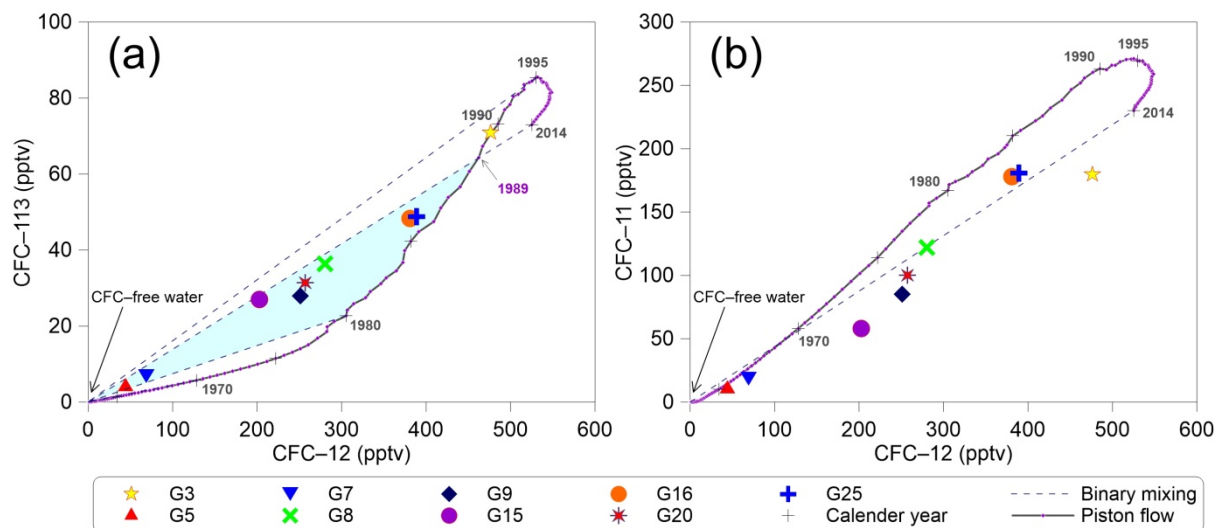


**Figure 11.** Plots showing relationships of (a) CFC-113 vs. CFC-12 and (b) CFC-11 vs. CFC-12 in pptv for the Northern Hemisphere air. The '+' denotes selected calendar years. The solid lines correspond to the piston flow (PF) and the short-dashed lines show the binary mixing (BM). The shaded regions in (a) indicate no post-1989 waters mixing. (It is Fig. 7 in the revised manuscript)

# Groundwater mean transit times, mixing and recharge in faulted-hydraulic drop alluvium aquifers using chlorofluorocarbons (CFCs) and tritium isotope ( $^3\text{H}$ ) Application of environmental tracers for investigation of groundwater mean residence time and aquifer recharge in faulted-hydraulic drop alluvium aquifers

Bin Ma<sup>1,2</sup>, Menggui Jin<sup>1,2,3</sup>, Xing Liang<sup>1,4</sup>, and Jing Li<sup>1</sup>

<sup>1</sup>School of Environmental Studies, China University of Geosciences, Wuhan, 430074, China

<sup>2</sup>State Key Laboratory of Biogeology and Environmental Geology, China University of Geosciences, Wuhan, 430074, China

<sup>3</sup>Laboratory of Basin Hydrology and Wetland Eco-restoration, China University of Geosciences, Wuhan, 430074, China

<sup>4</sup>Hubei Key Laboratory of Wetland Evolution & Ecological Restoration, China University of Geosciences, Wuhan, 430074, China

Correspondence to: Menggui Jin (mgjin@cug.edu.cn)

**Abstract.** Documenting ~~the groundwater transit residence~~ times and ~~the~~ recharge sources ~~of mixed groundwater~~ is crucial for water resource management in the alluvium aquifers of arid basins. Environmental tracers (CFCs,  $^3\text{H}$ ,  $^{14}\text{C}$ ,  $\delta^2\text{H}$ ,  $\delta^{18}\text{O}$ ) and ~~hydrochemistry of mixed groundwater~~ hydrochemical components were used ~~to assist our for understanding of assessing~~ groundwater mean ~~transit residence~~ times (~~MTTsMRTs~~), ~~mixing~~ and aquifer recharge in faulted-hydraulic drop alluvium aquifers in the Manas River Basin (China). ~~The very high  $^3\text{H}$  activities activity (41.1–60 TU) of in the groundwater decrease with distance to the mountain from 41.1–60 TU in the Manas River upstream (south of the fault) indicates, indicating the~~ rainfall recharge during the nuclear bomb tests (since the 1960s), ~~to as low as 1.1 TU in the downstream (north of the fault).~~ Carbon-14 groundwater ages increases with distance (3000–5000 yrs in the midstream to > 7000 yrs in the downstream) and depth, as well as with decreasing  $^3\text{H}$  activity (1.1 TU) and more depleted  $\delta^{18}\text{O}$  values, confirming that the deeper groundwater is derived from paleometeoric recharge in the semi-confined groundwater system. ~~MTTsMRTs~~ estimated using an exponential-piston flow model vary from 19 to 101 yrs for CFCs and from 19 to 158 yrs for  $^3\text{H}$ ; ~~which show much longer MTTs MRTs for  $^3\text{H}$  are much longer than those for CFCs may be probably~~ due to the time lag (liquid vs. gas phase) through the thick unsaturated zone. ~~The thrust faults were found to play a paramount role on groundwater flow paths and MTTs due to their block water features, where the relatively long MTTs were found near the Manas City with shorter distance and smaller hydraulic gradients.~~ The remarkable correlations between CFCs rather than  $^3\text{H}$  ~~MTTsMRTs~~ and pH,  $\text{SiO}_2$ , and  $\text{SO}_4^{2-}$  concentrations allow estimating first-order proxies of ~~MTTsMRTs~~ for groundwater at different times ~~to be made. The quite~~ Relatively modern–modern recharge is found in the south of the fault with young (post-1940) water fractions of 87–100 % ~~is obtained, while whereas~~ in the north of the fault in the midstream area the young, water fractions

vary from 12 to 91 % based on the CFC binary mixing ~~model~~method. This study shows that the combination of CFCs and  $^3\text{H}$  ~~transit~~residence time tracers ~~have potential to study~~can help analyse groundwater ~~MTTs~~MRTs and identify the recharge sources for the different mixing end-members.

## 35 **1 Introduction: ~~mean transit times~~**

Groundwater ~~supplies is~~ the world's largest freshwater resource, ~~supplies freshwater~~ to billions of people, and plays a central ~~part~~role in energy and food security, human health, and ecosystems (Gleeson et al., 2016). Documenting the ~~transit~~residence times of groundwater (~~i.e. time~~ from recharge to drainage in pumping wells, springs, or streams) reveals information about water storage, mixing, and transport in subsurface water systems (Cartwright et al., 2017; Dreuzy and Ginn, 2016; McGuire and McDonnell, 2006). ~~It~~This is particularly crucial in ~~the~~-alluvium aquifers where ~~the~~-fresh groundwater ~~may be renewable and potable resources rather than saline groundwater~~renewability is generally strong (Han et al., 2011; Huang et al., 2017), ~~thus functioning as potable water resources in the arid areas;~~ also, alluvium aquifers are ~~as well as~~more vulnerable to anthropogenic contaminants and land-use changes (Morgenstern and Daughney, 2012).

~~Mean transit times (MTTs) that determined from the transit time distributions (TTDs) cannot be measured directly in the field and may be inferred from transit time tracer concentrations by using the lumped parameter models (LPMs; Małozewski and Zuber, 1982; Jurgens et al., 2012), which has commonly assumed that the hydrologic system is in a steady state. Three types of transit time tracers have been widely referred to in the previous literatures. Because the residence time distribution in subsurface water systems cannot be empirically measured, a commonly used approach is parametric fitting of trial distributions to chemical concentrations (Leray et al., 2016; Suckow, 2014). The widely used lumped-parameter models (LPMs; Małozewski and Zuber, 1982; Jurgens et al., 2012), which commonly assume that the hydrologic system is at a steady-state, have been applied to subsurface water systems containing young water with modern tracers of variable input concentrations (e.g. seasonably variable stable isotope  $^2\text{H}$  and  $^{18}\text{O}$ , tritium, and  $^{85}\text{Kr}$ ; Cartwright et al., 2018; McGuire et al., 2005; Morgenstern et al., 2015; Stewart et al., 2010). The groundwater residence time tracers can be classified into three types depending on their time span. First, ~~as the water molecules, the~~-isotopes of water ( $^{18}\text{O}$ ,  $^2\text{H}$ ,  $^3\text{H}$ ) ~~make them~~are ideal tracers for determining ~~the~~-MTTs ~~mean residence times (MRTs)~~ shorter than ~~~~~approximately 5 yrs with stable isotopes (Kirchner et al., 2010; McGuire et al., 2005; Stewart et al., 2010) and up to ~~~~~approximately 100 yrs with  $^3\text{H}$  (Beyer et al., 2016; Cartwright and Morgenstern, 2015, 2016; Morgenstern et al., 2010). Second, ~~radioactive~~ solute tracers ~~like the radioisotopes of such as~~  $^{14}\text{C}$ ,  $^{36}\text{Cl}$ , and noble gases ( $^4\text{He}$ ,  $^{85}\text{Kr}$ ,  $^{39}\text{Ar}$ , and  $^{81}\text{Kr}$ ), as well as the ~~atmosphere~~-atmospheric concentrations of synthetic organic compounds (chlorofluorocarbons, CFC-11, CFC-12, and CFC-113; and sulfur hexafluoride,  $\text{SF}_6$ ), ~~permit their~~are used in determining groundwater ~~MTTs~~MRTs with a much wider ~~variabilities~~-time span (decades to hundred millenniums) due to the radioisotopes long-span half-lives (Aggarwal, 2013). Third, ~~concentrations of~~ major ions ~~concentrations like such as the~~-inert chloride (Cl) ions determine ~~the~~-MTTs/MRTs in a similar ~~function with way to~~ the stable isotopes depending on ~~the~~ damping of seasonal variation input cycles ~~on passing that pass~~ through a system into the~~

65 output. ~~MTTs~~MRTs determined ~~from~~through the seasonal tracer cycle method (e.g., stable isotope values or Cl concentrations), which, requires detailed ~~such as weekly or sub-weekly~~ time series measurements, ~~such as weekly or more frequent~~, may be more appropriate for water drainage through catchment and discharging into stream (Hrachowitz et al., 2009; Kirchner et al., 2010; McGuire et al., 2005) ~~over~~than for a groundwater system. Nevertheless, a strong correlation of major ion concentrations with groundwater age ~~permitting~~enables hydrochemistry to be used as proxy for or complementary ~~for~~to age via previously established relationships in closed lithological conditions (Beyer et al., 2016; Morgenstern et al., 2010, 2015).

70 ~~The only true age for water is Tritium ( $^3\text{H}$ ), a component of the water molecule with a half-life of 12.32 yrs, is the only true age tracer for waters~~ (Tadros et al., 2014). The Northern Hemispheric  $^3\text{H}$  ~~activities~~activity were ~~is~~ several orders of magnitude higher than that in the Southern Hemisphere (Clark and Fritz, 1997; Tadros et al., 2014) due to the atmospheric thermonuclear tests in the Northern Hemisphere ~~between~~the 1950s and 1960s, which ~~also~~ resulted in mean annual  $^3\text{H}$  ~~activities~~activity peaks reaching several hundred times the natural levels in the Northern Hemisphere. ~~As a result,~~ ~~the~~ ~~nowadays~~present-day rainfall  $^3\text{H}$  ~~activities~~activity in the Northern Hemisphere ~~is~~ still affected by the tail-end of the bomb-pulse, ~~in the Northern Hemisphere, which are~~and it is particularly high in the arid regions of northwest Northwest China due to both the continental effect (Tadros et al., 2014) and ~~superimposed over~~ the China atmospheric nuclear tests from 1964 to 1974. ~~Only about 5 % of the bomb test  $^3\text{H}$  activities mixed via the stratospheric circulation into the Southern Hemisphere (Morgenstern et al., 2010), and the  $^3\text{H}$  activities of remnant bomb pulse waters have now decayed below those of modern rainfall. Accordingly, recent studies in estimating MTTs by  $^3\text{H}$  in the Southern Hemisphere (e.g., Australia, Cartwright et al., 2018; Cartwright and Morgenstern, 2015, 2016; and New Zealand, Morgenstern et al., 2010, 2015; Morgenstern and Daughney, 2012) have used single  $^3\text{H}$  rainfall measurements as the input data. Thus, measurement of a single sample of  $^3\text{H}$  activity does not accurately assess the groundwater MRTs in the Northern Hemisphere (Cook et al., 2017), and ~~time-series  $^3\text{H}$  measurements may be used to estimate MTTs in the Northern Hemisphere by~~with LPMs are required (Han et al., 2007; Han et al., 2015).~~

80 ~~Contrasting~~In contrast to  $^3\text{H}$ , CFCs ~~degrade slowly in the atmosphere and~~ have relatively long ~~transit times in the atmosphere of between 44 yrs (CFC 11) and 180 yrs (CFC 12)~~degradation half-lives, which permits their uniform atmospheric distributions over large areas, ~~but~~. However, there is 1–2 yrs lag ~~time~~ for the Southern Hemisphere ~~than~~ compared with the Northern Hemisphere (Cartwright et al., 2017; Cook et al., 2017; Darling et al., 2012). The build-up of CFCs in the atmosphere ~~of CFCs~~ after the 1950s ~~combining~~coupled with their solubility (despite low solubility) in water ~~have~~enables them to be commonly ~~permitted~~them used as indicators of ~~transit times in~~ groundwater MRTs up to ~~approximately~~ 60 yrs (Darling et al., 2012; Han et al., 2012). ~~Though~~Although the atmospheric concentrations of CFC-11, CFC-12, and CFC-113 have declined between 1994 and 2002 (different CFCs peaked at different times; Cook et al., 2017) ~~and thus thereby leaving there are~~ rooms for ~~some~~ ambiguity in the CFC ratios plots (Darling et al., 2012); the different atmospheric CFCs ratios between ~~nowadays~~today and ~~before~~the pre-1990s (Plummer et al., 2006b) ~~make~~determining enable determination of groundwater ~~MTTs~~MRTs ~~by using~~ CFCs ~~possible~~.

viewed as alternatives to  $^3\text{H}$  for calculating ~~transit times in~~ groundwater ~~MRTs as with~~ the ~~decline in the~~ bomb-pulse  $^3\text{H}$  ~~activities-activity declined~~ (Cartwright et al., 2017; Cook et al., 2017; Qin et al., 2011). ~~However, the CFCs input would be limiting for estimating groundwater MTTs when they are entrapped excess air in the unsaturated zone during recharge (under estimation MTTs; Cook et al., 2006; Darling et al., 2012), contaminated in urban and industrial environments (under estimation MTTs; Carlson et al., 2011; Han et al., 2007; Mahlknecht et al., 2017; Qin et al., 2007), or degraded in anaerobic groundwater (over estimation MTTs; most notably CFC-11 and CFC-113; Cook and Solomon, 1995; Horneman et al., 2008; Plummer et al., 2006b) in the confined aquifers.~~ ~~However, groundwater MRTs may not be always be accurate when calculated using CFCs: for example, MRTs are much lower than the actual values if CFC inputs are entrapped excess air in the unsaturated zone during recharge (Cook et al., 2006; Darling et al., 2012) or contaminated in urban and industrial environments (Carlson et al., 2011; Han et al., 2007; Mahlknecht et al., 2017; Qin et al., 2007), and are much higher if CFC inputs are degraded in anaerobic groundwater (most notably CFC-11 and CFC-113; Cook and Solomon, 1995; Horneman et al., 2008; Plummer et al., 2006b).~~

Additionally, mixing between waters of different ages, which occurs both within the aquifer and pumping from long-screened wells (Cook et al., 2017; Custodio et al., 2018; Visser et al., 2013), ~~may result inposes difficulty-difficulties of interpreting for estimating transit time- MRTs using tracers data. like the aggregation errors that~~ The calculated ~~MTTsMRTs being will be~~ less than ~~the actual MTTs values~~ in mixed waters due to aggregation errors (Cartwright and Morgenstern, 2016; Kirchner, 2016; Stewart et al., 2017). ~~MTTsMRT estimation from the using a~~ multi-model approach based on incorporated ~~transit residence~~ time tracers should reduce the calculation uncertainty (Green et al., 2016; Visser et al., 2013) and ~~verify indicate~~ whether ~~the MTTsMRTs~~ can be realistically estimated (Cartwright et al., 2017).

Mixing-The hypothesis mixing within the aquifers and pumping from the long-screened wells is particularly true-common in the faulted-hydraulic drop alluvium aquifers of the Manas River Basin (MRB) in the arid regions of nNorthwest China (Fig. 1). In particular, Ppumping from ~~the~~ long-screened wells (of which there are over 10 000 boreholes, (Ma et al., 2018) makes groundwater mixing most likely. ~~The water table depth is 180 m and a level difference of 130 m hydraulic drop is observed due to the thrust fault in the alluvium aquifer (Fig. 1c). The MTTs that impacted by multiple scale mixing in the aquifers with contrasting geological settings and deep unsaturated zone are still insufficient recognition.~~ MRTs that result from a deep unsaturated zone (with a water table depth of 180 m) and contrasting geological settings (a level difference of 130 m hydraulic drop caused by the thrust fault) are still insufficiently recognised in the alluvium aquifer (Fig. 1c). ~~This study was designed~~ We aim to provide the first estimation of the ~~MTTsMRTs~~ of borehole groundwater drainage (e.g., well withdrawal) using CFC and  $^3\text{H}$  concentrations. ~~We then analyse T~~ the major ~~ion~~ hydrochemical ions ~~instry of~~ groundwater as first-order proxies for ~~MTTsMRTs were then analyzed~~. In addition, we identify the recharge sources for the different mixing end-members and constrain mixing rates.



## 2 Geological and hydrogeological setting

130 The bedrock of the upper Manas River catchment in the mountain area consists of granites, sedimentary formations of Devonian and Carboniferous age, and Mesozoic limestone (Jelinowska et al. 1995). ~~The p~~Pyroclastic rock is exposed in relatively small areas in the south mountain. The piedmont and oasis plains are filled with Cenozoic strata, including the Tertiary and Quaternary deposits with a total depth more than 5000 m in the piedmont area and decreasing to 500–1000 m in the center of the plain (Zhao 2010). The vertical cross section (Fig. 1c) shows that the Quaternary deposits consist of pebbles, sandy gravel, and sand in the piedmont plain. The clay content in the Quaternary deposits increases from the overflow spring zone to the north oasis plain, which consists of silty loam and clay. The Huoerguosi–Manas–Tugulu thrust faults ~~–anticline~~ occurred in the early Pleistocene and cut the Tertiary strata with a ~~total~~ length of approximately 100 km ~~length~~ in the piedmont alluvial fan (Figs. 1), which are water block features. ~~This~~ ~~These faults thrust fault anticline was were~~ ~~intermittent activity~~ ~~intermittently active~~ from the middle late–Pleistocene and then tended to be more active from the late Holocene (Cui et al., 2007).

135 In the mountain area, groundwater consists of metamorphic rock fissure water, magmatic rock fissure water, clastic rock fissure water and Tertiary clastic rock fissure water (Cui et al., 2007; Zhou, 1992). In the piedmont plain of Shihezi (SHZ) zone, groundwater is from a single–layer unconfined aquifer. From the overflow spring zone to the central oasis plain, groundwater consists of shallow unconfined water and deep confined water. The hydraulic gradient, hydraulic conductivity and transmissivity show a large range of variations due to changes in grain size and local increases of clay content (Wu 145 2007). The groundwater flow direction is ~~macroscopically similar to~~ ~~consistent with~~ the Manas River flow ~~direction~~. In the piedmont plain, the aquifer is recharged by the Manas River water and unconfined with saturated thickness more than 650 m, and is hydraulically connected to the hydrological network in the piedmont plain and north oasis plain (Ma et al., 2018; Wu 2007). The piedmont plain unconfined aquifer ~~buried~~ depth decreases gradually from south to north and has relatively fresh 150 groundwater with TDS of  $< 1 \text{ g L}^{-1}$ . Groundwater discharges via springs in the north area of SHZ (Fig. 1c). The shallow unconfined groundwater in the north oasis plain has TDS of  $> 3 \text{ g L}^{-1}$ , and the underlying confined groundwater show relatively fresh water with TDS of  $0.3\text{--}1.0 \text{ g L}^{-1}$  (Wu 2007). The water table depth is as ~~large~~ ~~deep~~ as 180 m and a level difference of 130 m hydraulic drop is observed due to the thrust fault in the south margin in SHZ (Fig. 1c).

## 3 Materials and methods

### 155 3.1 Water sampling

~~In total, 29 groundwater~~ Groundwater (pumped from ~~fully penetrating~~ well, of which 3 are from spring and 3 are from the artesian well) were ~~collected along the Manas River during June to August, 2015 (from G1 to G29 in Table 1 and Fig. 2).~~ ~~Groundwater were~~ separated into three clusters ~~along the Manas River motion (Table 1 and Fig. 2)~~ including the upstream groundwater (UG, south of the Wuyi Road), midstream groundwater (MG, area between the Wuyi Road and the West

160 Mmain Ceanal–Yisiqui), and downstream groundwater (north of the West Mmain Ceanal–Yisiqui) based on the  
hydrochemistry and stable isotope data. Groundwater were sampled from wells for irrigation and domestic supply, in which  
shallow wells were pumped for a minimum 5 min before sampling and deep wells were active for irrigation for more than 10  
days prior to the sampling. Surface water samples (river water, ditch and reservoir water) and groundwater samples data  
165 ~~from G30 to G39 were reported by Ji (2016) and Ma et al. (2018).~~ ~~Groundwater were sampled from wells for irrigation and~~  
~~domestic supply, in which shallow wells were pumped for a minimum 5 min before sampling and deep wells were active for~~  
~~irrigation for more than 10 days prior to the sampling.~~

Water temperature (T), pH values, electrical conductivity (EC) and dissolved oxygen (DO) were measured (Table 1) in the  
field using calibrated Hach (HQ40d) conductivity and pH meters, which had been calibrated before use. Bicarbonate was  
determined by titration with 0.05 N HCl on site. Samples to be analyzed for chemical and stable isotopic values were filtered  
170 on site through 0.45  $\mu\text{m}$  millipore syringe filters and stored in pre-cleaned polypropylene bottles at 4 °C until analysis. For  
cation and strontium isotope analysis, the samples were acidified to  $\text{pH} < 2$  with ultrapure  $\text{HNO}_3$ .

Extreme precautions are needed to be taken to avoid contamination from equipment such as pumps and tubing (Cook et al.,  
2017; Darling et al., 2012; Han et al., 2012) for CFCs samples. After purging the wells, water samples were collected  
directly from the borehole using a copper tube sampling pipe for CFC analysis. One end of the pipe was connected to the  
175 well casing, and the other end was placed in the bottom of a 120 mL borosilicate glass bottle, inside a 2000 mL beaker. The  
well water was allowed to flow through the tubing for ten minutes, thoroughly flushing the tubing with well water. The  
bottle was submerged, filled and capped underwater when there was no bubbles appeared in the bottle, following the  
protocols described by Han et al. (2007). In this study, 5 bottles were collected at each well and 3 of which were analyzed. A  
total of 10 wells were collected for CFC (CFC–11, CFC–12 and CFC–113) analysis. Unfiltered samples for  $^3\text{H}$  analysis were  
180 collected and stored in 500 mL airtight polypropylene bottles. Dissolved inorganic carbon (DIC) for  $^{14}\text{C}$  activity analysis was  
precipitated in field from 180 to 240 L water samples to  $\text{BaCO}_3$  by addition of excess  $\text{BaCl}_2$  previously brought to  $\text{pH} \geq 12$   
by addition of  $\text{NaOH}$ , which then were sealed in 500 mL polypropylene bottles, following the procedure reported by Chen et  
al. (2003).

### 3.2 Analytical techniques

185 The CFC concentrations were analysed within 1 month of sample collection at the Groundwater Dating Laboratory of the  
Institute of Geology and Geophysics, Chinese Academy of Sciences (IGG–CAS) using a purge–and trap gas  
chromatography procedure with an Electron Capture Detector (ECD), which has been reported by Han et al. (2012, 2015)  
and Qin et al. (2011). The procedures were ~~followed after~~ by Oster et al. (1996). The detection limit for each CFC is about  
0.01  $\text{pmol L}^{-1}$  of water, with the error less than  $\pm 5\%$ . The obtained results are shown in Table 1.

190 The  $^3\text{H}$  and  $^{14}\text{C}$  activities of groundwater were measured using liquid scintillation spectrometry (1220 Quantulus ultra–  
low–level counters, PerkinElmer, Waltham, MA, USA) at the State Key Laboratory of Biogeology and Environmental  
Geology, China University of Geosciences in Wuhan. Water samples for  $^3\text{H}$  were distilled and electrolytically enriched prior

to being analysed. Detailed procedures were followed after by Morgenstern and Taylor (2009).  $^3\text{H}$  activities were expressed as tritium unit (TU), with 1 TU corresponding to a  $^3\text{H}/^1\text{H}$  ratio of  $1 \times 10^{-18}$ . For  $^{14}\text{C}$  samples, the obtained  $\text{BaCO}_3$  samples were first converted to  $\text{CO}_2$ , then to acetylene ( $\text{C}_2\text{H}_2$ ) which in turn was trimerized catalytically to  $\text{C}_6\text{H}_6$  as described by Polach (1987), prior to being analysed.  $^{14}\text{C}$  activities were reported as percent modern carbon (pMC). The achieved precision for  $^3\text{H}$  and  $^{14}\text{C}$  were  $\pm 0.2$  TU and  $\pm 0.4$  pMC respectively.

The cation, anion and stable isotope measurements were performed at the State Key Laboratory of Biogeology and Environmental Geology, China University of Geosciences in Wuhan. Cations were analysed using an inductively coupled plasma atomic emission spectrometry (ICP–AES) (IRIS Intrepid II XSP, Thermo Elemental). Anions were analysed on filtered unacidified samples using ion chromatography (IC) (Metrohm 761 Compact IC). Analytical errors were inferred from the mass balance between cations and anions (with  $\text{HCO}_3^-$ ), and are within  $\pm 6\%$ . Stable isotopic values ( $\delta^2\text{H}$  and  $\delta^{18}\text{O}$ ) analyses were measured using a Finnigan MAT–253 mass spectrometer (Thermo Fisher, USA, manufactured in Bremen, Germany), with the TC/EA method. The  $\delta^2\text{H}$  and  $\delta^{18}\text{O}$  values (Table 1) were presented in  $\delta$  notation in ‰ with respect to the Vienna Standard Mean Ocean Water (VSMOW), with an analytical precision of 0.5 ‰ vs. VSMOW for  $\delta^2\text{H}$  and of 0.1 ‰ for  $\delta^{18}\text{O}$ .

### 3.3 Apparent CFC age estimation Groundwater dating

#### 3.3.1 CFCs indicating modern water recharge

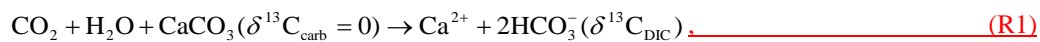
Knowledge of the history of the local atmospheric mixing ratios of CFCs in precipitation concentrations is first required for indicating modern water recharge groundwater dating. The difference between the local and global background atmospheric mixing ratios of CFCs concentrations in the Northern Hemisphere – CFC excess – refers to as CFC excess which varies largely substantially based on the industrial development. Elevated CFC concentrations of (10–15 % higher than those of the Northern Hemisphere) have been reported in the air of urban environments such as Las Vegas, Tucson, Vienna, and Beijing (Barletta et al., 2006; Carlson et al., 2011; Han et al., 2007; Qin et al., 2007), while whereas in Lanzhou and Yinchuan (Northwest China) they were about approximately 10 % less lower (Barletta et al., 2006). In this study, MRB–Manas River Basin is located in the Northwest of China (Fig. 1a), has a with very low population density, and is far from the industrial cities, and there is no clear difference in the atmospheric CFC concentrations between North America and low latitude countries. To evaluate CFC ages, the time series trend of Northern Hemisphere atmospheric mixing ratio (Fig. 3; 1940–2014, <http://water.usgs.gov/lab/software/air/cure/>) was adopted in this study.

Measured CFC concentrations (in  $\text{pmol L}^{-1}$ ) can be interpreted in terms of partial pressures of CFCs (in pptv) in solubility equilibrium with the water sample based on Henry's Law law solubility. Concrete computational process was conducted followed following that by Plummer et al. (2006a). In the arid Northwest China, estimating the local shallow groundwater temperature as recharge temperature is was more suitable than the annual mean surface air temperature to be estimated for the recharge temperature (Qin et al., 2011) as because the local low precipitation usually cannot reach the groundwater.

225 ~~Previous studies in~~ On the MRB (Ji, 2016; Wu, 2007) have also indicated ~~that~~ much less vertical recharge water from the local precipitation ~~as~~ compared with ~~to the~~ abundant groundwater lateral flow recharge and river leakage from the mountain to the piedmont areas. In this study, the measured groundwater temperature, which that vary varied from 11.5 to 15.7 °C ~~from each~~ between wells (Table 1), was used as the recharge temperature ~~was used~~ to estimate the ~~water ages~~ groundwater input CFC concentrations. Surface elevations of the recharge area vary from 316 to 755 m. The ~~apparent age~~ modern water recharge is ~~was~~ then determined by comparing the calculated partial pressures of CFCs in solubility equilibrium with the water samples with historical CFC concentrations in the air (Fig. 3) ~~based on the hypothesis of piston flow~~.

### 3.3.2 The apparent <sup>14</sup>C ages

235 Carbon-14 (<sup>14</sup>C, half-life: 5730 yrs) activity in groundwater is often used to estimate groundwater age over time periods of approximately 200 and 30 000 yrs, and to determine the recharge from mixing water in various climate conditions (Cook, et al., 2017; Custodio et al., 2018; Huang et al., 2017). Calculation of <sup>14</sup>C groundwater age may be complicated if dissolved inorganic carbon is derived from a mixture of sources or <sup>14</sup>C originating from the atmosphere or soil zone is significantly diluted by the dissolution of <sup>14</sup>C-free carbonate minerals in the aquifer matrix and biochemical reactions along the groundwater flow paths (Clark and Fritz, 1997). Although only minor carbonate dissolution is likely, determination of groundwater residence times requires <sup>14</sup>C correction (Atkinson et al., 2014). When the dissolution of carbonate during recharge or along the groundwater flow path may dilute the initial soil CO<sub>2</sub>, <sup>δ</sup><sup>13</sup>C can be used to trace the process (Clark and Fritz, 1997). An equation for the reaction between CO<sub>2</sub>-containing water with a carbonate mineral is commonly written as follows (modified after Pearson and Hanshaw, 1970):



245 where <sup>δ</sup><sup>13</sup>C<sub>carb</sub> is the dissolved carbonate <sup>δ</sup><sup>13</sup>C value (approximately 0; Clark and Fritz, 1997), and <sup>δ</sup><sup>13</sup>C<sub>DIC</sub> is the measured <sup>δ</sup><sup>13</sup>C value in groundwater.

Depending on knowing the measured <sup>14</sup>C activity after adjustment for the geochemical and physical dilution processes in the aquifer (without radioactive decay), the groundwater apparent <sup>14</sup>C ages (t) can be calculated from the following decay equation:

$$t = -\frac{1}{\lambda_{14\text{C}}} \times \ln \frac{a^{14}\text{C}}{a_0^{14}\text{C}}, \quad \text{(1)}$$

250 where  $\lambda_{14\text{C}}$  is the <sup>14</sup>C decay constant ( $\lambda_{14\text{C}} = \ln 2/5730$ ), and  $a^{14}\text{C}$  is the measured <sup>14</sup>C activity of the DIC in groundwater. As mentioned above, the estimated ages are really apparent ages due to the mixture of waters with wide range of ages (Custodio et al., 2018; Suckow, 2014).

Previous studies in the arid northwest China (Edmunds et al., 2006; Huang et al., 2017) have concluded that a volumetric value of 20 % “dead” carbon derived from the aquifer matrix was recognized, which is consistent with the value (10–25 %)

255 obtained by Vogel (1970). Therefore, the initial  $^{14}\text{C}$  activity ( $a_0^{14}\text{C}$ ) of 80 pMC is used to correct groundwater  $^{14}\text{C}$  ages (results are shown in Table 1), despite this simple correction makes no attempt to correct the age of individual samples that may have experienced different water–rock interaction histories.

### **3.4 Mean transit times estimated by $^3\text{H}$ and CFCs**

#### **3.3.3 Groundwater mean residence time estimation**

260 Groundwater mixing may occur both within the aquifer and in the long–screened wells (Cook et al., 2017; Custodio et al., 2018; Visser et al., 2013). The groundwater residence times (ages) often display a wide range because recharge occurs under various climate conditions (Custodio et al., 2018). With the aid of gaseous tracers (e.g.  $^3\text{H}$ , CFCs,  $\text{SF}_6$  and  $^{85}\text{Kr}$ ) one can describe the mixing distribution using a mixing model (Stewart et al., 2017; Zuber et al., 2005) to obtain the groundwater MRTs. LPMs is an alternative approach to interpret MRTs for water flow through the subsurface systems to the output. The  
265 widely used lumped parameter models (LPMs) that exist is based on the assumptions that the hydrologic system is considered as a closed system, sufficiently homogeneous, being at steady state, having a defined input and a corresponding output in the form of pumping wells, springs or streams draining the system (Małoszewski and Zuber, 1982). For the steady–state subsurface hydrologic system, on accounting of the  $^3\text{H}$  and CFCs tracers entering groundwater with precipitation are injected proportionally to the volumetric flow rates by nature itself natural processes;  
270 the output concentration in water at the time of sampling relating to the input  $^3\text{H}$  and CFCs can be described by the following convolution integrals (Małoszewski and Zuber, 1982):

$$C_{\text{out}}(t) = \int_0^{\infty} C_{\text{in}}(t-\tau) g(\tau) e^{-\lambda_{^3\text{H}}\tau} d\tau \quad \text{for } ^3\text{H} \text{ tracer} \quad (\text{4a2a})$$

$$C_{\text{out}}(t) = \int_0^{\infty} C_{\text{in}}(t-\tau) g(\tau) d\tau \quad \text{for CFCs tracer,} \quad (\text{4b2b})$$

where  $C_{\text{out}}$  is the tracer output concentration,  $C_{\text{in}}$  is the tracer input concentration,  $\tau$  is the transit/residence time,  $t-\tau$  is  
275 the time when water entered the catchment,  $\lambda_{^3\text{H}}$  is the  $^3\text{H}$  decay constant ( $\lambda_{^3\text{H}} = \ln 2/12.32$ ), and  $g(\tau)$  is the system response function that describes the transit/residence time distributions (RTDs) in the subsurface hydrologic system.

In this study, the CFC concentrations from the time series trend of the Northern Hemisphere atmospheric mixing ratio (Fig. 3) and  $^3\text{H}$  concentrations in precipitation in Urumqi (Fig. 4) are treated as proxies for CFC and  $^3\text{H}$  recharge concentrations ( $C_{\text{in}}$ ), respectively. The historical precipitation  $^3\text{H}$  activity in the Urumqi station (Fig. 4) is reconstructed with the data  
280 available from the International Atomic Energy Agency (IAEA) using a logarithmic interpolation method. The precipitation  $^3\text{H}$  activity between 1969 and 1983 at Hong Kong and Irkutsk with different latitudes are used (data is available at <<https://www.iaea.org/>>). The time series of  $^3\text{H}$  activity (Fig. 4) was used as the input data are based on the following considerations. First, the MRB is located in the Northern Hemisphere, where the bomb–pulse  $^3\text{H}$  activity is several orders of

magnitude higher than in the Southern Hemisphere (Clark and Fritz, 1997; Tadros et al., 2014) and was superimposed with the China atmospheric nuclear tests from 1964 to 1974 in the arid regions of Northwest China; thus, the remnant  $^3\text{H}$  activity remains affected by the tail-end of the bomb pulse. Second, the study area is more than 3500 km away from the western Pacific, where the atmospheric  $^3\text{H}$  activity is much higher than that at coastal sites due to the continental effect (Tadros et al., 2014). Furthermore, although the atmospheric  $^3\text{H}$  activity varies between seasons (Cartwright and Morgenstern, 2016; Morgenstern et al., 2010; Tadros et al., 2014), the mean annual values (Fig. 4) were considered in this study.

Several ~~TTDs of various models~~RTDs have been described (Małozzewski and Zuber, 1982; Jurgens et al., 2012) and have been widely used in studies of variable timescales and catchment areas (Cartwright and Morgenstern, 2015, 2016; Cartwright et al., 2018; Hrachowitz et al., 2009; Morgenstern et al., 2010, 2015; McGuire et al., 2005), ~~of which t~~The selection of each model depends on the hydrogeological situations in the hydrologic system to which it is applicable. ~~The exponential-piston flow model (EPM) describes an aquifer that contain a segment of the exponential flow followed by a segment of piston flow. The piston flow model assumes minimal water mixing from different flow lines and little or no recharge in the confined aquifer; the exponential flow model assumes a full mixing of water in the unconfined aquifer and the receipt of areally distributed recharge (Jurgens et al., 2012; Małozzewski and Zuber, 1982). The weighting function of this model is given by~~In this study, the exponential-piston flow model (EPM), the dispersion model (DM), and the exponential mixing model (EMM) were given below as transit time distribution function:

~~Exponential piston flow model~~

$$g(\tau) = 0 \quad \text{for } \tau < \tau_m(1-1/\eta) \quad (2a3a)$$

$$g(\tau) = \frac{\eta}{\tau_m} e^{(-\eta\tau/\tau_m + \eta - 1)} \quad \text{for } \tau \geq \tau_m(1-1/\eta) \quad (2b3b)$$

~~The D~~dispersion model (DM) mainly measures the relative importance of dispersion to advection, and is applicable for confined or partially confined aquifers (Małozzewski, 2000). Its RTD is given by

$$g(\tau) = \frac{1}{\tau \sqrt{4\pi D_p \tau / \tau_m}} e^{-\left(\frac{(1-\tau/\tau_m)^2}{4\pi D_p \tau / \tau_m}\right)} \quad (34)$$

~~The E~~weighting function of the exponential mixing ~~Model~~model (EMM) is

$$g(\tau) = \frac{1}{\tau_m} e^{(-\tau/\tau_m)}, \quad (45)$$

where  $\tau_m$  is the mean ~~transit~~residence time,  $\eta$  is the ratio defined as  $\eta = (l_p + l_e)/l_e = l_p/l_e + 1$ , where  $l_e$  (or  $l_p$ ) is the length of area at the water table (or not) receiving recharge,  $D_p$  is the dispersion parameter, which is the reciprocal of the Peclet number ( $Pe$ ) and defined as  $D_p = D/(vx)$ , where  $D$  is the dispersion coefficient ( $\text{m}^2 \text{day}^{-1}$ ),  $v$  is velocity ( $\text{m day}^{-1}$ ), and  $x$  is distance (m).

Each RTD has one or two parameters. MRT ( $\tau_m$ ) is determined by convoluting the input (the time series  $^3\text{H}$  and CFCs input in rainfall) to each model to match the output (the measured  $^3\text{H}$  and CFC concentrations in groundwater), and other parameters ( $\eta$  and  $D_p$ ) are determined depending on the hydrogeological conditions. To interpret the ages of the MRB data set, EPM ( $\eta=1.5$  and  $2.2$ ), DM ( $D_p=0.03$  and  $0.1$ ), and EMM models were used, after which MRTs with different RTDs were cross-referenced.

### 3.5 The $^{14}\text{C}$ age model

The calculation of  $^{14}\text{C}$  ages may be complicated if groundwater dissolved inorganic carbon (DIC) is derived from a mixture of sources or/and the  $^{14}\text{C}$  originating from the atmosphere or soil zone is often significantly diluted by the dissolution of  $^{14}\text{C}$ -free carbonate minerals in the aquifer matrix and biochemical reactions along the groundwater flow paths (Clark and Fritz, 1997). While only minor carbonate dissolution is likely, determination of groundwater transit times requires  $^{14}\text{C}$  correction to be taken into account (Atkinson et al., 2014). When dissolution of carbonate during recharge or along the groundwater flow path may dilute the initial soil  $\text{CO}_2$ ,  $\delta^{13}\text{C}$  can be used to trace the process (Clark and Fritz, 1997). An equation for the reaction between carbon dioxide containing water with a carbonate mineral is commonly written as (modified after Pearson and Hanshaw, 1970):



where  $\delta^{13}\text{C}_{\text{carb}}$  is the dissolved carbonate  $\delta^{13}\text{C}$  value (approximately 0; Clark and Fritz, 1997), and  $\delta^{13}\text{C}_{\text{DIC}}$  is the measured  $\delta^{13}\text{C}$  value in groundwater.

If it assumed that any dissolution that occurs under truly open-system conditions will equilibrate both  $^{14}\text{C}$  and  $^{13}\text{C}$  in the recharging water and that closed system dissolution of calcite in the aquifers is the major process (Atkinson et al., 2014), the initial  $^{14}\text{C}$  activity ( $a_0^{14}\text{C}$ ) may be calculated from the following equation:

$$a_0^{14}\text{C} = a_{\text{rech}}^{14}\text{C} \frac{\delta^{13}\text{C}_{\text{DIC}} - \delta^{13}\text{C}_{\text{carb}}}{\delta^{13}\text{C}_{\text{rech}} - \delta^{13}\text{C}_{\text{carb}}}, \quad (5)$$

where  $a_{\text{rech}}^{14}\text{C}$  is the recharging water  $^{14}\text{C}$  activity (assumed to be 100 pMC), and  $\delta^{13}\text{C}_{\text{rech}}$  is the recharging water  $\delta^{13}\text{C}$  value in the recharge zone depending on vegetation type (C3 or/and C4).

Depending on knowing the measured  $^{14}\text{C}$  activity after adjustment for the geochemical and physical dilution processes in the aquifer (without radioactive decay), then the groundwater  $^{14}\text{C}$  ages ( $t$ ) can be calculated from the following decay equation:

$$t = -\frac{1}{\lambda_{^{14}\text{C}}} \times \ln \frac{a^{14}\text{C}}{a_0^{14}\text{C}}, \quad (6)$$

where  $\lambda_{^{14}\text{C}}$  is the  $^{14}\text{C}$  decay constant ( $\lambda_{^{14}\text{C}} = \ln 2/5730$ ), and  $a^{14}\text{C}$  is the measured  $^{14}\text{C}$  activity of the DIC in groundwater.

340 Previous studies in the arid northwest China (Edmunds et al., 2006; Huang et al., 2017) have concluded that a volumetric value of 20 % “dead” carbon derived from the aquifer matrix was recognized, which is consistent with the value (10–25 %) obtained by Vogel (1970). Once below the  $^3\text{H}$  detection limit, the initial  $^{14}\text{C}$  activity can be considered as the initial value by plotting the  $^3\text{H}$  value versus the  $^{14}\text{C}$  activity, and based on that, the maximum  $^{14}\text{C}$  activity of 79.8 pMC with  $^3\text{H}$  value below the detection limit in the Baiyang River Basin, 260 km northwest to our study area, was obtained (Huang et al., 2017).  
345 Therefore, the initial  $^{14}\text{C}$  activity ( $a_0^{14}\text{C}$ ) of 80 pMC is used to correct groundwater  $^{14}\text{C}$  ages (results are shown in Table 1), despite this simple correction makes no attempt to correct the age of individual samples that may have experienced different water–rock interaction histories.

## 4 Results and discussion

### 4.1 Stable isotope and major ion hydrochemistry

350 The  $\delta^2\text{H}$  and  $\delta^{18}\text{O}$  values in the study area vary from  $-75.88$  to  $-53.40$  ‰ and  $-11.62$  to  $-6.76$  ‰ for the surface water, and from  $-82.45$  to  $-62.16$  ‰ and  $-12.19$  to  $-9.01$  ‰ for the groundwater. Figure 3a–5a shows the  $\delta^2\text{H}$  and  $\delta^{18}\text{O}$  values of surface water and groundwater in relation to the precipitation isotopes of the closest GNIP station (Urumqi station in Fig. 1a). Both the linear slope (7.3) and intercept (3.1) of the Local Meteoric Water Line (LMWL) are lower than that of the Global Meteoric Water Line (GMWL, 8 and 10, respectively; Craig 1961). Surface water (ditch, river and reservoir water) are more  
355 enriched in heavy isotopes and defined an evaporation line with a slope of 4.5 (Fig. 3b5b), which is much higher than that solely calculated from the upstream river water and reservoir water (slope=3.2 from Ma et al., 2018).

Groundwater deuterium excess values ( $d$ -excess =  $\delta^2\text{H} - 8\delta^{18}\text{O}$ , Fig. 3b5b) defined by Dansgaard (1964) lie close to the annual mean LMWL ( $d_{\text{LMWL}}=13$  ‰), which also suggest little isotope fractionation by evaporation as  $d$ -excess value decreases when water evaporates (Han et al. 2011; Ma et al., 2015). The  $d$ -excess values of surface water decrease from  
360 17.12 ‰ in the upstream area to 0.68 ‰ in the downstream area, indicating strong evaporation effect, which is also demonstrated by the low slope (evaporation slope=4.5) of the surface waters. A recent study (Benettin et al., 2018) indicated that the evaporation line obtained from various sources of water is often not the true evaporation line. All samples of surface water in the present study were collected in the summer of 2015 and were recharged from the mountain areas in the same season. Although they were collected from different areas (ditch water, reservoir water, and Manas River water), the linear trend obtained may have implications for surface water evaporation.

365 The hydrochemistry compositions of surface water and groundwater in the MRB reflect the evolution from the fresh  $\text{HCO}_3\text{-SO}_4\text{-Ca}$  water type to the  $\text{HCO}_3\text{-SO}_4\text{-Na-Ca}$  type and further to the  $\text{HCO}_3\text{-SO}_4\text{-Na}$  type, and finally to the brine  $\text{Cl-SO}_4\text{-Na}$  water type along the groundwater flow paths (Fig. 46). Groundwater in the unconfined aquifers (e.g., intermountain depression and piedmont plain aquifers in Fig. 1c) is dominated by  $\text{Ca}^{2+}$  and  $\text{HCO}_3^-$  with a relatively low concentration of  
370  $\text{Na}^+$  (Fig. 46). Groundwater in the confined aquifers is characterized by a wide range with progressively increasing  $\text{Na}^+$



and  $\text{Cl}^-$  ions, ~~meanwhile-whereas~~  $\text{Ca}^{2+}$  and  $\text{Mg}^{2+}$  ions decrease progressively towards the more concentrated end of the salinity spectrum (Fig. 46). The concentration of  $\text{SO}_4^{2-}$  ion gradually increases in the unconfined aquifers and becomes less dominant in the confined aquifers along the groundwater flow paths (Fig. 46).

## 4.2 Groundwater ages

375 Groundwater ages are shown in Table 1 for  $^{14}\text{C}_{\text{corr}}$  and in Table 2 for CFCs. Figure 5 shows the estimated CFC atmospheric partial pressures.  $^3\text{H}$  activities of groundwater and the reconstructed precipitation time series results are shown in Fig. 6. Figure 7 shows the distributions of tracer concentrations (Fig. 7a) and ages (Fig. 7b) with distance to mountain.

### 4.2.1 Apparent CFC ages

380 As can be seen in Table 1, groundwater with well depths between 13 and 150 m contain detectable CFC concentrations (0.17–3.77  $\text{pmol L}^{-1}$  for CFC 11, 0.19–2.18  $\text{pmol L}^{-1}$  for CFC 12, and 0.02–0.38  $\text{pmol L}^{-1}$  for CFC 113) both in the upstream and midstream areas, indicating at least a small fraction of young groundwater components (post 1940). The highest concentration was observed in the UG (G3), south of the fault, median and the lowest were respectively observed in the west and east bank of the ‘East main canal’ in the MG, north of the fault. In the midstream area (Fig. 2), CFC concentrations generally decrease with well depth at the south of reservoirs (G25, G8, and G9), while increase with well depth at the north of reservoirs (G15 and G16), which might indicate the different groundwater flow paths (e.g., downward or upward flow directions). The estimated CFC atmospheric partial pressures and apparent ages are shown in Table 2 and  
385 Fig. 5, with the apparent ages varying from 25 to 54.5 yrs. The UG (G3) has the same CFC 113 and CFC 12 apparent ages (Table 2), indicating piston flow recharge in the upstream area. The MG CFC 11 based ages agreed within 2–4 yrs with that based on CFC 12 concentrations, while that the CFC 113 based ages were much 2–9 yrs younger than that based on CFC  
390 11 and CFC 12 concentrations, indicating mixtures of young and old groundwater components in the midstream area.

Despite apparent CFC ages presuppose that the measured water is the result of simple piston flow with no mixing, they provide a good first approximation for groundwater age (Darling et al., 2012; Han et al., 2015). The time lag for CFCs transport through the thick unsaturated zone (Cook and Solomon, 1995), as well as degradation especially for CFC 11 is being common in the anaerobic groundwater (Horneman et al., 2008; Plummer et al., 2006b), which both are important  
395 consideration when dating groundwater using CFC concentrations. In this study, the groundwater aerobic environment (Table 1, DO values vary from 0.7 to 9.8  $\text{mg L}^{-1}$ ) make CFC degradation under anoxic conditions unlikely. The groundwater were mainly recharged by the river fast leakage in the upstream area and piedmont plain (Ma et al., 2018), where the soil texture is consisted of pebbles and sandy gravel (Fig. 1e), which confirm one to assume that the unsaturated zone air CFC closely follows that of the atmosphere and thus the recharge time lag through the unsaturated zone is not consideration.  
400 Nevertheless, CFC 11 has shown a greater propensity for degradation and/or contamination than CFC 12 (Plummer et al., 2006b). Therefore, one assign the CFC 12 apparent age in the following discussions.

The youngest groundwater apparent age is in the upstream area (G3 with 25 yrs), which is most likely due to the shortest flow paths from recharge sources compared to the piedmont groundwater samples in the midstream area. The distribution of CFC-12 apparent ages with distance to mountain (Fig. 7b) reveals two different trends from the upstream to midstream areas. First, groundwater ages increased with elevated distance along the Manas River motion from the upstream to the midstream areas, suggesting longer flow paths towards the north orientation in the West 'East main canal'. Second, the oldest ages of groundwater (G5 and G7) were located in the East 'East main canal' in the midstream area with much shorter distance than that in the reservoir north (G15 and G16), this could be explained by the lower groundwater velocities in the East 'East main canal', where the hydraulic gradient (Fig. 2) is much smaller than the West. Furthermore, it can be seen from Table 2 and Fig. 2 that groundwater ages increased from 29 to 38 yrs with well depth increasing from 48 to 100 m at the reservoir south (G25, G8 and G9), while that in the reservoir north decreased from 40.4 to 29.6 yrs with well depth increasing from 23 to 56 m (G15 and G16). The different trends for the relationship between groundwater age and well depth might be ascribed to the different flow paths among the two sites (e.g., reservoir south and north).

#### 4.2.2 $^3\text{H}$ and $^{14}\text{C}$ ages

$^3\text{H}$  activity of groundwater samples vary from 60 to 1.1 TU (Fig. 6 and Table 1), with the highest value in the UG (G4) and the relatively low values in the MG (mean 12.4 TU) and DG (mean 4.5 TU). The historical precipitation  $^3\text{H}$  activity in Urumqi station (Fig. 6) was reconstructed from the available data in the International Atomic Energy Agency (IAEA) following the method described by Han et al. (2015). The estimated results show that precipitation  $^3\text{H}$  activity has been decreasing since the 1960s and the estimated current tritium level has since stabilized around 31.5 TU (Fig. 6). All of the measured UG (G1, G2, and G4) and G23 (belong to MG)  $^3\text{H}$  data were higher than 34.3 TU, which indicates some fractions of the 1960s precipitation recharge. Groundwater with  $^3\text{H}$  activity lower than 5.6 TU contains some pre-1950s recharge.

The distribution of  $^3\text{H}$  activity with distance to mountain (Fig. 7a) also reveals two different trends from the upstream to midstream areas. First,  $^3\text{H}$  activities of groundwater in the upstream area increase from 41.1 (G1 and G2) to 60 TU (G4) with distance, which probably indicate that more fractions of the 1960s precipitation recharge was occurred for G4 than G1 and G2 groundwater samples. It is seen from Fig. 2 that nearing G4 samples shows the highest hydraulic gradient values, which imply that more fractions of the 1960s precipitation recharge was possible. Second,  $^3\text{H}$  activities of groundwater in the midstream area showed an obvious reduction trends along the Manas River motion from 37.5 (G23) to 1.1 TU (G14) with distance, indicating that more fractions of pre-bomb precipitation recharge may have occurred along the groundwater flow direction in the north of the fault. Furthermore, the  $^{14}\text{C}$  activity in the MG showed small increases with distance (Fig. 7a) from 43.4 to 54.6 pMC, with the exception of sample G12 at approximately 54 km of 86.9 pMC that has an  $^{14}\text{C}_{\text{eff}}$  age of 684 yrs (modern recharge), while in the DG decreased to 23.5 pMC. The presence of detectable  $^3\text{H}$  (2.9–6.91 TU) in DG with low  $^{14}\text{C}$  values (23.5–34.3 pMC) indicated that some mixing with post-bomb precipitation recharge may be occurred.

The distribution of groundwater both  $^3\text{H}$  ages (estimated by comparing the  $^3\text{H}$  activity in precipitation decayed to 2014 and in groundwater (Fig. 6) on condition that a piston flow recharge was across the study area) and  $^{14}\text{C}_{\text{eff}}$  ages (calculated

435 from Eq. (6)) with distance to mountain (Fig. 7b) were heterogeneous with no relationship along lateral groundwater flow  
paths. The great age differences between  $^3\text{H}$  (28.8–60 yrs) and  $^{14}\text{C}_{\text{eff}}$  ages (3158–10 127 yrs) from midstream to downstream  
440 areas (Fig. 7b) imply that mixing with variable proportions of young and old water have occurred. Although there is an  
overall  $^{14}\text{C}_{\text{eff}}$  age increase from the midstream to downstream areas (Fig. 7b), inversely a decrease in age with distance in  
the MG is observed. This probably be ascribed to the largely vertical mixing processes (Ma et al., 2018) within the confined  
aquifers in the reservoir north in the midstream area, because an increase in groundwater age with distance is usually  
observed within the confined aquifers but not in the unconfined aquifers (Batlle-Aguilar et al., 2017). Another speculative  
possibility that aquifers in the midstream area have received significant volume of its recharge from the upstream unconfined  
groundwater by lateral flow with different flow paths, which is still not yet confirmed.

## 4.2.3 Modern and paleo-meteoric recharge features

### 445 4.2.1 Stable isotope indications

Stable isotopes ( $\delta^2\text{H}$  and  $\delta^{18}\text{O}$ ), components of the water molecule that record the atmospheric conditions at the time of  
recharge (Batlle-Aguilar et al., 2017; Chen et al., 2003), provide valuable information on groundwater recharge processes.  
Generally, there are two possible meteoric recharge sources including precipitation in the modern climate and in the  
paleoclimate. Groundwater whose isotopic values are more depleted than the modern precipitation usually would be ascribed  
450 to two recharge sources including snowmelt/precipitation at higher elevation and precipitation fallen during cooler climate.  
Figure 3–5 shows that groundwater generally lie along the LMWL but do not define evaporation trend, implying little  
evaporation and isotope exchange between groundwater and the rock matrix have occurred (Ma et al., 2018; Négrel et al.,  
2016). Transpiration over evaporation is likely to be dominant in the soil when infiltration as soil water uptake by root is not  
significantly isotope fractionated (Dawson and Ehleringer 1991).

455 Three groundwater clusters can be identified in the  $\delta^2\text{H}$ – $\delta^{18}\text{O}$  plot (Fig. 3b5b), suggesting ~~the~~ different recharge sources  
among the upstream, midstream, and downstream areas. The first group with average  $\delta^2\text{H}$  and  $\delta^{18}\text{O}$  average-values of  $-68.24$   
and  $-10.08$  ‰, respectively, is was from UG<sub>7</sub>, and is located much closer to the summer rainfall (Fig. 3a5a), reflecting more  
enriched summer rainfall inputs. Negligible evaporation trends was were observed in ~~the~~ UG, although the recharge is was  
mostly in the summer due to the fast river leakage in the intermountain depression through highly permeable pebbles and  
460 gravel deposits (Fig. 1c). Furthermore, the detectable CFC concentrations and high  $^3\text{H}$  activity ies (Table 1) also indicate ~~the~~  
a modern precipitation recharge. An overlap between surface water and UG indicates the same recharge sources, as because  
some alignment of river water and groundwater isotopic values may indicatesuggest a qualitative recharge under climate  
conditions similar to contemporary conditions (Huang et al., 2017).

465 The second group with average  $\delta^2\text{H}$  and  $\delta^{18}\text{O}$  values of  $-73.10$  and  $-11.0$  ‰, respectively, overlapping-overlapped with  
the annual amount-weighted mean rainfall isotopic value is from MG. Such isotopic values are comparable to the modern  
annual amount-weighted mean rainfall  $\delta^2\text{H}$  and  $\delta^{18}\text{O}$  values ( $-74.7$  and  $-11.0$  ‰, respectively; Fig. 3a5a), probably

reflecting ~~year-round~~annual modern precipitation recharge. ~~However, there could be a~~ another explanation for the relatively ~~much highly~~ scattered MG isotopic values in the  $\delta^2\text{H}$ - $\delta^{18}\text{O}$  plot (Fig. ~~3b5b~~), ~~which~~ is mixing with different time-scales ~~recharges~~ of variable isotopic values at different aquifers and sites along the groundwater flow paths. Groundwater isotopes in the piedmont plain are ~~totally~~ relatively ~~enriched~~ in heavy isotopes (Fig. ~~3b5b~~), which ~~overlapping-overlap~~ with the river water, indicating ~~the~~ fast river leakage recharge ~~through-in a~~ short time (Ma et al., 2018). Groundwater isotopes in the oasis plain diverge from ~~that-those~~ in the piedmont plain (Fig. ~~3b5b~~), ~~as well as and~~ do not ~~show~~ alignment with surface water, indicating ~~the~~ recharge with longer flow paths rather than ~~the~~ fast river leakage recharge.

The third group, ~~with~~ the most depleted in heavy isotopes ( $-82.36$  and  $-12.03$  ‰), ~~is-was~~ from DG, and ~~is-was~~ located much closer to the winter rainfall in the  $\delta^2\text{H}$ - $\delta^{18}\text{O}$  plot (Fig. ~~3b5b~~). ~~Previous s~~Studies (Ji, 2016; Ma et al., 2018) have shown that vertical recharge from the winter rainfall in the downstream area is ~~mostly~~ unlikely. As the altitude effects of precipitation recharge (Clark and Fritz, 1997) and paleo-meteoric recharge during ~~the~~ cooler climate (Chen et al., 2003) could collectively account for the isotopically depleted groundwater, it is usually not easy to distinguish the precipitation recharge sources at ~~a~~ higher elevation from paleo-meteoric recharge. However, the positive altitude gradient of isotopes in precipitation (Kong and Pang, 2016) over North Tianshan Mountain (Fig. 1a) ~~was ascribed-attributed~~ to ~~the~~ moisture recycling, and sub-cloud evaporation effects would ~~give rise to~~ yield more enriched isotopes from higher-altitude precipitation recharge. The isotopically enriched UG (Fig. ~~3b5b~~) in the intermountain depression with higher altitude (Fig. 1c) ~~are-was~~ recharged from the high mountains, ~~which likewise~~ This also demonstrates that DG ~~being-is unlikely to be~~ from the high mountain recharge ~~is mostly unlikely~~. ~~Therefore~~ Accordingly, ~~the-its~~ depleted isotopic values ~~from DG~~ (Fig. ~~3b5b~~) ~~should be~~ ~~were~~ ~~ascribed-attributed~~ to the paleo-meteoric recharge in a cooler climate. ~~In the las glacial period, t~~Temperatures ~~depressions of -10 °C~~ in Xinjiang region (Li et al., 2015) and ~~6-9 °C in~~ North China Plain (Chen et al., 2003) ~~were in the last glacial period-cooler~~ by approximately  $10$  °C and  $6-9$  °C, respectively, compared with ~~than~~ the ~~modern have been observe~~ present day. Groundwater ~~that has had a~~ depleted  $\delta^{18}\text{O}$  value of ~~around~~  $-12.0$  ‰ from the paleo-meteoric recharge ~~have been widely acknowledged~~ in the arid ~~regions of n~~Northwest China, ~~like-such as~~ in ~~the~~ Minqin basin (Edmunds et al., 2006), ~~and both as well as~~ in ~~the~~ East (Li et al., 2015) and West (Huang et al., 2017) Junggar Basin (Fig. 1a).

#### 4.2.2 CFCs indications

Table 1 shows that groundwater with well depths of 13–150 m contained detectable CFC concentrations ( $0.17$ – $3.77$  pmol L<sup>-1</sup> for CFC-11,  $0.19$ – $2.18$  pmol L<sup>-1</sup> for CFC-12, and  $0.02$ – $0.38$  pmol L<sup>-1</sup> for CFC-113) in both the upstream and midstream areas, indicating at least a small fraction of young groundwater components (post-1940). The highest concentration was observed in the UG (G3), south of the fault. The median and the lowest were observed in the west and east banks, respectively, of the East Main Canal in the MG, north of the fault. In the midstream area (Fig. 2), CFC concentrations generally decreased with well depth south of the reservoirs (G25, G8, and G9), and increased with well depth north of the reservoirs (G15 and G16), which might indicate different groundwater flow paths (e.g., downward or upward flow directions).

500 The groundwater aerobic environment (Table 1, DO values vary from 0.7 to 9.8 mg L<sup>-1</sup>) makes CFC degradation under anoxic conditions unlikely. Nevertheless, CFC-11 has shown a greater propensity for degradation and contamination than CFC-12 (Plummer et al., 2006b). Therefore, we use CFC-12 to interpret the modern groundwater recharge in the following discussions. The estimated CFC partial pressure and possible recharge year are shown in Table 2 and Fig. 3. The UG (G3) CFC-113 and CFC-12 both indicate the 1990 precipitation recharge (Table 2), probably a piston flow recharge in the  
505 upstream area. The MG CFC-11-based modern precipitation recharge was in agreement with that based on CFC-12 concentrations within 2–8 yrs, whereas the CFC-113-based recharge was as much as 4–11 yrs later than that the other two, signifying recharge of a mixture of young and old groundwater components in the midstream area. The most recent groundwater recharge was in the upstream area (G3 with 1990 rainfall recharge), which was most likely because the flow paths from recharge sources here were shorter than those of the piedmont groundwater samples in the midstream area.

510 G5 and G7 were located in the east bank of the East Main Canal in the midstream area and were closer than G15 and G16 north of the reservoir, showing that the modern recharge was much earlier than that of G15 and G16 (Table 2). This could be explained by the lower groundwater velocities in the east bank of the East Main Canal, where the hydraulic gradient (Fig. 2) was much smaller than that in the west. Furthermore, groundwater recharge became earlier with increasing well depth from 48 to 100 m south of the reservoir (G25, G8 and G9), whereas that north of the reservoir became later with increasing well  
515 depth from 23 to 56 m (G15 and G16; Table 2, Fig. 2). The different trends for the relationship between groundwater recharge year and well depth might be due to the different flow paths between the two sites (e.g., reservoir south and north).

Comparing CFC concentrations helps to indicate samples containing young (post-1940) and old (CFC-free) water (Han et al., 2007; Han et al., 2012; Koh et al., 2012) or exhibiting contamination or degradation (Plummer et al., 2006b). The cross-plot of the concentrations for CFC-113 and CFC-12 (Fig. 7a) demonstrates that all of the groundwater can be characterised  
520 as binary mixtures between young and older components, though there is still room for some ambiguity around the crossover in the late 1980s (Darling et al., 2012). As shown in Fig. 7a, all of the MG samples are located in the shaded region, representing no post-1989 water recharge. The UG (G3) sample is clearly relatively modern and seems to have been recharged in 1990 through piston flow or mixed with old water and post-1995 water. Using the method described by Plummer et al. (2006b) with the binary mixing model, the fractions of young water were found to vary from 12 to 91 %  
525 (Table 2) for the MG samples with the relatively low young fractions of 12 and 18 % in the MG samples (G5 and G7) from east bank of the East Main Canal. These two well water table were deeper than 40 m, probably indicating a relatively slow and deep circulated groundwater flow. This hypothesis is also suggested by the lower DO (3.7–4.6 mg L<sup>-1</sup>; Table 1) and nitrate concentrations (8.6–9.5 mg L<sup>-1</sup> from Ma et al., 2018) and considerably smaller hydraulic gradient (Fig. 2). Furthermore, a fraction of young water as high as 100 % was obtained for G3 sample with the recharge water from 1990, and  
530 a 87 % fraction was obtained by from the binary mixture of post-1989 water and old water (Table 2). The relatively modern recharge for the G3 sample was likewise explained by its high DO (9.8 mg L<sup>-1</sup>; Table 1) and relatively low nitrate concentration (7.9 mg L<sup>-1</sup> from Ma et al., 2018), which represented the contribution of high-altitude recharge rather than the old water.

535 CFC contamination and sorption in the unsaturated zone during recharge considerably influenced the interpretation of  
groundwater recharge. Points off the curves in the cross-plot of CFC concentrations may indicate contamination from the  
urban air with CFCs during sampling (Carlson et al., 2011; Cook et al., 2006; Mahlknecht et al., 2017) or the degradation or  
sorption of CFC-11 or CFC-113 (Plummer et al., 2006b). Figure 7 demonstrates that the urban air with CFC contaminations,  
which generally increased CFC concentrations above the global background atmospheric CFC concentrations for the  
Northern Hemisphere, are unlikely. Elevated CFC concentrations have been reported in the air of urban environments such  
540 as Las Vegas, Tucson, Vienna and Beijing (Barletta et al., 2006; Carlson et al., 2011; Han et al., 2007; Qin et al., 2007)  
rather than in the arid regions of Northwest China (Barletta et al., 2006). Hence, the anomalous ratios of CFC-11/CFC-12  
(Fig. 7b) off the model lines might be attributed to sorption in the unsaturated zone during recharge rather than the  
degradation of CFC-11 (Cook et al., 2006; Plummer et al., 2006b) under anoxic conditions (Table 1, DO values vary from  
0.7 to 9.8 mg L<sup>-1</sup>). Nevertheless, the small deviations (Fig. 7b) indicate a low sorption rate. A higher CFC sorption rate  
545 occurs with high clay fraction and high organic matter in soils (Russell and Thompson, 1983), and vice versa (Carlson et al.,  
2011). Therefore, the hypothesis of a low sorption rate due to the low clay fraction and low organic matter content in the  
intermountain depression and the piedmont plain (Fig. 1c) seems reasonable.

The time lag for CFC transport through the thick unsaturated zone (Cook and Solomon, 1995), as well as degradation,  
especially for CFC-11 being common in anaerobic groundwater (Horneman et al., 2008; Plummer et al., 2006b), are both  
550 important considerations when interpreting groundwater recharge using CFC concentrations. The time lag for CFC  
diffusions through the deep unsaturated zone in simple porous aquifers, a function of the tracer solubility in water, tracer  
diffusion coefficients, and soil water content (Cook and Solomon, 1995), have been widely proved (Darling et al., 2012; Qin  
et al., 2011). The small differences in CFC-11 and CFC-12 recharge years (Table 2) demonstrate that the time lag should be  
short in the faulted-hydraulic drop alluvium aquifers with the deep unsaturated zone (Fig. 1c). Studies on the MRB (Ma et  
555 al., 2018; Wang, 2007; Zhou, 1992) have shown that groundwater mainly recharged by the river fast leakage in the upstream  
area and piedmont plain, where the soil texture consists of pebbles and sandy gravel (Fig. 1c); this suggests that the  
unsaturated zone air CFC closely follows that of the atmosphere, so the recharge time lag through the unsaturated zone is not  
considered.

#### **4.2.3 <sup>3</sup>H and <sup>14</sup>C indications**

560 Groundwater recharge was determined using <sup>14</sup>C activity in groundwater for time intervals from centuries to millenniums  
(Custodio et al., 2018), and <sup>3</sup>H has been used for modern precipitation recharge, especially during the nuclear bomb periods  
(Cook et al., 2017; Huang et al., 2017). Groundwater <sup>3</sup>H activity varied from 60 to 1.1 TU (Fig. 4 and Table 1), with the  
highest value in UG (G4), followed by MG (mean 12.4 TU) and DG (mean 4.5 TU). All of the <sup>3</sup>H values in UG (G1, G2,  
and G4) and G23 (belonging to MG) were higher than 34.3 TU, which indicated some fractions of the 1960s precipitation  
565 recharge. Groundwater with <sup>3</sup>H activity lower than 5.6 TU contained some pre-1950s recharge.

Both  $^3\text{H}$  and  $^{14}\text{C}$  activities showed large variations with the distance to the mountainous region along groundwater flow paths in the midstream area (Fig. 8), suggesting recharge over a mixture of short to long timescales. Two different trends for the distribution of  $^3\text{H}$  activity with distance to the mountainous region (Fig. 8) from the upstream to midstream areas were observed. First, increase in  $^3\text{H}$  activity in groundwater in the upstream area from 41.1 (G1 and G2) to 60 TU (G4) with distance indicated a larger fraction of 1960s precipitation for G4 than for G1 and G2; indeed, as seen in Fig. 2, near G4 samples exhibited the highest hydraulic gradient values. Second,  $^3\text{H}$  activity in groundwater in the midstream area showed an obvious reduction trend along the Manas River from 37.5 (G23) to 1.1 TU (G14), indicating that more fractions of pre-bomb precipitation recharge may have occurred along the groundwater flow direction in the north of the fault. Furthermore,  $^{14}\text{C}$  activity in the MG showed small increases with distance (Fig. 8) from 43.4 to 54.6 pMC, with the exception of sample G12 at approximately 54 km (86.9 pMC with a  $^{14}\text{C}_{\text{corr}}$  age of -684 yrs; modern recharge; Table 1), whereas that in the DG decreased to 23.5 pMC. The presence of detectable  $^3\text{H}$  (2.9–6.91 TU) in DG with low  $^{14}\text{C}$  values (23.5–34.3 pMC) indicated that some mixing with post-bomb precipitation recharge may have occurred.

Combined use of CFCs and  $^3\text{H}$  may help resolve even more complicated recharge features due to the large difference of the temporal pattern in the input functions between CFCs and  $^3\text{H}$ . Compared with plots comparing tracer ratios, tracer-tracer concentration plots have some advantages because they reflect more directly the measured quantities and potential mixtures (Plummer et al., 2006b), such as mixing with irrigation water (Han et al., 2012, 2015; Koh et al., 2012) or young water mixtures in different decades (Han et al., 2007; Qin et al., 2011). The plot of  $^3\text{H}$  vs. CFC-12 (Fig. 9; CFC-11 and CFC-113 can substitute for CFC-12) shows that some samples (G9, G15 and G20) are slightly above the piston flow line, whereas in Fig. 7a they are away from the piston flow line but on the binary mixing lines. G15 and G20 had the shallowest well depths of 23 and 13 m, respectively. The G9 sample was collected from the piedmont plain near Manas River (Fig. 2), which features pebbles and sandy gravel deposits. This situation may be explained by (i) binary mixing between post-1989 water and older water recharged between 1950 and 1970 that did not contain CFC-free water (pre-1940) or (ii) mixing of two end-members with one end-member containing various mixtures of young (but pre-1989) and old water and the other end-member having post-1989 water. The second explanation requires samples to contain at least some post-bomb fractions from the 1960s (revealed by  $^3\text{H}$  concentrations; Fig. 9) and both post-1989 and pre-1940 water, which is not consistent with CFC data (Fig. 7a). If the first explanation is true, the binary mixing hypothesis and the young water (post-1940) fractions in Table 2 for these three samples should be adjusted accordingly.

Because atmospheric  $^3\text{H}$  concentrations have been elevated for a long time, old water components can be identified by  $^3\text{H}$  concentrations that are anomalously low compared with those of CFCs (Plummer et al., 2006b). The G5 sample contained very low CFC-113 with a  $^3\text{H}$  concentration of 3.8 TU (Table 1), indicating that this sample was likely mixed by the older water (pre-1940) and 1960–1970 water. The low  $^3\text{H}$  concentration can be attributed to the dilution by a high fraction of old water, and thus the “ $^3\text{H}$  bomb-peak” cannot be recognised. The G16 sample, outside of the shaded region (Fig. 9), has low  $^3\text{H}$  but a substantial CFC concentration. This situation may be explained by (i) exposure to the atmosphere before sampling during large water table fluctuations due to groundwater pumping or the addition of excess air to water through the fractured

600 system or (ii) river water or reservoir water  $^3\text{H}$  concentration but minimal  $^3\text{H}$  recharge. Furthermore, the  
relatively high fractions of young water (89 %; Table 2) preclude the dilution effect by the old water. Irrigation re-  
infiltration can cause a shift of the CFC concentrations to higher values but does not alter the  $^3\text{H}$  concentration (Han et al.,  
2015). However, the relatively low  $\text{NO}_3^-$  concentrations (4.51 mg  $\text{L}^{-1}$ ; data from Ma et al., 2018) of the G16 sample  
605 suggested that irrigation re-infiltration did not have a significant effect. Therefore, river or reservoir water with very low  
 $\text{NO}_3^-$  concentration (2.7–7.3 mg  $\text{L}^{-1}$ ; data from Ma et al., 2018) recharge is possible.

#### 4.4.3 Groundwater mean ~~transit~~residence times

##### 4.34.1 $^3\text{H}$ and CFCs

610 ~~In this study the input CFCs concentrations are from the time series trend of Northern Hemisphere atmospheric~~  
~~mixing ratio (Fig. 5). The time series  $^3\text{H}$  activities as the input data (Fig. 6) are still necessary that is based on the~~  
~~following two considerations. First, the study area is located in the Northern Hemisphere, where the bomb test  $^3\text{H}$~~   
~~activities were several orders of magnitude higher than in the Southern Hemisphere (Clark and Fritz, 1997; Tadros~~  
~~et al., 2014).  $^3\text{H}$  activity in the atmosphere was superimposed over the China atmospheric nuclear tests from 1964 to~~  
615 ~~1974 in the arid northwest China, and thus the remnant  $^3\text{H}$  activities are still affected by the tail end of the bomb~~  
~~pulse. Second, the study area is more than 3500 km far away from the western pacific, where  $^3\text{H}$  activity in the~~  
~~atmosphere is evidently much higher than coastal sites due to the continental effect (Tadros et al., 2014). Furthermore,~~  
~~though  $^3\text{H}$  activity in the atmosphere is known to vary between seasons (Cartwright and Morgenstern, 2016;~~  
~~Morgenstern et al., 2010; Tadros et al., 2014), the year-round mean values (Fig. 6) were adopted in this study.~~

Each ~~transit~~RTD time distribution functions (Eqs. (23) to (45)) ~~has its~~are suited to specific hydrogeological situations ~~in~~  
~~the hydrologic system to which it is applicable~~ (Maloszewski and Zuber, 1982); ~~which the~~ EPM is particularly useful for  
620 interpretation of MTTsMRTs in aquifers that have regions of both exponential and piston flow (Cartwright et al., 2017). The  
unconfined aquifers ~~that~~ adjacent to the rivers (Fig. 1 c) are likely to exhibit exponential flow, and recharge through the  
unsaturated zone (Fig. 1c) will most likely resemble piston flow (Cartwright and Morgenstern, 2015; Cook and Böhlke,  
2000). For the time series  $^3\text{H}$  and CFCs inputs, MTTsMRTs (Fig. 810) were initially calculated using ~~the~~ EPM, with an EPM  
ratio of 1.5 obtained using Eqs. (2) and (3) ( $I_E$  in Eq. (23)) is determined by adding the intermountain depression to the  
625 piedmont plain in Fig. 1c) ~~via Eqs. (1) and (2)~~. River leakage and rainfall input were possible from the piedmont plain (Ma et  
al., 2018), thus a less proportion of piston flow by the EPM with an EPM ratio of 2.2 ( $I_E$  in Eq. (23)) is only in the piedmont  
plain in Fig. 1c) was also used. To test the veracity the DM with  $D_p$  of 0.03 and 0.1 and the EMM were also used to  
calculate the MTTsMRTs via Eqs. (42), (34) and (45). Plots of the output concentrations for  $^3\text{H}$  (Fig. 8a10a) and CFCs  
(CFC-11 in Fig. 8b10b, CFC-12 in Fig. 8e-10c and CFC-113 in Fig. 8d10d) vs. MTTsMRTs for different lumped parameter  
630 models show wide MTTsMRTs ranges that increase with the increasing MTTsMRTs.

Figure 9-11 shows that different LPMs yield different MTTsMRTs for the same time ~~series~~series of  $^3\text{H}$  activities and  
CFC concentrations; ~~which~~ MTTsMRTs obtained from different LPMs tend toward to become more discrete discretized by  
model with ~~their~~ increasing MRTs. For the CFCs rainfall inputs (Fig. 9a, b), MTTsMRTs from ~~the~~ EPM with an EPM ratio



of 1.5 (Fig. 9a11a) varied from 19 to 101 yrs with a (median: of 51 yrs) for the CFC-12 rainfall input, from 33 to 115 yrs  
635 with a (median: of 62.3 yrs) for the CFC-11 rainfall input, and from 18 to 92 yrs with a (median: of 50.2 yrs) for the CFC-  
113 rainfall input. Good linear relationships for the ~~MTTsMRTs~~ between the different CFCs rainfall inputs were obtained  
using the same EPM (EPM (1.5) in Fig. 9a-11a and EPM (2.2) in Fig. 9b11b). ~~MTTsMRTs~~ increased with the decreasing  
EPM ratios (from 2.2 to 1.5; Fig. 9b11b), implying that the longer flow paths that were recharged from the intermountain  
depression. For the range of CFC-12 concentrations in the UG and in the west bank of the 'East Main Canal' of MG,  
640 similar ~~MTTsMRTs~~ were estimated from the different ~~lumped-parameter-modelLPMs~~ (Fig. 9b11b) with mean values  
varying from 28.6 to 64.8 yrs, while-whereas those in the east bank of the 'East main canal' (Figs. 9b 2 and 11b and Table 2)  
of MG show larger differences with mean values varying from 129.2 to 173 yrs. ~~TotallyOverall~~, the youngest value was  
observed for-in the G3 sample (south of the fault), while-and the oldest was for-in the G5 sample (east bank of the 'East  
~~mMain eCanal~~'; Fig. 2).

645 ~~By-In~~ contrast with-to the CFCs rainfall inputs, ~~MTTsMRTs~~ estimated using the <sup>3</sup>H rainfall inputs by different LPMs (Fig.  
9e11c) show larger uncertainties and wider ranges. For the EPM with an EPM ratio of 1.5, ~~MTTsMRTs~~ vary from 19 to 158  
yrs with a median of 112.2 yrs (Fig. 9e11c), which are much longer than those calculated from the CFCs rainfall inputs by  
the same model (Fig. 9b11b). The differences could be due to the longer travel times through the thick unsaturated zone for  
<sup>3</sup>H than CFCs. <sup>3</sup>H moves principally in the liquid phase, while-whereas CFCs travel in the gas phase through the unsaturated  
650 zone (Cook and Solomon, 1995). The more rapid transport for gas-phase than liquid-phase in the unsaturated zone would be  
expected to give rise to longer ~~transitresidence~~ times from <sup>3</sup>H than those determined from CFCs (Cook, et al., 2017).  
Furthermore, the ranges in ~~MTTsMRTs~~ estimated from the EPM with EPM ratios of 1.5 and 2.2, the-DM with  $D_p$  of 0.03  
and 0.1, and the-EMM are 16–158 yrs, 72–285 yrs, and 30–360 yrs, respectively. Similar ~~MTTsMRT~~ trends were with that  
calculated from the CFC-12 input were-observed (Fig. 9b11b), in which separate the west and east banks of the 'East Main  
655 ~~Canal~~' of MG and DG were separated from each other. Uncertainties increase with the increasing ~~MTTsMRTs~~ among the  
different models, especially when ~~MTTsMRTs~~ > are higher than 130 yrs (Fig. 9e11c), which the samples are mainly  
~~occurred in samples~~ collected from the east bank of the 'East Main Canal' of MG and DG.

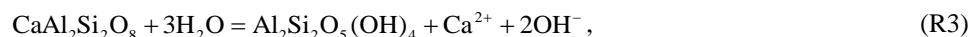
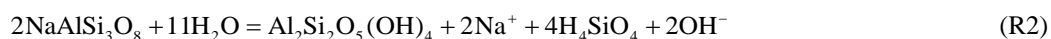
~~The-Because the~~ east bank of the 'East main canal' groundwater with had a relatively short distance to mountain (Fig. 7b)  
and with a much smaller hydraulic gradient (Fig. 2), have much the older ~~MTTsMRTs~~ (Fig. 9b, e) were much longer than  
660 those in the west bank. That in the west bank shows an overall increasing trend with the distance to mountain in MG and DG  
(Fig. 9b11b, c) as the longer and deeper flow paths usually give rise to the longer ~~MTTsMRTs~~ (Cartwright and Morgenstern,  
2015, 2016; McGuire et al., 2005). Despite the influence from the uncertainties of the input concentrations and different  
models (Cartwright and Morgenstern, 2015, 2016), ~~MTTsMRTs~~ have been identified to vary on account of more complex  
interplay of factors like mixing and dispersion in the flow systems, which may result in significantly different ~~MTTsMRTs~~  
665 from results calculated by LPMs assuming a homogeneous aquifer with a simple geometry to the actual results (Cartwright  
et al., 2017; Kirchner, 2016; Stewart et al., 2017). Nevertheless, in this study the homogeneous aquifers, being at steady-  
state, have been assumed to justifying the use the-of LPMs to calculate the ~~MTTsMRTs~~.

#### 4.43.2 Hydrochemistry evolution

670 Strong correlations ~~of-between~~ hydrochemical~~stry~~ components ~~with-and~~ groundwater age ~~permitting-permit the~~  
~~hydrochemistry to be used~~ their use as proxies ~~for~~ or complementary ~~for-to~~ age via previously established relationships in  
close lithological conditions. ~~For example, A~~an excellent correlation between silica (SiO<sub>2</sub>) and ~~MTTsMRTs with the~~  
~~correlation coefficient (R<sup>2</sup>-of=0.997)~~ was reported (Morgenstern et al., 2010), which ~~shows-was~~ much higher ~~R<sup>2</sup>~~-than in Fig.  
~~10-12~~ and in other results (Morgenstern et al., 2015). ~~Silica~~-(SiO<sub>2</sub>-(Fig. ~~10a12a~~), sulfate (SO<sub>4</sub><sup>2-</sup>), bicarbonate (HCO<sub>3</sub><sup>-</sup>)<sub>2</sub> and  
675 total dissolved solids (TDS) (Fig. ~~10b12b~~) ~~both-all~~ show good correlations with groundwater age, indicating that mineral  
dissolutions ~~by-through~~ water-rock interactions dominate ~~the~~ hydrochemical~~stry~~ changes (Ma et al., 2018), ~~during-whichand~~  
major ion concentrations increase with groundwater age. However, ~~MTTsMRTs~~ estimated ~~by-using~~ <sup>3</sup>H ~~activities-activity~~  
showed poor correlations with the ions (data not shown). ~~Besides~~Moreover, the lithology type groundwater flow through  
within the aquifer and the likely evolutionary path ways play an important role in the hydrochemical~~stry~~ compositions. The  
negative saturation indices (~~SI~~) with respect to gypsum of all waters (Ma et al., 2018) indicated d that the high SO<sub>4</sub><sup>2-</sup>  
680 concentrations (Fig. ~~10b12b~~) ~~would-be-ascribed-were due~~ to the gypsum dissolution in the ~~t~~Tertiary stratum. Also note that  
high SO<sub>4</sub><sup>2-</sup> can be originated from the geothermal water (Morgenstern et al., 2015), in contrast to studies such as Guo et al.  
(2014) and Guo et al. (2017), and can be biased due to anoxic SO<sub>4</sub><sup>2-</sup> reduction. However, the groundwater with relatively  
low temperatures and aerobic environment (Table 1) make the two cases above unlikely.

The combination of hydrochemistry concentrations and groundwater age data is also a powerful tool for investigating the  
685 groundwater flow processes and flow through conditions (McGuire and McDonnell, 2006; Morgenstern et al., 2010, 2015),  
identifying the natural groundwater evolution and the impact of anthropogenic contaminants (Morgenstern et al., 2015;  
Morgenstern and Daughney, 2012), ~~and-giving-more-accurate-prediction-of-the-contaminants-like-nitrate-than-either-source-of~~  
~~information~~. The pH of groundwater decreases s from 10.1 to 8.6 over the age range from 19 to 101 yrs, with a log law fit of  
pH = 0.72 × ln(MTTs) + 11.85, R<sup>2</sup> = 0.65 (Fig. ~~10a12a~~). On the contrary, a trend of increasing pH with increasing  
690 groundwater age has been reported in New Zealand (the dashed red line shown in Fig. ~~10a12a~~; Morgenstern et al., 2015),  
where the pH values were overall less than 7.2. These two discrepant trends can be explained by the relationship between the  
pH and HCO<sub>3</sub><sup>-</sup> concentrations in water (inserted plot in Fig. ~~10a12a~~), which the pH increase with increasing HCO<sub>3</sub><sup>-</sup>  
concentrations only when the pH is less than 8.34, otherwise decrease with increasing HCO<sub>3</sub><sup>-</sup> concentrations. Therefore, the  
trend of increasing HCO<sub>3</sub><sup>-</sup> concentrations with increasing groundwater age (Fig. ~~10b12b~~) in this study indicates that  
695 decreasing trend for the pH (from 10.1 to 8.6) is reasonable.

The soda waters with the overall pH higher than 8.1 (Table 1) are in disequilibrium with primary rock-forming minerals  
of the host rocks. The incongruent dissolutions of the albite and anorthite through hydrolysis reaction are:



700 where all the chemical components of the albite and anorthite release into the solution phase and produce  $\text{OH}^-$  with simultaneous precipitation of kaolinite. A trend of increasing pH with ~~increasing~~-well depth (Table 1) suggests that groundwater with pH ~~<lower than~~ 9 was likely recharged by  $\text{CO}_2$ -containing water, because ~~the~~- $\text{OH}^-$  generally interacts with  $\text{CO}_2$  and/or organic acids in the soil to form  $\text{HCO}_3^-$  ~~in the water~~ (Wang et al., 2009). ~~Likewise~~Similarly, the trend of decreasing pH with increasing ~~MTTs~~MRTs (Fig. ~~10a~~12a) indicates ~~higher-that water~~  $\text{CO}_2$ -containing ~~higher~~  $\text{CO}_2$  concentrations ~~water-with~~has longer ~~MTTs~~MRT, which seems to suggest the anthropogenic input. The nitrate ( $\text{NO}_3^-$ ) concentrations ~~varied~~ from 4.5 to 20.2  $\text{mg L}^{-1}$  with a median of 12.2  $\text{mg L}^{-1}$  (~~data~~ not shown), which exceeded the natural nitrate concentration in groundwater of 5–7  $\text{mg L}^{-1}$  (Appelo and Postma, 2005). The development of the plough after the 1950s, N- $\text{NO}_3$  fertilizer (with low  $^{87}\text{Sr}/^{86}\text{Sr}$  ratios; Ma et al., 2018) and the extensive groundwater withdrawal ~~groundwater~~ for irrigation (Ji, 2016) suggest that irrigation infiltration could account for the ~~groundwater~~-high groundwater  $\text{NO}_3^-$  concentrations in the piedmont plain. However, little irrigation infiltration was observed in the downstream area with groundwater  $\text{NO}_3^-$  concentrations of ~~<less than~~ 5  $\text{mg L}^{-1}$  (Ma et al., 2018) due to the water-saving irrigation style, which ~~had non-contributes~~ did not contribute to groundwater recharge in the arid regions of Northwest China.

#### 4.5 Groundwater mixing

##### 4.5.1 CFC ratios

715 ~~Comparing CFC concentrations has provided a powerful tool to recognize samples containing co-existence of young (post-1940) water with old (CFC-free) water (Han et al., 2007; Han et al., 2012; Koh et al., 2012) or exhibiting contamination or degradation (Plummer et al., 2006b). The cross-plot of the concentrations for CFC-113 and CFC-12 (Fig. 11a) demonstrates that all of the groundwater can be characterized as binary mixtures between young and older components, though there is still room for some ambiguity around the crossover in the late 1980s (Darling et al., 2012). As shown in Fig. 11a, all of the MG samples are located in the shaded region, representing no post-1988.5 waters recharge. The UG (G3) sample is clearly quite 'modern' and seems to be recharged in 1989.5 through piston flow or mixed by the old water and post-1988.5 water. Using the method described by Plummer et al. (2006b) with the binary mixing model (BMM), the fractions of young water vary from 12 to 91 % (Table 2) for the MG samples with the relatively low young fractions of 12 and 18 % in the east bank of the 'East main canal' of MG samples (G5 and G7). These two well water table depths are more than 40 m, probably indicating a relatively slow and deep-circulated groundwater flow. This hypothesis is also suggested by lower DO (3.7–4.6  $\text{mg L}^{-1}$ ; Table 1) and nitrate concentrations (8.6–9.5  $\text{mg L}^{-1}$  from Ma et al., 2018) and relatively much smaller hydraulic gradient (Fig. 2). Furthermore, as high as 100 % fraction of young water for G3 sample is obtained with the recharge water from 1989.5, or 87 % fraction is obtained by the binary mixture between post-1988.5 water and old water (Table 2). The quite 'modern' recharge for G3 sample is likewise explained by its highest DO (9.8  $\text{mg L}^{-1}$ ; Table 1) and relatively low nitrate concentration (7.9  $\text{mg L}^{-1}$  from Ma et al., 2018), which represent the contribution of high-altitude recharge rather than the old-age water.~~

720  
725  
730

The apparent ages (Table 2 and Fig. 5) estimated from the PFM and MTTs (Fig. 9a) estimated from the EPM (1.5) using CFC-113 concentrations are both generally lower than those obtained using CFC-11 and CFC-12, indicating that mixing processes are prevailing and that the simple EPM (1.5) is also not an appropriate description of the groundwater flow processes. All of the MG samples, located in the shaded region (Fig. 11a), can be regarded either as simple binary mixtures of young (1980–1988.5) water and old (CFC-free) water, or be regarded as waters with exponential piston and exponential age distributions, which seems to represent no post-1988.5 waters recharge. It should be noted that the EMM line lies at the boundary of the shaded region (Fig. 11a), suggesting that the binary mixing and EMM can be distinguished from each other for the MG samples. While waters collected from the east bank (G5, G7 and G8) and one from the west bank (G15) of the ‘East main canal’ of MG seems cannot be distinguished from the binary mixing and EPM (1.5).

Points lying off the curves in the cross-plot CFC concentrations may indicate that contaminations from the urban air with CFC compounds during sampling (Carlson et al., 2011; Cook et al., 2006; Mahlknecht et al., 2017) or degradation/sorption of CFC-11 or CFC-113 (Plummer et al., 2006b) have occurred. Figure 11 demonstrates that the urban air with CFC compounds contaminations, which generally cause elevated CFC concentrations than the global background atmospheric CFC concentrations (Northern Hemisphere), are unlikely. Elevated CFC concentrations have been reported in the air of urban environments such as Las Vegas, Tucson, Vienna and Beijing (Barletta et al., 2006; Carlson et al., 2011; Han et al., 2007; Qin et al., 2007), contrary to that in the arid northwest China (Barletta et al., 2006). Hence, the anomalous CFC-11/CFC-12 (Fig. 11b) and CFC-113/CFC-11 (Fig. 11c) ratios plotting off the model lines might be ascribed to the following two hypotheses:

First, sorption in the unsaturated zone during recharge rather than the degradation of CFC-11 (Cook et al., 2006; Plummer et al., 2006b) under anoxic conditions (Table 1, DO values vary from 0.7 to 9.8 mg L<sup>-1</sup>). Nevertheless, the small deviations (Fig. 11b, c) indicate that the hypothesized sorption rate was low. Higher CFC sorption rate with high clay fraction and high organic matter in soils have been proved (Russell and Thompson, 1983), and vice versa (Carlson et al., 2011). Therefore, the hypothesis of a low sorption rate due to the low clay fraction and low organic matter content in the intermountain depression and the piedmont plain (Fig. 1c) seems reasonable.

Second, the time lag for CFCs movement both in dissolved and gas phases through deep unsaturated zone. The time lag for the diffusive transport of CFCs through deep unsaturated zone in simple porous aquifers, a function of the tracer solubility in water, tracer diffusion coefficients and soil water content (Cook and Solomon, 1995), have been widely proved (Darling et al., 2012; Qin et al., 2011). The little or no separation in CFC-11 and CFC-12 apparent ages (Table 2) demonstrates that the time lag would be short in the faulted hydraulic drop alluvium aquifers with deep unsaturated zone (Fig. 1c), meaning that groundwater CFCs ages obtained in this study effectively represent transit times since recharge reached the water table.

#### 4.5.2 CFC-12 vs. tritium data

Combined use of CFCs and <sup>3</sup>H may provide further help to resolve even more complicated mixing scenarios due to the large difference of the temporal pattern of the input functions between CFCs and <sup>3</sup>H. Tracer-tracer concentration plots have some advantages over plots comparing apparent ages and tracer ratios because they reflect more directly the measured quantities

and potential mixtures (Plummer et al., 2006b), such as mixing with irrigation water (Han et al., 2012, 2015; Koh et al., 2012) or young water mixtures in different decades (Han et al., 2007; Qin et al., 2011). Plot of  $^3\text{H}$  vs. CFC-12 (Fig. 11d; CFC-11 and CFC-113 can substitute for CFC-12) shows that some samples (G9, G15 and G20) plot on or slight upward deviation to the piston flow line, while in Fig. 11a plot away from the piston flow line but on the binary mixing lines. G15 and G20 samples have the shallowest well depths of 23 and 13 m, respectively. G9 sample is collected from the piedmont plain with pebbles and sandy gravel deposits, nearing the Manas River (Fig. 2). There are two possible explanations for this situation: (i) binary mixing between post-1988.5 water and older water recharged from 1950 to 1970, not containing CFC-free waters (pre-1940) (ii) mixtures from two end-members with one end-member has an age distribution close to the EPM (1.5) or EMM and the other end-member has post-1988.5 water. The second explanation requires that the samples contain at least some post-bomb fractions in the 1960s (revealed by  $^3\text{H}$  concentrations; Fig. 11d), and it also allows that the samples contain both post-1988.5 and pre-1940 waters, which however not revealed by CFC data (Fig. 11a). If the first explanation valid, the binary mixing hypothesis and the young water (post-1940) fractions in Table 2 for these three samples should be adjusted accordingly.

Because atmospheric  $^3\text{H}$  concentrations have been elevated for a long time, old water components can be identified by anomalously low  $^3\text{H}$  activities in comparison with CFCs (Plummer et al., 2006b). G5 sample contain very low CFC-113 with  $^3\text{H}$  of 3.8 TU (Table 1), likely indicating that this sample was mixed by the older water (pre-1940) and 1960–1970 water. The low  $^3\text{H}$  concentration can be ascribed to the dilution by a high fraction of old water, and thus the ‘ $^3\text{H}$  bomb peak’ cannot be recognized. G16 sample, outside of the shaded region (Fig. 11d), has low  $^3\text{H}$  but significant CFC concentration. Two possible explanations have been obtained: (i) exposed to the atmosphere before sampling during large water table fluctuations due to groundwater pumping or add excess air to water through fractured system, (ii) river water or reservoir water with high CFC but minimal  $^3\text{H}$  recharge. Furthermore, the relatively high fractions of young water (89 %; Table 2) preclude the dilution effect by the old water. Irrigation re-infiltration can cause a shift of the CFC concentrations to higher values but not alter the  $^3\text{H}$  concentration (Han et al., 2015). However, the relatively low  $\text{NO}_3^-$  concentrations ( $4.51 \text{ mg L}^{-1}$ ; data from Ma et al., 2018) of G16 sample suggest that irrigation re-infiltration is also not significant compared to the two explanations mentioned above. It seems that river water or reservoir water with very low  $\text{NO}_3^-$  concentrations ( $2.7\text{--}7.3 \text{ mg L}^{-1}$ ; data from Ma et al., 2018) recharge is possible.

## 5 Conclusions

In this study, ~~the we used~~ environmental tracers and hydrochemistry ~~have enabled us~~ to identify the modern and paleo-meteoric recharge sources, to constrain the different end-members mixing ~~rates/ratios~~, and ~~to~~ study the mixed groundwater ~~mean transit times~~ MRTs in faulted-hydraulic drop alluvium aquifer systems. The paleo-meteoric recharge in a cooler climate ~~was distinguished from~~ ~~rather than~~ the lateral flow from the higher elevation precipitation in the Manas River downstream area ~~was distinguished~~. The thrust faults were found to play a paramount role on groundwater flow paths and

mean transit times due to their block water features, where ~~the quite relatively~~ modern<sup>2</sup> groundwater with young (post-  
800 1940) water fractions of 87–100 % was obtained, indicating a small ~~mixing degree~~ extent of mixing in the south of the fault. The short ~~mean transit time~~ MRTs (19 yrs) along with the higher ~~than natural~~ NO<sub>3</sub><sup>-</sup> concentration (7.86 mg L<sup>-1</sup>) ~~than natural~~ groundwater (5 mg L<sup>-1</sup>) in the south of the fault (headwater area), ~~implying the~~ indicated the invasion of modern contaminants, ~~invading, which should arouse people's~~ This finding warrants particular attention. ~~Large-High amplitudes of~~ mixing rate ~~amplitudes~~ varying from 12 to 91 % were widespread in ~~the~~ north of the fault due to the varying depths of long-  
805 screened boreholes ~~or as well as~~ within the aquifer itself. Furthermore, ~~the mixing diversity was highlighted by~~ the large ~~substantial~~ water table fluctuations during groundwater pumping, vertical recharge through the thick unsaturated zone, and young water mixtures in different decades ~~highlight the mixing diversity~~. The ~~obtained~~ strong correlations between groundwater ~~mean transit time~~ MRTs and hydrochemical ~~istry~~ concentrations ~~allow the~~ enable a first-order proxy at different times to be ~~made used~~. In addition, ~~our~~ this study has ~~also highlighted~~ revealed that ~~mean transit time~~ MRTs estimated by  
810 CFCs ~~rather than~~ <sup>3</sup>H were more appropriate ~~than those using~~ <sup>3</sup>H due to the highly complex groundwater systems in the arid ~~MRB~~ with a thick unsaturated zone.

*Author contributions.* Xing Liang and Jing Li were responsible for the <sup>3</sup>H and <sup>14</sup>C analyses. Bin Ma undertook the sampling program and oversaw the analysis of the hydrochemistry and CFCs. Bin Ma and Mengui Jin prepared the manuscript.

*Competing interests.* The authors declare that they have no conflict of interest.

815 *Acknowledgements.* This research was financially supported by the National Natural Science Foundation of China (~~2015–2018~~, no. U1403282 and no. 41807204). ~~The authors would like to thank Dr. Yunquan Wang for the valuable discussions and suggestions for this paper. We wish to thank Dr. Xumei Mao, Dr. Dajun Qin and Mr. Yalei Liu for sampling and laboratory works. We also wish to thank the editor and anonymous referees for their valuable suggestions and insightful comments.~~

## 820 References

- Aggarwal, P. K.: Introduction, in: Isotope Methods for Dating Old Groundwater, Suckow, A., Aggarwal, P. K., and Araguas-Araguas, L. (Eds.), International Atomic Energy Agency, Vienna, Austria, 1–4, 2013.
- Appelo, C. A. J. and Postma, D.: Geochemistry, groundwater and pollution, 2<sup>nd</sup> ed., Balkema, Dordrecht, Netherlands, 2005.
- Atkinson, A. P., Cartwright, I., Gilfedder, B. S., Cendón, D. I., Unland, N. P., and Hofmann, H.: Using <sup>14</sup>C and <sup>3</sup>H to  
825 understand groundwater flow and recharge in an aquifer window, Hydrol. Earth Syst. Sci., 18, 4951–4964, doi:10.5194/hess-18-4951-2014, 2014.

- Barletta, B., Meinardi, S., Simpson, I. J., Rowland, F. S., Chan, C. Y., Wang, X., Zou, S., Chan, L. Y., and Blake, D. R.: Ambient halocarbon mixing ratios in 45 Chinese cities, *Atmos. Environ.*, 40, 7706–7719, doi:10.1016/j.atmosenv.2006.08.039, 2006.
- 830 Battle–Aguilar, J., Banks, E. W., Batelaan, O., Kipfer, R., Brennwald, M. S., and Cook, P. G.: Groundwater residence time and aquifer recharge in multilayered, semi–confined and faulted aquifer systems using environmental tracers, *J. Hydrol.*, 546, 150–165, doi:10.1016/j.jhydrol.2016.12.036, 2017.
- [Benettin, P., Volkmann, T. H. M., Freyberg, J., Frentress, J., Penna, D., Dawson, T. E., and Kirchner, J. W.: Effects of climatic seasonality on the isotopic composition of evaporating soil waters, \*Hydrol. Earth Syst. Sci.\*, 22, 2881–2890, doi:10.5194/hess-22-2881-2018, 2018.](#)
- 835 Beyer, M., Jackson, B., Daughney, C., Morgenstern, U., and Norton, K.: Use of hydrochemistry as a standalone and complementary groundwater age tracer, *J. Hydrol.*, 543, 127–144, doi:10.1016/j.jhydrol.2016.05.062, 2016.
- Carlson, M. A., Lohse, K. A., McIntosh J. C., and McLain J. E. T.: Impacts of urbanization on groundwater quality and recharge in a semi–arid alluvial basin, *J. Hydrol.*, 409, 196–211, doi:10.1016/j.jhydrol.2011.08.020, 2011.
- 840 Cartwright, I., Cendón, D., Currell, M., and Meredith, K.: A review of radioactive isotopes and other residence time tracers in understanding groundwater recharge: Possibilities, challenges, and limitations, *J. Hydrol.*, 555, 797–811, doi:10.1016/j.jhydrol.2017.10.053, 2017.
- Cartwright, I., Irvine, D., Burton, C., and Morgenstern, U.: Assessing the controls and uncertainties on mean transit times in contrasting headwater catchments, *J. Hydrol.*, 557, 16–29, doi:10.1016/j.jhydrol.2017.12.007, 2018.
- 845 Cartwright, I. and Morgenstern, U.: Contrasting transit times of water from peatlands and eucalypt forests in the Australian Alps determined by tritium: implications for vulnerability and source of water in upland catchments, *Hydrol. Earth Syst. Sci.*, 20, 4757–4773, doi:10.5194/hess-20-4757-2016, 2016.
- Cartwright, I. and Morgenstern, U.: Transit times from rainfall to baseflow in headwater catchments estimated using tritium: the Ovens River, Australia, *Hydrol. Earth Syst. Sci.*, 19, 3771–3785, doi:10.5194/hess-19-3771-2015, 2015.
- 850 Chen, Z., Qi, J., Xu, J., X, J., Ye, H., and Nan, Y.: Paleoclimatic interpretation of the past 30 ka from isotopic studies of the deep confined aquifer of the North China Plain, *Appl. Geochem.*, 18, 997–1009, doi:10.1016/S0883-2927(02)00206-8, 2003.
- Clark, I. D. and Fritz, P.: *Environmental Isotopes in Hydrogeology*, Lewis, New York, USA, 1997.
- Craig, H.: Isotopic variations in meteoric waters, *Science*, 133, 1702–1703, doi:10.1126/science.133.3465.1702, 1961.
- 855 Cook, P. G., and Böhlke, J. K.: Determining timescales for groundwater flow and solute transport, in: *Environmental Tracers in Subsurface Hydrology*, Cook, P. G. and Herczeg, A. L. (Eds.), Kluwer, Boston, Netherlands, 1–30, 2000.
- Cook, P., Dogramaci, S., McCallum, J., and Hedley, J.: Groundwater age, mixing and flow rates in the vicinity of large open pit mines, Pilbara region, northwestern Australia, *Hydrogeol. J.*, 25, 39–53, doi:10.1007/s10040-016-1467-y, 2017.

- Cook, P. G., Plummer, L. N., Solomon, D. K., Busenberg, E., and Han, L. F.: Effects and processes that can modify apparent  
860 CFC age, in: Use of Chlorofluorocarbons in Hydrology: A Guidebook, Gröning, M., Han, L. F., and Aggarwal, P. (Eds.),  
International Atomic Energy Agency, Vienna, Austria, 31–58, 2006.
- Cook, P. G. and Solomon, D. K.: Transport of atmospheric tracer gases to the water table: Implications for groundwater  
dating with chlorofluorocarbons and krypton 85, *Water Resour. Res.*, 31, 263–270, doi:10.1029/94WR02232, 1995.
- Cui, W. G., Mu, G. J., Wen, Q., and Yue, J.: Evolution of alluvial fans and reaction to the regional activity at rase front of  
865 Manas River Valley, *Res. Soil Water Conserv.*, 14, 161–163, 2007.
- [Custodio, E., Jódar, J., Herrera, C., Custodio-Ayala, J., and Medina, A.: Changes in groundwater reserves and radiocarbon  
and chloride content due to a wet period intercalated in an arid climate sequence in a large unconfined aquifer, \*J. Hydrol.\*  
556, 427–437, doi:10.1016/j.jhydrol.2017.11.035, 2018.](#)
- Dansgaard, W.: Stable isotopes in precipitation, *Tellus*, 16, 436–468, doi:10.1111/j.2153-3490.1964.tb00181.x, 1964.
- 870 Darling, W. G., Gooddy, D. C., MacDonald, A. M., and Morris, B. L.: The practicalities of using CFCs and SF<sub>6</sub> for  
groundwater dating and tracing, *Appl. Geochem.*, 27, 1688–1697, doi:10.1016/j.apgeochem.2012.02.005, 2012.
- Dawson, T. E. and Ehleringer, J. R.: Streamside trees do not use stream water, *Nature*, 350, 335–337, 1991.
- Dreuzy, J. R. D. and Ginn, T. R.: Residence times in subsurface hydrological systems, introduction to the Special Issue, *J.*  
*Hydrol.*, 543, 1–6, doi:10.1016/j.jhydrol.2016.11.046, 2016.
- 875 Edmunds, W. M., Ma, J., Aeschbach–Hertig, W., Kipfer, R., and Darbyshire, D. P. F.: Groundwater recharge history and  
hydrogeochemical evolution in the Minqin Basin, North West China, *Appl. Geochem.*, 21, 2148–2170,  
doi:10.1016/j.apgeochem.2006.07.016, 2006.
- Gleeson, T., Befus, K. M., Jasechko, S., Luijendijk, E., and Cardenas, M. B.: The global volume and distribution of modern  
groundwater, *Nat. Geosci.*, 9, 161–167, doi:10.1038/NGEO2590, 2016.
- 880 Guo, H., Wen, D., Liu, Z., Jia, Y., and Guo, Q.: A review of high arsenic groundwater in Mainland and Taiwan, China:  
Distribution, characteristics and geochemical processes, *Appl. Geochem.*, 41, 196–217,  
doi:10.1016/j.apgeochem.2013.12.016, 2014.
- Guo, Q., Planer–Friedrich, B., Liu, M., Li, J., Zhou, C., and Wang, Y.: Arsenic and thioarsenic species in the hot springs of  
the Rehai magmatic geothermal system, Tengchong volcanic region, China, *Chem. Geol.*, 453, 12–20,  
885 doi:10.1016/j.chemgeo.2017.02.010, 2017.
- Green, C. T., Jurgens, B. C., Zhang, Y., Starn, J. J., Singleton, M. J., and Esser, B. K.: Regional oxygen reduction and  
denitrification rates in groundwater from multi–model residence time distributions, San Joaquin Valley, USA, *J. Hydrol.*,  
543, 155–166, doi:10.1016/j.jhydrol.2016.05.018, 2016.
- Han, D., Cao, G., McCallum, J., and Song, X.: Residence times of groundwater and nitrate transport in coastal aquifer  
890 systems: Daweijia area, northeastern China, *Sci. Total Environ.*, 538, 539–554, doi:10.1016/j.scitotenv.2015.08.036, 2015.
- Han, D., Song, X., Currell, M. J., Cao, G., Zhang, Y., and Kang, Y.: A survey of groundwater levels and hydrogeochemistry  
in irrigated fields in the Karamay Agricultural Development Area, northwest China: Implications for soil and groundwater



- salinity resulting from surface water transfer for irrigation, *J. Hydrol.*, 405, 217–234, doi:10.1016/j.jhydrol.2011.03.052, 2011.
- 895 Han, D. M., Song, X. F., Currell, M. J., and Tsujimura, M.: Using chlorofluorocarbons (CFCs) and tritium to improve conceptual model of groundwater flow in the South Coast Aquifers of Laizhou Bay, China, *Hydrol. Process.*, 26, 3614–3629, doi:10.1002/hyp.8450, 2012.
- Han, L., Hacker, P., and Gröning, M.: Residence times and age distributions of spring waters at the Semmering catchment area, Eastern Austria, as inferred from tritium, CFCs and stable isotopes, *Isot. Environ. Healt. S.*, 43, 31–50, 900 doi:10.1080/10256010601154015, 2007.
- Horneman, A., Stute, M., Schlosser, P., Smethie Jr. W., Santella, N., Ho, D. T., Mailloux, B., Gorman, E., Zheng, Y., and van Geen, A.: Degradation rates of CFC–11, CFC–12 and CFC–113 in anoxic shallow aquifers of Araihaazar Bangladesh, *J. Contam. Hydrol.*, 97, 27–41, doi:10.1016/j.jconhyd.2007.12.001, 2008.
- Hrachowitz, M., Soulsby, C., Tetzlaff, D., Dawson, J. J. C., Dunn, S. M., and Malcolm, I. A.: Using long–term data sets to 905 understand transit times in contrasting headwater catchments, *J. Hydrol.*, 367, 237–248, doi:10.1016/j.jhydrol.2009.01.001, 2009.
- Huang, T., Pang, Z., Li, J., Xiang, Y., and Zhao, Z.: Mapping groundwater renewability using age data in the Baiyang alluvial fan, NW China, *Hydrogeol. J.*, 25, 743–755, doi:10.1007/s10040-017-1534-z, 2017.
- IAEA: <http://isohis.iaea.org/water>, last access: 27 January 2016, 2006.
- 910 Jelinowska, A., Tucholka, P., Gasse, F., and Fontes, J. C.: Mineral magnetic record of environment in Late Pleistocene and Holocene sediments, Lake Manas, Xinjiang, China, *Geophys. Res. Lett.*, 22, 953–956, doi:10.1029/95GL00708, 1995.
- Ji, L.: Using stable hydrogen and oxygen isotope to research the conversion relationship of surface water and groundwater in Manas River Basin, M.S. thesis, Shihezi University, China, 58 pp., 2016.
- Jurgens, B. C., Böhlke, J. K., and Eberts, S. M.: TracerLPM (Version 1): An Excel® workbook for interpreting groundwater 915 age distributions from environmental tracer data: U.S. Geological Survey Techniques and Methods Report 4–F3, Reston, USA, 60 pp., 2012.
- Kirchner, J. W.: Aggregation in environmental systems – Part 1: Seasonal tracer cycles quantify young water fractions, but not mean transit times, in spatially heterogeneous catchments, *Hydrol. Earth Syst. Sci.*, 20, 279–297, doi:10.5194/hess-20-279-2016, 2016.
- 920 Kirchner, J. W., Tetzlaff, D., and Soulsby C.: Comparing chloride and water isotopes as hydrological tracers in two Scottish catchments, *Hydrol. Process.*, 24, 1631–1645, doi:10.1002/hyp.7676, 2010.
- Koh, D. C., Ha, K., Lee, K. S., Yoon, Y. Y., and Ko, K. S.: Flow paths and mixing properties of groundwater using hydrogeochemistry and environmental tracers in the southwestern area of Jeju volcanic island, *J. Hydrol.*, 432–433, 61–74, doi:10.1016/j.jhydrol.2012.02.030, 2012.
- 925 Kong, Y. and Pang, Z.: A positive altitude gradient of isotopes in the precipitation over the Tianshan Mountains: Effects of moisture recycling and sub–cloud evaporation, *J. Hydrol.*, 542, 222–230, doi:10/1016/j.jhydrol.2016.09.007, 2016.

- Li, J., Pang, Z., Froehlich, K., Huang, T., Kong, Y., Song, W., and Yun, H.: Paleo-environment from isotopes and hydrochemistry of groundwater in East Junggar Basin, Northwest China, *J. Hydrol.*, 529, 650–661, doi:10.1016/j.jhydrol.2015.02.019, 2015.
- 930 Ma, B., Jin, M., Liang, X., and Li, J.: Groundwater mixing and mineralization processes in a mountain–oasis–desert basin, northwest China: hydrogeochemistry and environmental tracer indicators, *Hydrogeol. J.*, 26, 233–250, doi:10.1007/s10040-017-1659-0, 2018.
- Ma, B., Liang, X., Jin, M., Li, J., and Niu, H.: Characteristics of fractionation of hydrogen and oxygen isotopes in evaporating water in the typical region of the North China Plain, *Adv. Water Sci.*, 26, 639–648, 935 doi:10.14042.j.cnki.32.1309.2015.05.005, 2015.
- Mahlknecht, J., Hernández–Antonio, A., Eastoe, C. J., Tamez–Meléndez, C., Ledesma–Ruiz, R., Ramos–Leal, J. A., and Ornelas–Soto, N.: Understanding the dynamics and contamination of an urban aquifer system using groundwater age ( $^{14}\text{C}$ ,  $^3\text{H}$ , CFCs) and chemistry, *Hydrol. Process.*, 31, 2365–2380, doi:10.1002/hyp.11182, 2017.
- 940 [Małozzewski, P.: Lumped-parameter models as a tool for determining the hydrological parameters of some groundwater systems based on isotope data. IAHS–AISH Publication, 271–276, 2000.](#)
- Małozzewski, P. and Zuber, A.: Determining the turnover time of groundwater systems with the aid of environmental tracers, 1. Models and their applicability, *J. Hydrol.*, 57, 207–231, doi:10.1016/0022-1694(82)90147-0, 1982.
- McGuire, K. J. and McDonnell, J. J.: A review and evaluation of catchment transit time modeling, *J. Hydrol.*, 330, 543–563, doi:10.1016/j.jhydrol.2006.04.020, 2006.
- 945 McGuire, K. J., McDonnell, J. J., Weiler, M., Kendall, C., McGlynn, B. L., Welker, J. M., and Seibert, J.: The role of topography on catchment–scale water residence time, *Water Resour. Res.*, 41, 302–317, doi:10.1029/2004WR003657, 2005.
- Morgenstern, U. and Daughney, C. J.: Groundwater age for identification of baseline groundwater quality and impacts of land–use intensification – The National Groundwater Monitoring Programme of New Zealand, *J. Hydrol.*, 456–457, 79– 950 93, doi:10.1016/j.jhydrol.2012.06.010, 2012.
- Morgenstern, U., Daughney, C. J., Leonard, G., Gordon, D., Donath, F. M., and Reeves, R.: Using groundwater age and hydrochemistry to understand sources and dynamics of nutrient contamination through the catchment into Lake Rotorua, New Zealand, *Hydrol. Earth Syst. Sci.*, 19, 803–822, doi:10.5194/hess-19-803-2015, 2015.
- Morgenstern, U., Stewart, M. K., and Stenger, R.: Dating of streamwater using tritium in a post nuclear bomb pulse world: 955 continuous variation of mean transit time with streamflow, *Hydrol. Earth Syst. Sci.*, 14, 2289–2301, doi:10.5194/hess-14-2289-2010, 2010.
- Morgenstern, U. and Taylor, C. B.: Ultra low–level tritium measurement using electrolytic enrichment and LSC, *Isot. Environ. Healt. S.*, 45, 96–117, doi:10.1080/10256010902931194, 2009.
- Négre, P., Petelet–Giraud, E., and Millot, R.: Tracing water cycle in regulated basin using stable  $\delta^2\text{H}$ – $\delta^{18}\text{O}$  isotopes: The 960 Ebro river basin (Spain), *Chem. Geol.*, 422, 71–81, doi:10.1016/j.chemgeo.2015.12.009, 2016.

- Oster, H., Sonntag, C., and Münnich, K. O.: Groundwater age dating with chlorofluorocarbons, *Water Resour. Res.*, 32, 1989–3001, doi:10.1029/96WR01775, 1996.
- Pearson, F. J. and Hanshaw, B. B.: Sources of dissolved carbonate species in groundwater and their effects on carbon-14 dating, in: *Proceedings of A Symposium on Use of Isotopes in Hydrology*, International Atomic Energy Agency, Vienna, Austria, 271–286, 1970.
- 965 Plummer, L. N., Busenberg, E., and Cook, P. G.: Principles of Chlorofluorocarbon dating, in: *Use of Chlorofluorocarbons in Hydrology: A Guidebook*, Gröning, M., Han, L. F., and Aggarwal, P. (Eds.), International Atomic Energy Agency, Vienna, Austria, 17–29, 2006a.
- Plummer, L. N., Busenberg, E., and Han, L. F.: CFCs in binary mixtures of young and old groundwater, in: *Use of Chlorofluorocarbons in Hydrology: A Guidebook*, Gröning, M., Han, L. F., and Aggarwal, P. (Eds.), International Atomic Energy Agency, Vienna, Austria, 59–72, 2006b.
- 970 Polach, H. A.: Evaluation and status of liquid scintillation counting for radiocarbon dating, *Radiocarbon*, 29, 1–11, doi:10.1017/S0033822200043502, 1987.
- Qin, D.: Decline in the concentrations of chlorofluorocarbons (CFC–11, CFC–12 and CFC–113) in an urban area of Beijing, China, *Atmos. Environ.*, 41, 8424–8430, doi:10.1016/j.atmosenv.2007.07.005, 2007.
- 975 Qin, D., Qian, Y., Han, L., Wang, Z., Li, C., and Zhao, Z.: Assessing impact of irrigation water on groundwater recharge and quality in arid environment using CFCs, tritium and stable isotopes, in the Zhangye Basin, Northwest China, *J. Hydrol.*, 405, 194–208, doi:10.1016/j.jhydrol.2011.05.023, 2011.
- Russell, A. D. and Thompson, G. M.: Mechanisms leading to enrichment of the atmospheric fluorocarbons CCl<sub>3</sub>F and CCl<sub>2</sub>F<sub>2</sub> in groundwater, *Water Resour. Res.*, 19, 57–60, doi:10.1029/WR019i001p00057, 1983.
- 980 Stewart, M. K., Morgenstern, U., Gusyev, M. A., and Małozewski, P.: Aggregation effects on tritium-based mean transit times and young water fractions in spatially heterogeneous catchments and groundwater systems, *Hydrol. Earth Syst. Sci.*, 21, 4615–4627, doi:10.5194/hess-21-4615-2017, 2017.
- Stewart, M. K., Morgenstern, U., and McDonnell, J. J.: Truncation of stream residence time: how the use of stable isotopes has skewed our concept of stream water age and origin, *Hydrol. Process.*, 24, 1646–1659, doi:10.1002/hyp.7576, 2010.
- 985 [Suckow, A.: The age of groundwater – Definitions, models and why we do not need this term, \*App. Geochem\*, 50, 222–230, doi:10.1016/j.apgeochem.2014.04.016, 2014.](https://doi.org/10.1016/j.apgeochem.2014.04.016)
- Tadros, C. V., Hughes, C. E., Crawford, J., Hollins, S. E., and Chisari, R.: Tritium in Australian precipitation: A 50 year record, *J. Hydrol.*, 513, 262–273, doi:10.1016/j.jhydrol.2014.03.031, 2014.
- 990 Visser, A., Broers, H. P., Purtschert, R., Sültenfuß, J., and de Jonge, M.: Groundwater age distributions at a public drinking water supply well field derived from multiple age tracers (<sup>85</sup>Kr, <sup>3</sup>H/<sup>3</sup>He, and <sup>39</sup>Ar), *Water Resour. Res.*, 49, 7778–7796, doi:10.1002/2013WR014012, 2013.
- Vogel, J. C.: Carbon-14 dating of groundwater, in: *Proceedings of A Symposium on Use of Isotopes in Hydrology*, International Atomic Energy Agency, Vienna, Austria, 225–239, 1970.

- 995 Wang, Y., Shvartsev, S. L., and Su, C.: Genesis of arsenic/fluoride-enriched soda water: A case study at Datong, northern China, *Appl. Geochem.*, 24, 641–649, doi:10.1016/j.apgeochem.2008.12.015, 2009.
- Wu, B.: Study on groundwater system evolvement law and water environment effect of Shihezi City, Ph.D. thesis, Xinjiang Agricultural University, China, 132 pp., 2007.
- Zhao, B. F.: Recharge on water resources characteristics and its rational development pattern for arid areas: a case of Manas River Basin, Ph.D. thesis, Chang'an University, China, 182 pp., 2010.
- 1000 [Zhou, H. C.: Groundwater system and recharge from the remote river in Southwestern margin of the Jungger Basin. Ph.D. thesis. Chinese Academy of Geological Sciences, China, 116 pp., 1992.](#)

**Table 1.** Chemical–physical parameters, stable isotopes, tritium ( $^3\text{H}$ ),  $^{14}\text{C}$ , and CFC concentrations in groundwater samples in the Manas River Basin.

Sample ID	Sampling date (d/m/y)	Elevation (m a.s.l.) <sup>a</sup>	Well depth (m)	pH	T (°C)	EC ( $\mu\text{S cm}^{-1}$ )	DO ( $\text{mg L}^{-1}$ )	$\delta^2\text{H}$ (‰)	$\delta^{18}\text{O}$ (‰)	CFC–11 ( $\text{pmol L}^{-1}$ )	CFC–12 ( $\text{pmol L}^{-1}$ )	CFC–113 ( $\text{pmol L}^{-1}$ )	$^3\text{H}$ (TU)	$a^{14}\text{C}$ (pMC)	$^{14}\text{C}_{\text{corr}}$ age (years)
<i>Upstream groundwater (UG)</i>															
G1	5/6/2015	1083	170 <sup>b</sup>					−67.60	−10.15				41.07		
G2	5/6/2015	1107	170 <sup>b</sup>					−67.40	−10.17				41.13		
G3	9/8/2015	755	150	10.1	11.5	387	9.8	−70.39	−10.50	3.14	2.18	0.38			
G4	6/6/2015	532	58					−66.80	−9.91				60.04		
<i>Midstream groundwater (MG)</i>															
G5	8/8/2015	467	100	8.6	13.4	896	4.6	−69.35	−10.73	0.17	0.19	0.02	3.80		
G6	8/6/2015	472	175										28.90		
G7	7/8/2015	422	100	8.8	15.7	620	3.7	−69.87	−10.98	0.27	0.27	0.03			
G8	7/8/2015	412	90	9.3	13.6	513	2.1	−69.92	−11.08	1.99	1.21	0.18	5.00		
G9	8/8/2015	484	100	9.1	14.5	612	9.1	−74.58	−11.01	1.31	1.03	0.13	7.10		
G10	8/6/2015	463	145					−72.30	−11.05				9.09		
G11	8/6/2015	439	60					−68.50	−10.47				15.75		
G12	7/8/2015	368	260	9.3	19.0	327	6.7	−69.33	−10.73					86.9	−684
G13	4/8/2015	370	300	9.4	17.1	307	1.2	−76.20	−11.22					54.6	3158
G14	4/8/2015	370	60	9.0	13.2	556	1.4	−68.96	−10.43				1.10		
G15	5/8/2015	364	23	8.1	12.7	1650	1.0	−69.45	−9.86	0.99	0.91	0.14	7.10		
G16	5/8/2015	357	56	9.0	15.2	291	0.7	−76.59	−11.57	2.69	1.54	0.22	4.80		
G17	5/8/2015	367	280	9.8	17.2	263	2.5	−82.45	−12.19					53.2	3373
G18	6/8/2015	377	350 <sup>b</sup>	9.0	15.3	233	6.6	−75.97	−11.50					46.8	4432
G19	6/8/2015	381	118 <sup>b</sup>	9.0	15.4	309	5.2	−76.46	−11.46				6.90		
G20	6/8/2015	381	13	8.7	12.6	615	2.1	−74.99	−11.27	1.68	1.14	0.16	8.20		

Sample ID	Sampling date (d/m/y)	Elevation (m a.s.l.) <sup>a</sup>	Well depth (m)	pH	T (°C)	EC (μS cm <sup>-1</sup> )	DO (mg L <sup>-1</sup> )	δ <sup>2</sup> H (‰)	δ <sup>18</sup> O (‰)	CFC-11 (pmol L <sup>-1</sup> )	CFC-12 (pmol L <sup>-1</sup> )	CFC-113 (pmol L <sup>-1</sup> )	<sup>3</sup> H (TU)	<i>a</i> <sup>14</sup> C (pMC)	<sup>14</sup> C <sub>corr</sub> age (years)
G21	5/8/2015	424	180	8.8	15.6	378	8.0	-77.30	-11.60					43.4	5056
G22	6/6/2015	428	150					-69.72	-10.41				26.29		
G23	6/6/2015	446	70					-67.63	-9.92				37.50		
G24	8/8/2015	453	110	9.1	14.7	571	8.6	-77.35	-11.23	1.53	C <sup>c</sup>	C			
G25	8/8/2015	457	48	9.5	13.6	512	9.8	-77.91	-11.36	2.93	1.67	0.24			
<i>Downstream groundwater (DG)</i>															
G26	10/6/2015	348	40					-85.19	-12.11				6.91		
G27	29/7/2015	323	280	9.0	18.3	244		-79.83	-12.21					23.5	10127
G28	3/8/2015	353	45	9.0	13.2	246	8.0	-78.02	-11.47				2.90		
G29	11/6/2015	347	380					-86.39	-12.33				3.64	34.3	7001

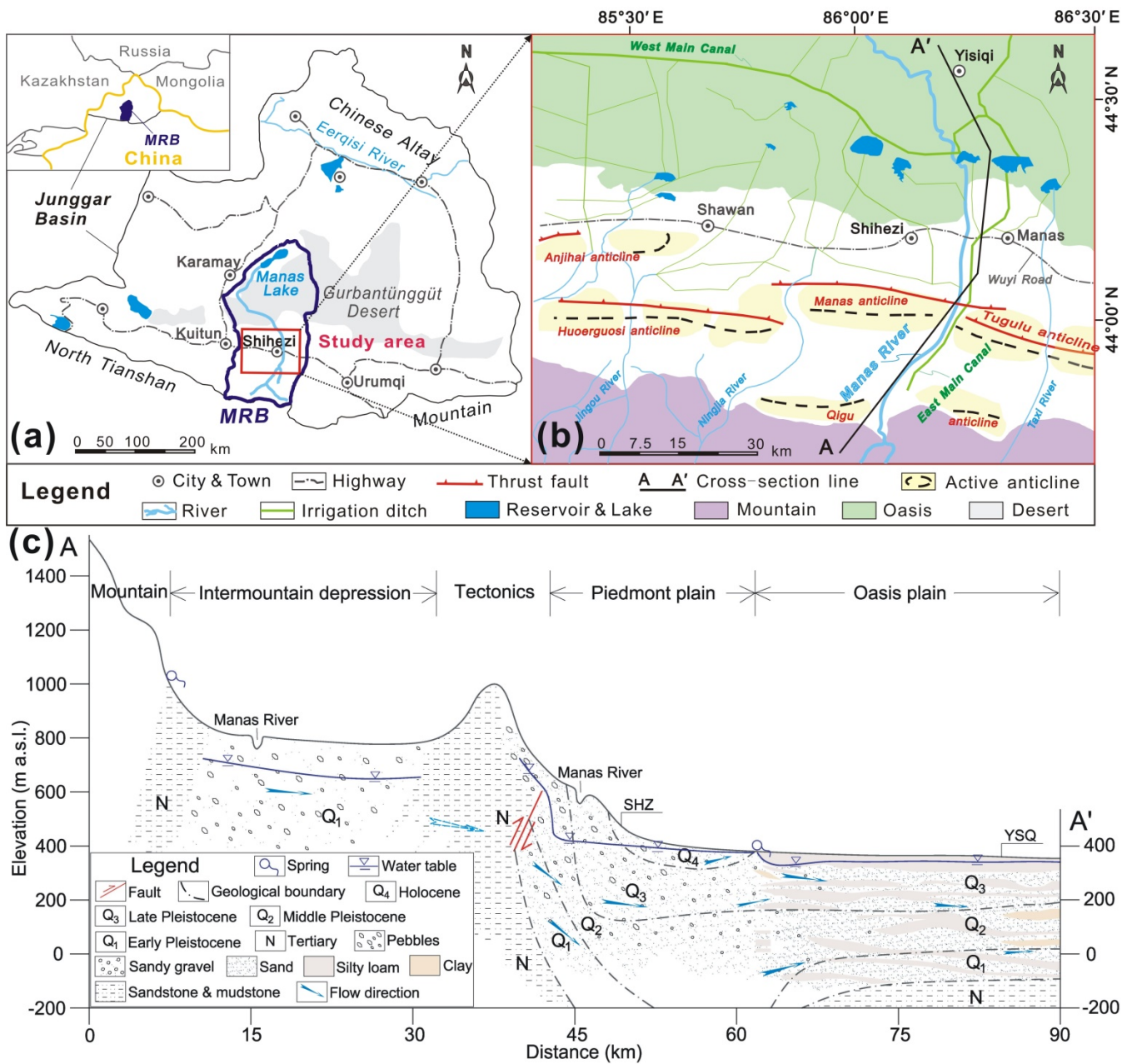
<sup>a</sup> m a.s.l. = m above sea level. <sup>b</sup> Artesian well. <sup>c</sup> Contamination.

**Table 2.** Calculated results for CFC atmospheric partial pressures (pptv), ~~groundwater apparent ages (PFM)~~ modern precipitation recharge year, fraction of post-1940 water, ~~(BMM)~~ and mean transit/residence times (DM, EPM, EMM).

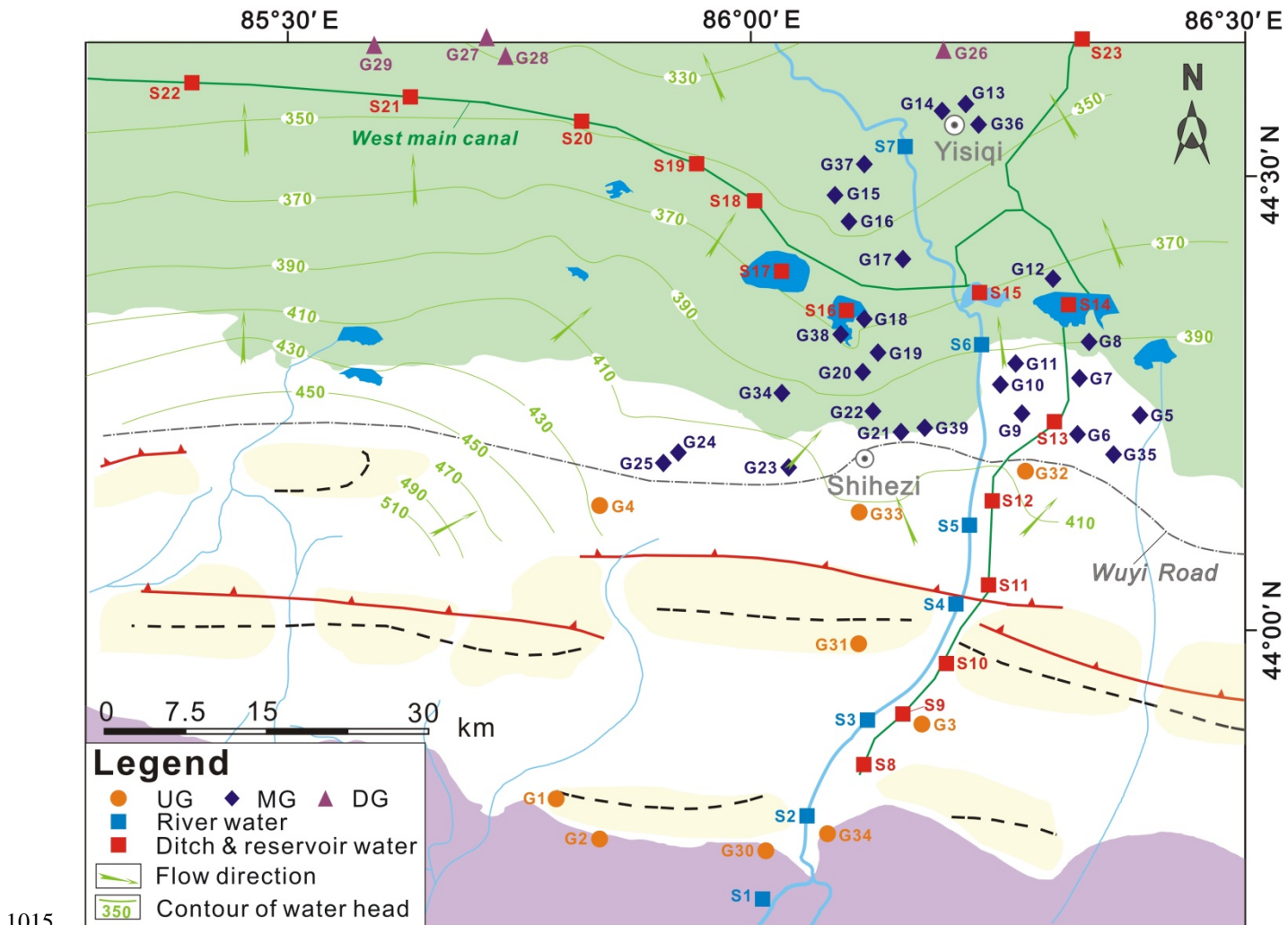
Sample ID	Atmospheric partial pressures (pptv)			Mixing post-1940 water in decimal year (F12/F113)	Fraction of post-1940 water (BMM <sup>a</sup> , %)	<u>Apparent age (PFM) modern precipitation recharge year (calendar years)<sup>b</sup></u>			Mean <u>transit/residence</u> times (F12) (years) <sup>eb</sup>					
	CFC-11	CFC-12	CFC-113			CFC-11	CFC-12	CFC-113	EPM (1.5)	EPM (2.2)	DM (0.03)	DM (0.1)	EMM	
	G3	179.59	476.18			70.88	<del>1989.590</del> <del>2002.53</del>	100 87	<del>32.8198</del> <u>2</u>	<del>251990</del> <u>2</u>	<del>251990</del> <u>2</u>	19	22	39
G5	10.42	43.99	4.04	1983	12	<del>54.5196</del> <u>0</u>	<del>52.7196</del> <u>2</u>	<del>471968</del> <u>2</u>	101	73	91	160	440	
G7	18.49	68.99	6.85	1984 <del>.55</del>	18	<del>51.2519</del> <u>63</u>	<del>49.2196</del> <u>5</u>	<del>43.21971</del> <u>5</u>	89	66	82	139	270	
G8	122.11	280.24	36.42	1987 <del>.58</del>	64	<del>391976</del> <u>3</u>	<del>36.2197</del> <u>8</u>	<del>30.71984</del> <u>8</u>	43	39	52	71	49	
G9	85.03	251.10	27.96	1985	66	<del>41.9197</del> <u>3</u>	<del>381977</del> <u>3</u>	<del>32.91982</del> <u>3</u>	47	42	54	76	58	
G15	58.15	202.68	26.99	1988	45	<del>44.5197</del> <u>0</u>	<del>40.4197</del> <u>4</u>	<del>33.41981</del> <u>4</u>	55	47	59	86	77	
G16	177.81	380.91	48.36	1987	89	<del>331982</del> <u>5</u>	<del>29.6198</del> <u>5</u>	<del>28.31986</del> <u>5</u>	30	31	45	57	29	
G20	100.11	257.11	31.36	1986 <del>.57</del>	62	<del>40.5197</del> <u>4</u>	<del>37.8197</del> <u>7</u>	<del>321983</del> <u>7</u>	45	41	54	75	56	
G24	99.90					<del>40.7197</del> <u>4</u>								
G25	180.79	388.92	48.83	1984 <del>.95</del>	91	<del>32.6198</del> <u>4</u>	<del>291986</del> <u>4</u>	<del>28.31986</del> <u>4</u>	30	30	44	56	28	

<sup>a</sup> ~~BMM=~~binary mixing model, assuming a mixture of old water with young water (post-1940). <sup>b</sup> ~~PFM=~~piston flow model, apparent ages are calculated by contrasting the Northern Hemisphere atmospheric air curve (<http://water.usgs.gov/lab/software/air/curve/>) based on the PFM. <sup>e</sup> <sup>b</sup> Lumped parameter models: DM=dispersion model with  $D_p$  (in Eq. (3)) of 0.1 and 0.03, EPM=exponential ~~–~~piston ~~–~~flow model with  $\eta$  (in Eq. (2)) of 2.2 and 1.5, EMM=exponential mixing model. F12 is short for CFC-12.



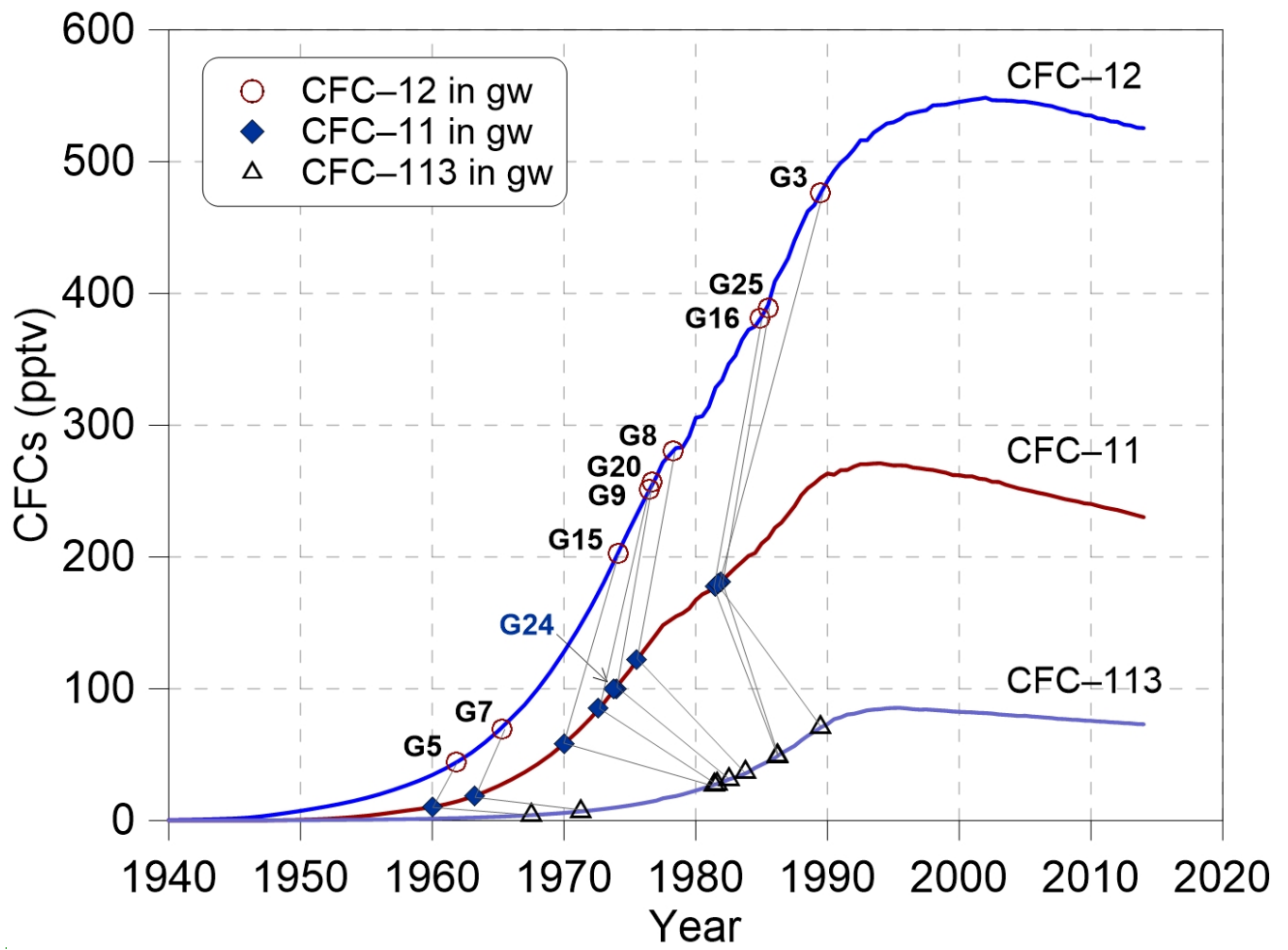


**Figure 1.** Maps showing (a) regional location of the Manas River Basin (modified after Ma et al., 2018), (b) surface water (river, reservoir and irrigation ditch) system (modified after Cui et al, (2007) and Ji, (2016)) and (c) geological cross-section of the study area for A–A' line shown in (b).



**Figure 2.** Water sampling sites and unconfined groundwater head contours (in meters) in the headwater catchments of Manas River. UG=Upstream Groundwater, MG=Midstream Groundwater, DG=Downstream Groundwater.

1015



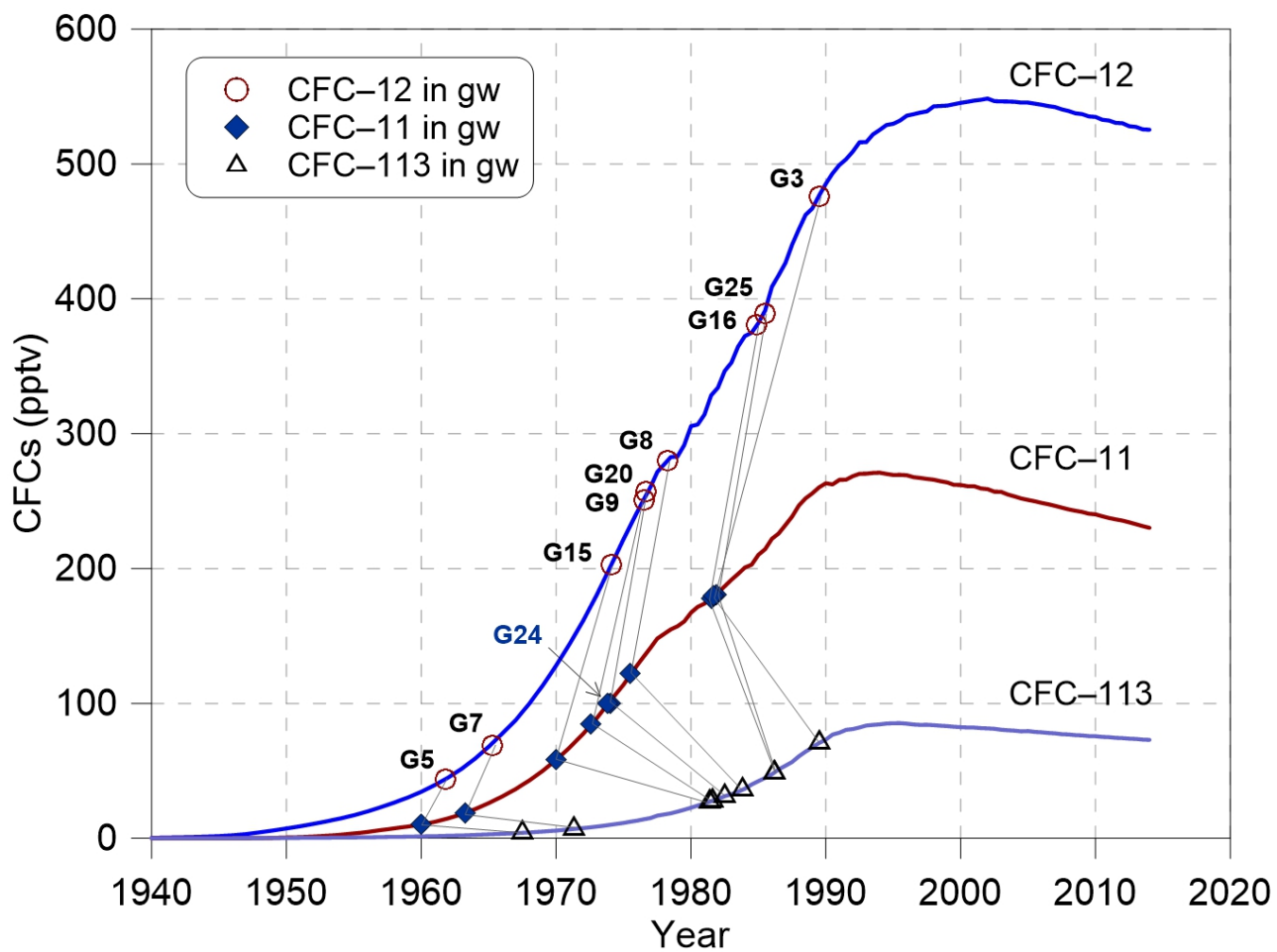


**Figure 53.** Concentrations of CFC-11, CFC-12 and CFC-113 (pptv) in the groundwater of this study area sampled in 2015 compared with the time series trend of Northern Hemisphere atmospheric mixing ratio at a recharge temperature of 10 °C. Data is available at < <http://water.usgs.gov/lab/software/air/cure/>>.

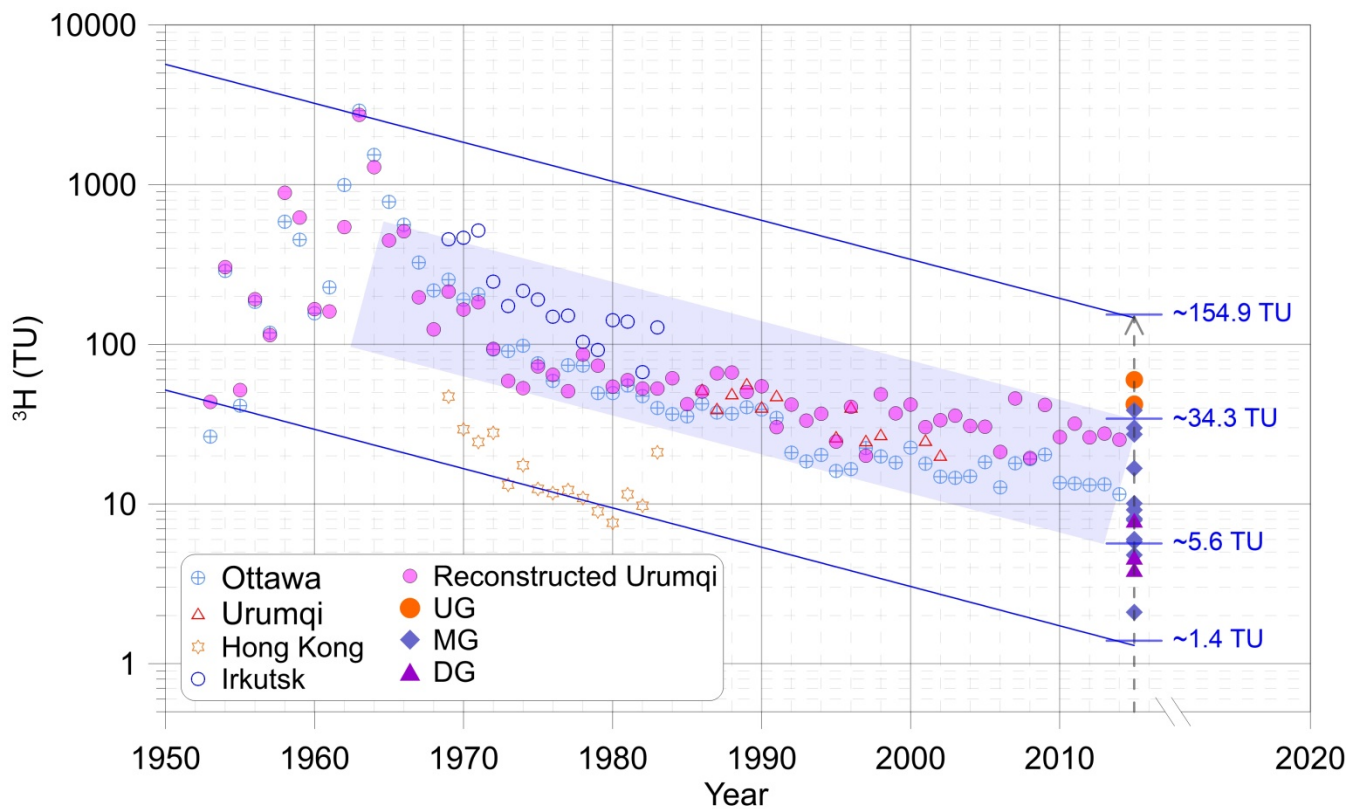
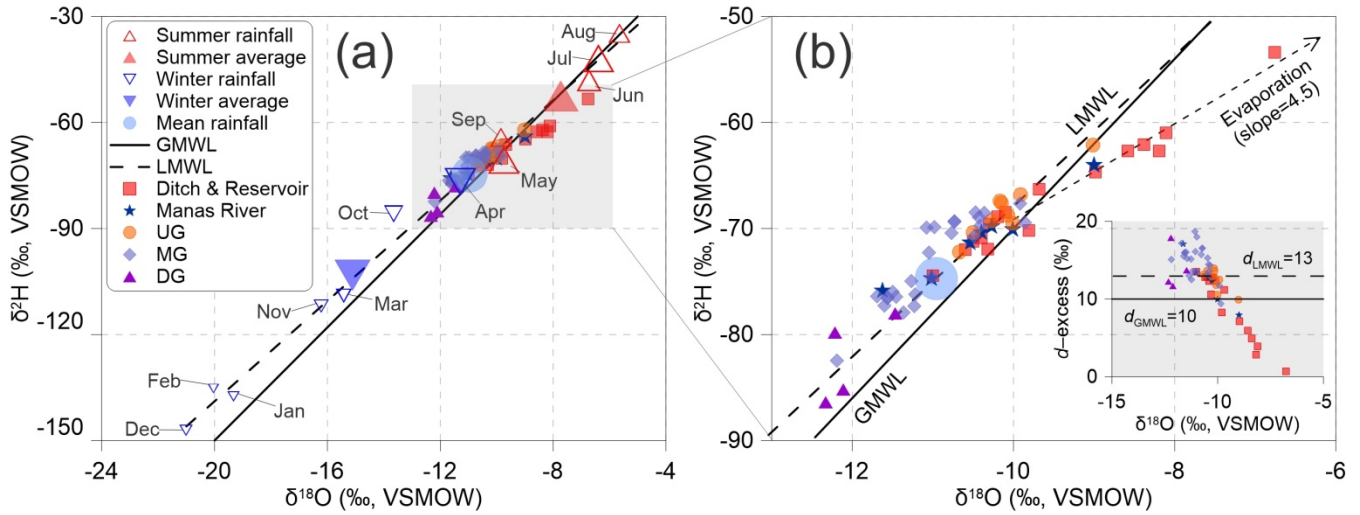


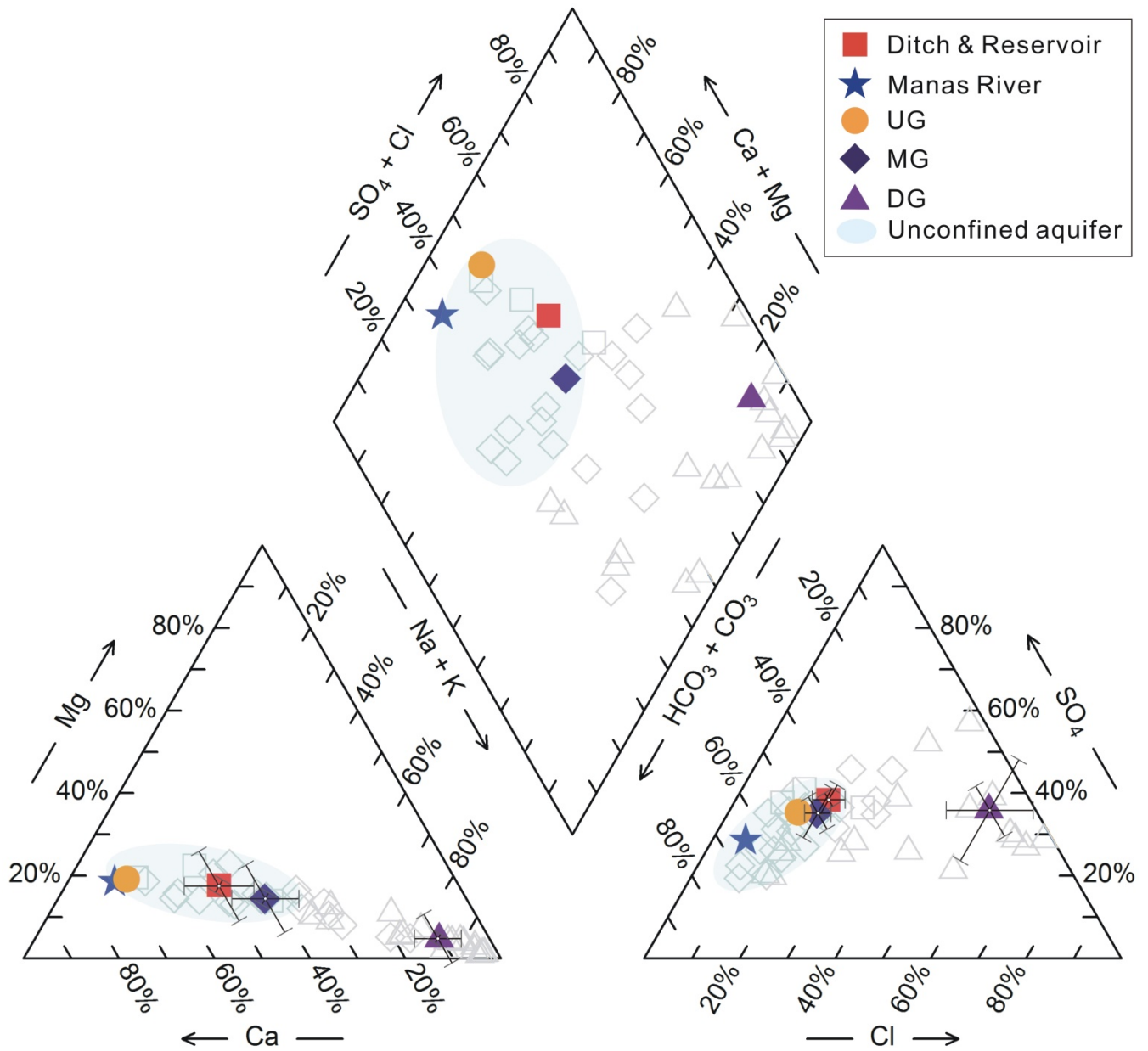
**Figure 4.** Tritium concentration (TU) of the upstream groundwater (UG), midstream groundwater (MG), and downstream groundwater (DG). Time series of tritium concentration in precipitation at Ottawa, Urumqi, Hong Kong, and Irkutsk were obtained by GNIP in IAEA (<https://www.iaea.org/>). The blue solid lines and shaded field were drawn using the half-life (12.32 yrs) of tritium decayed to 2014.

1030



1035 | **Figure 35.** (a) Plot of stable isotopes of surface water and groundwater from the mountain to the oasis plain as compared to the global meteoric water line (GMWL; Craig, 1961) and the local meteoric water line (LMWL, rainfall in Urumqi station of International Atomic Energy Agency (IAEA) networks during 1986 and 2003; IAEA, 2006). The size of the hollow triangles stands for the relative amount of precipitation. “Mean rainfall” refers to the annual amount-weighted mean rainfall isotopic value. (b) Plot of  $\delta^2\text{H}$  vs.  $\delta^{18}\text{O}$  and inserted plot  $d$ -excess vs.  $\delta^{18}\text{O}$ . UG=Upstream Groundwater, MG=Midstream Groundwater, DG=Downstream Groundwater.

1040



1045 | **Figure 46.** Piper diagram highlights the  $\text{HCO}_3\text{-SO}_4\text{-Na}$  type of waters. The coloured symbols represent the mean values calculated from the hydrochemistry data (light grey hollow symbols) reported by Ma et al. (2018). The error bars are shown in the cation and anion diagrams.

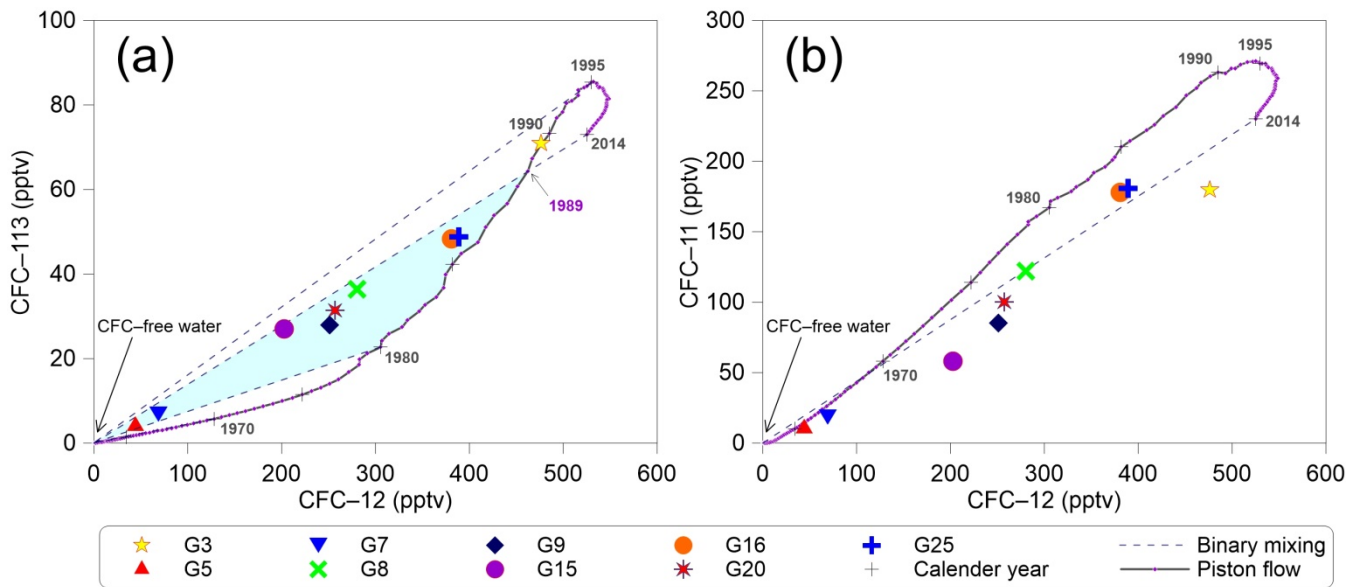


**Figure 7.** Plots showing relationships of (a) CFC-113 vs. CFC-12 and (b) CFC-11 vs. CFC-12 in pptv for the Northern Hemisphere air. The '+' denotes selected calendar years. The solid lines correspond to the piston flow and the short-dashed lines show the binary mixing. The shaded regions in (a) indicate no post-1989 waters mixing.

1050



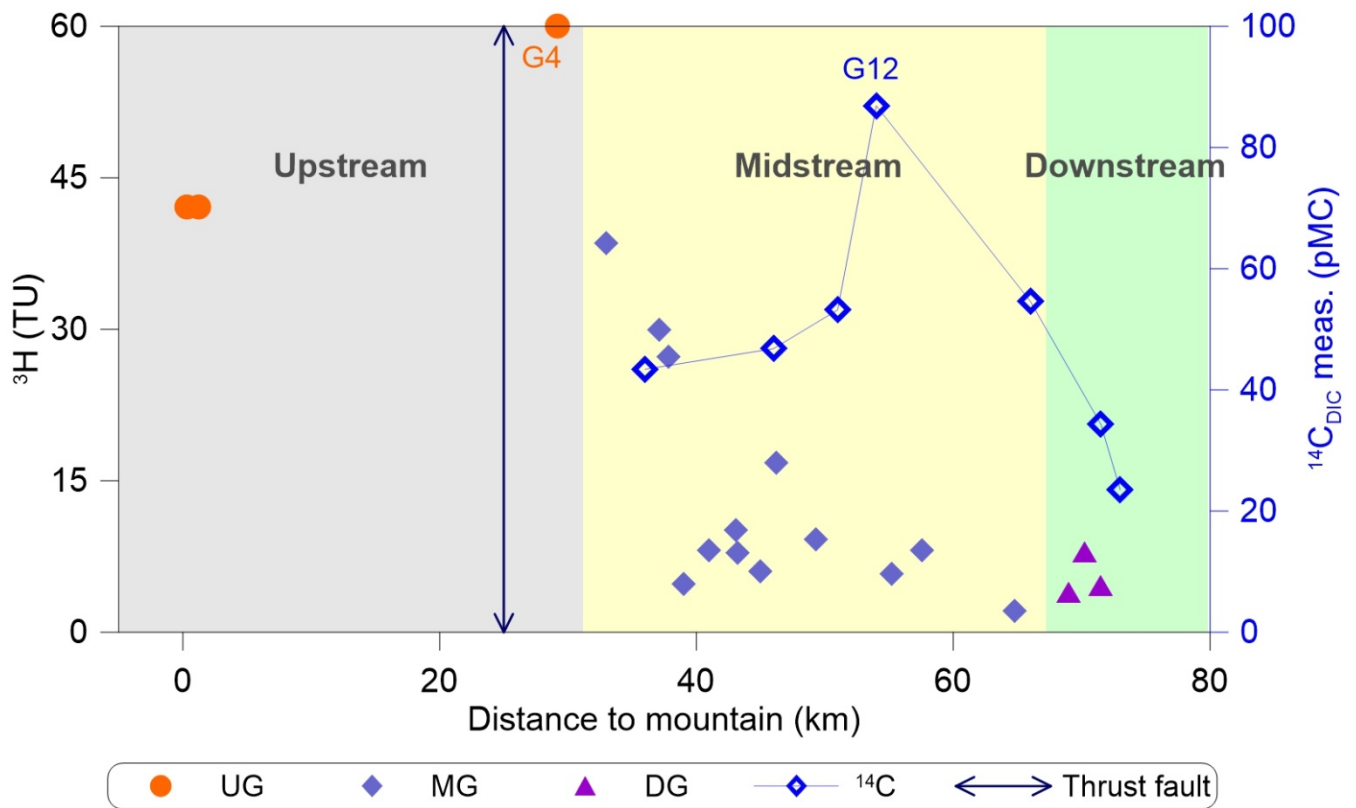


**Figure 8.** Distributions of  $^3\text{H}$  and  $^{14}\text{C}$  activities with distance to mountain. The shaded regions indicate the upstream, midstream and downstream of Manas River.

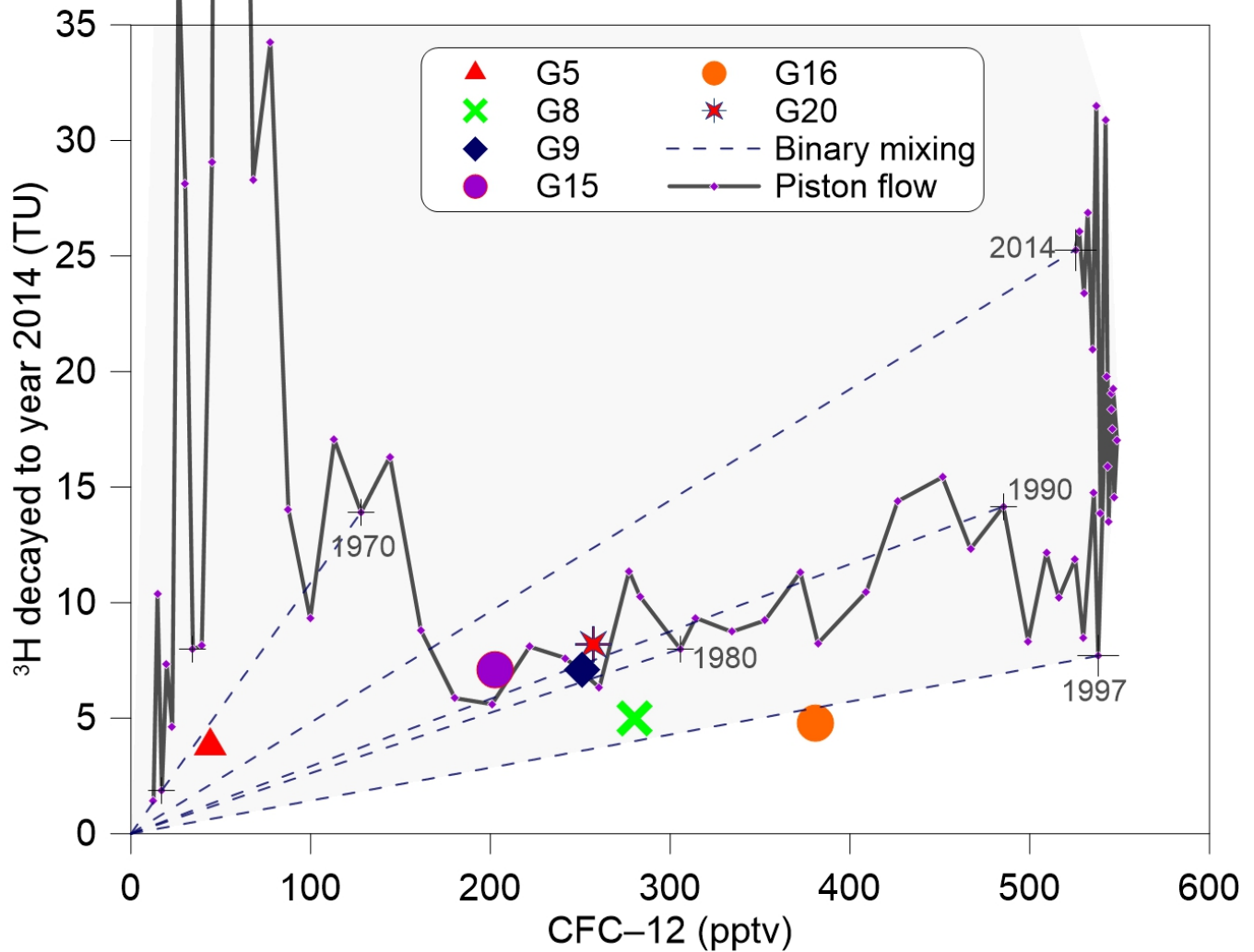


**Figure 9.**  $^3\text{H}$  activity (TU) in Urumqi precipitation decayed to 2014 vs. CFC-12 in pptv for Northern Hemisphere air. The '+' denotes selected calendar years. The solid lines correspond to the piston flow and the short-dashed lines show the binary mixing. The shaded region indicates concentrations that could arise due to mixing water of different ages.

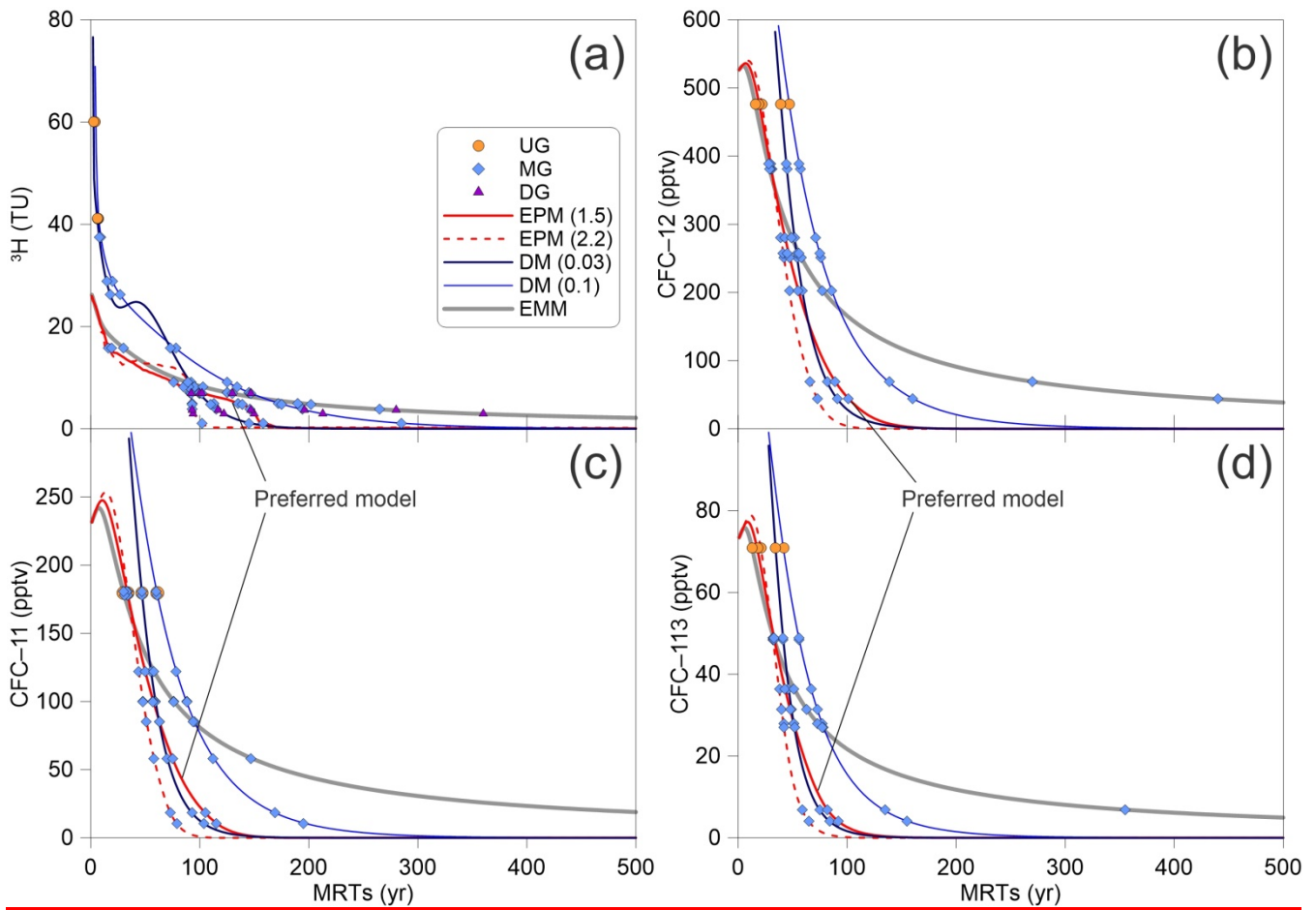


**Figure 10.** Tritium and CFCs (CFC-11, CFC-12 and CFC-113) output vs. mean residence times for different lumped-parameter models estimated using Eqs. (2) to (5). The input  $^3\text{H}$  activity and CFCs concentration are using the estimated  $^3\text{H}$  activity in precipitation in Urumqi station (Fig. 4) and the Northern Hemisphere atmospheric mixing ratio (Fig. 3), respectively.

1065

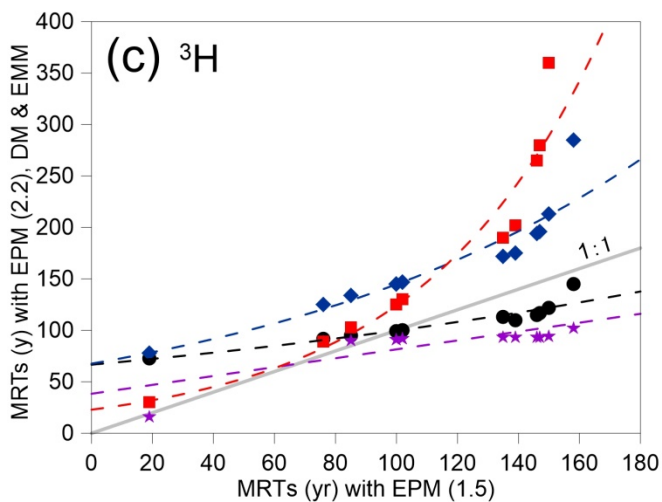
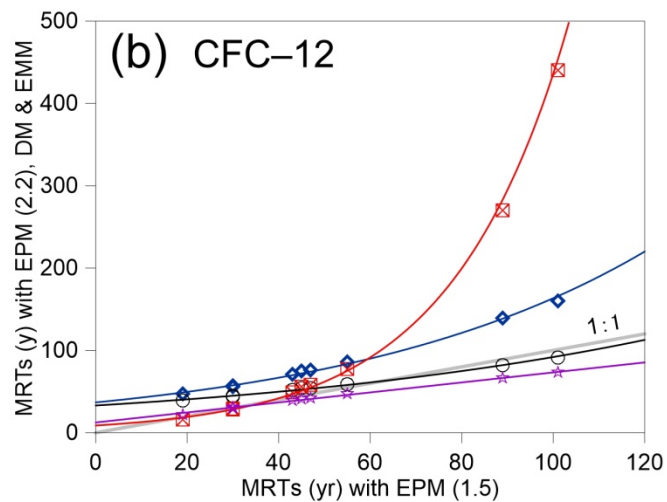
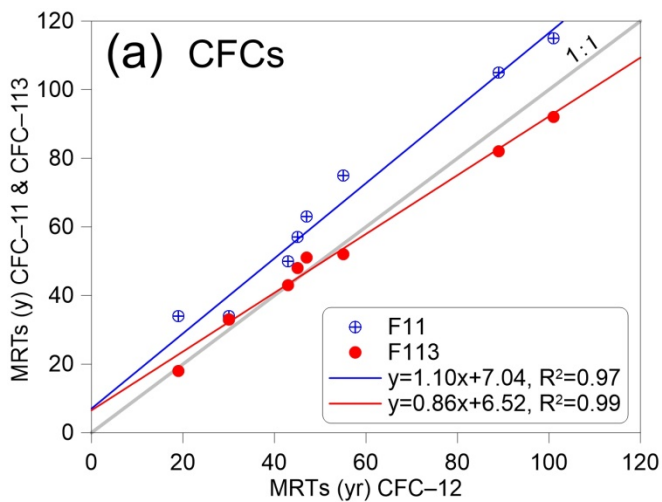


**Figure 11.** (a) MRTs with EPM (1.5) of CFC-12 vs. CFC-11 & CFC-113, (b) CFC-12 MRTs with EPM (1.5) vs. EPM (2.2), DM & EMM, and (c) 3H MRTs with EPM (1.5) vs. EPM (2.2), DM & EMM.

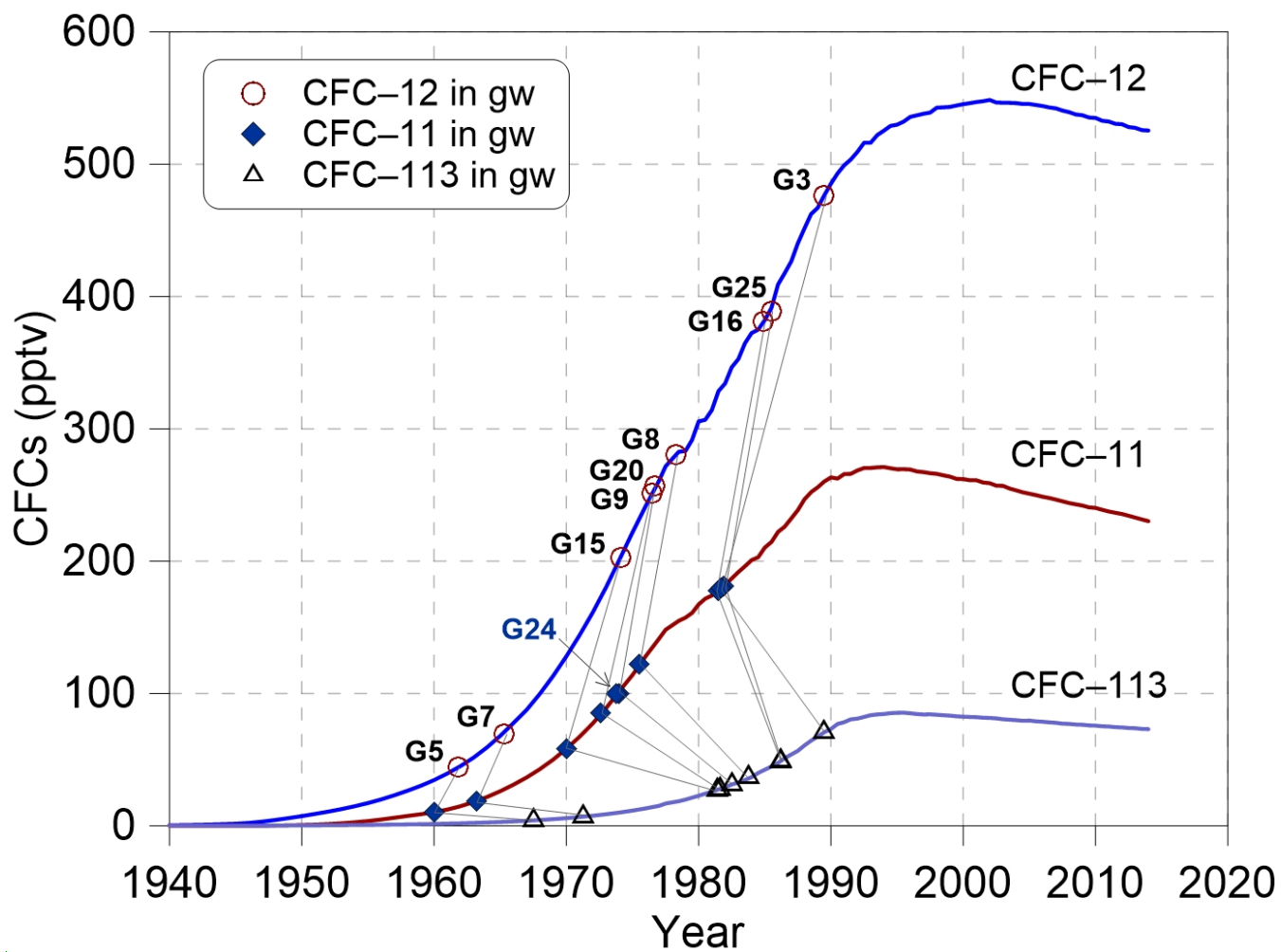


Figure 5. Concentrations of CFC-11, CFC-12 and CFC-113 (pptv) in the groundwater of this study area sampled in 2015 compared with the time series trend of Northern Hemisphere atmospheric mixing ratio at a recharge temperature of 10 °C. Data is available at <http://water.usgs.gov/lab/software/air/euro/>

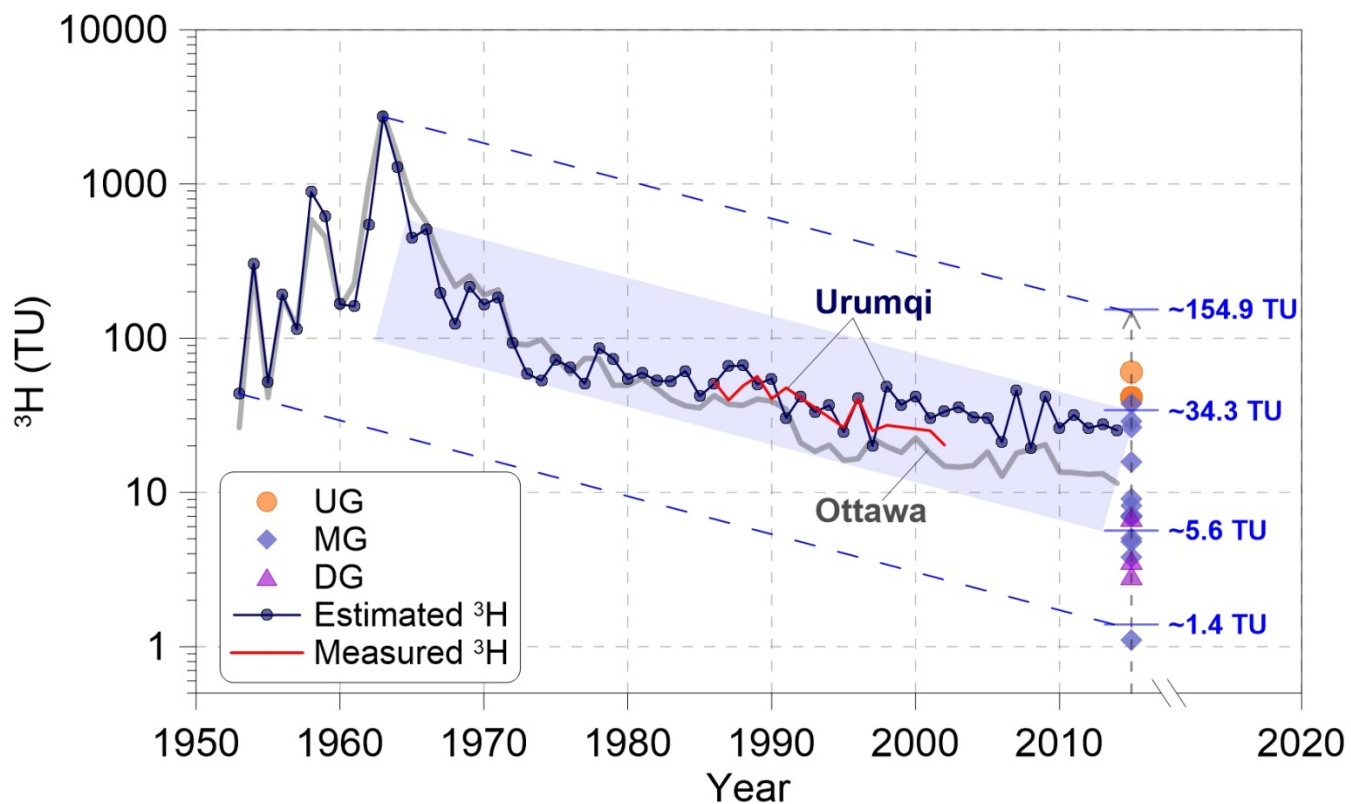
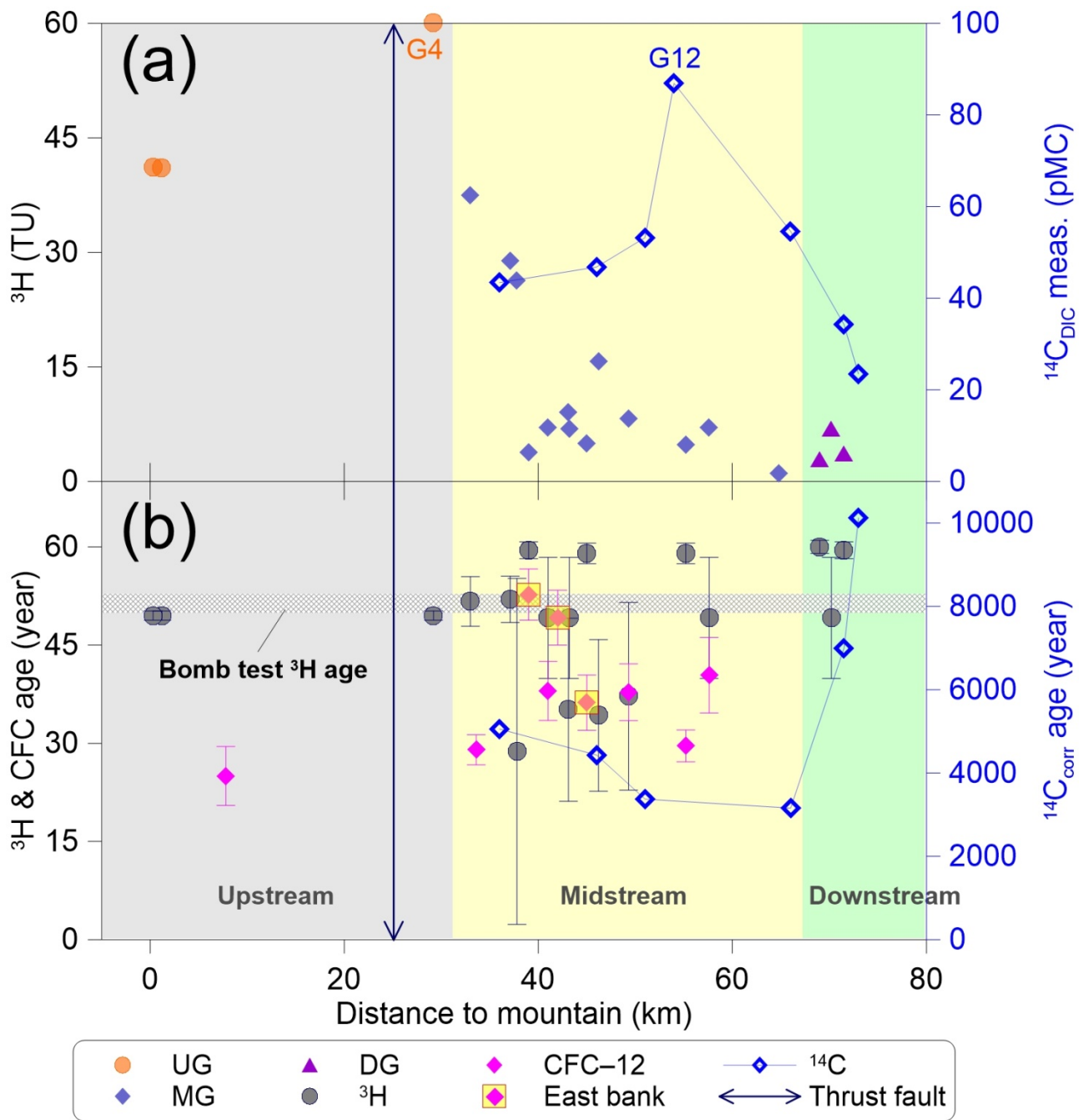
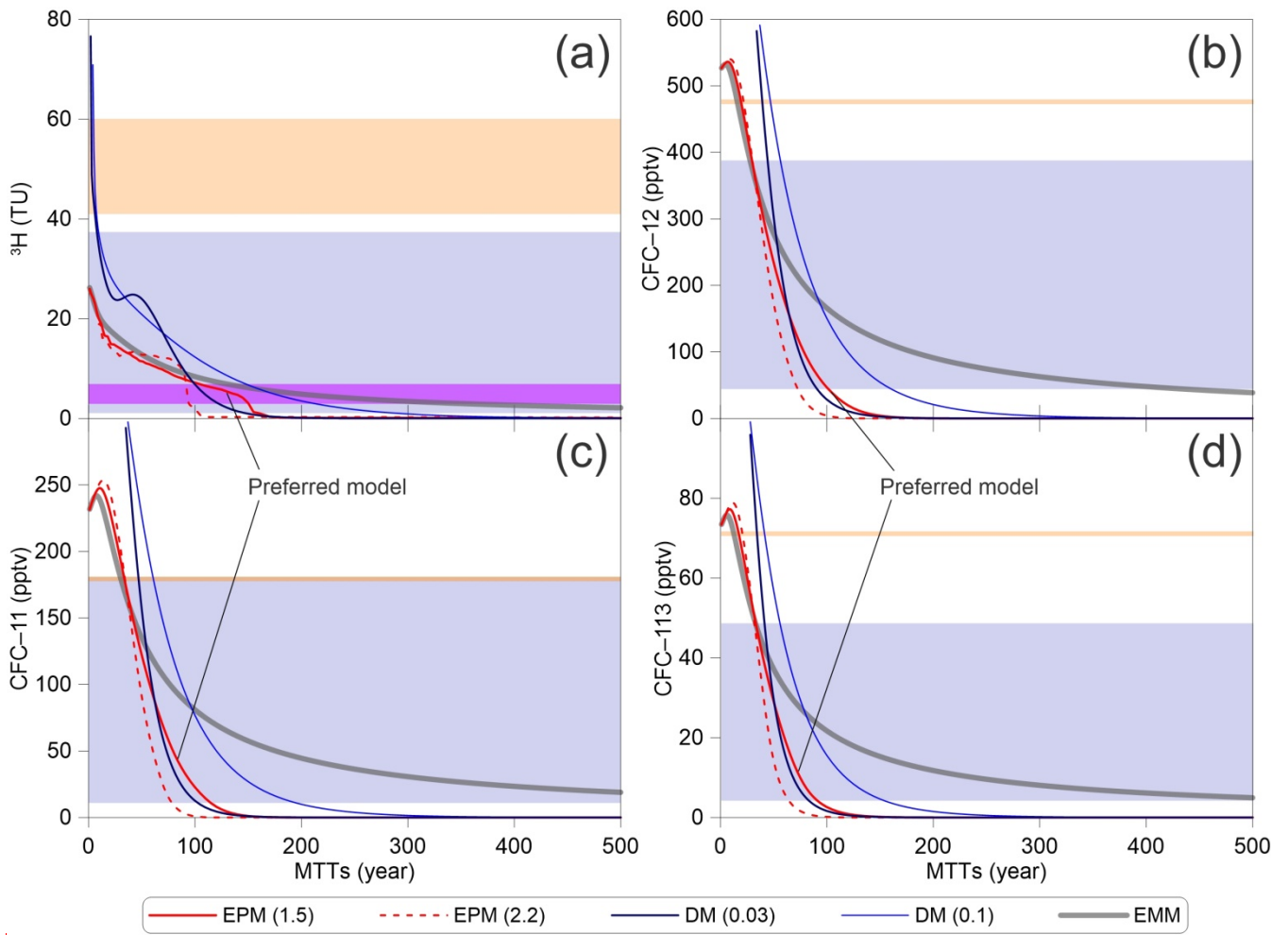


Figure 6. Plot of the reconstructed and measured time-series of  $^3\text{H}$  activities in precipitation in Urumqi station between 1953 and 2014. The blue dashed lines and shaded field were drawn using the half-life (12.32 yrs) of tritium decayed to 2014.



1080

**Figure 7.** (a) Distributions of  $^3\text{H}$  and  $^{14}\text{C}$  activities with distance to mountain; (b) Distributions of  $^3\text{H}$ , CFC-12 and  $^{14}\text{C}_{\text{corr}}$  ages with distance to mountain. 'East bank' refers to groundwater CFC-12 apparent ages in the east bank of the 'East main canal'.



1085 **Figure 8.** Tritium and CFCs (CFC-11, CFC-12 and CFC-113) output vs. mean transit times for different lumped parameter models estimated using Eqs. (1) to (4). The input  $^3\text{H}$  activity and CFCs concentration are using the estimated  $^3\text{H}$  activities in precipitation in Urumqi station (Fig. 6) and Northern Hemisphere atmospheric mixing ratio (Fig. 5), respectively. The UG (orange), MG (light blue) and DG (purple)  $^3\text{H}$  activities and CFC concentrations are shown by shaded fields.



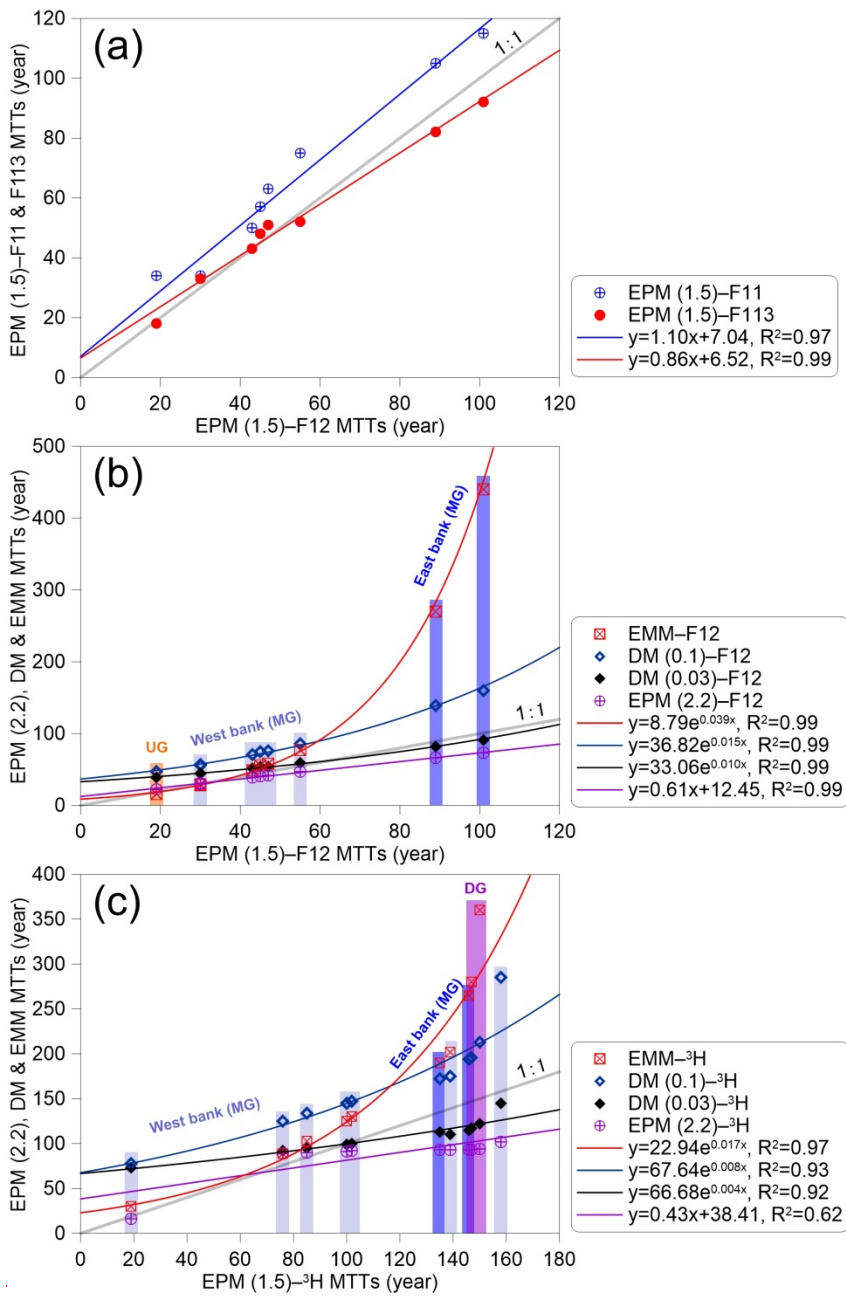


**Figure 9.** (a) EPM (1.5) MTTs and (b) EPM (2.2), DM & EMM MTTs vs. EPM (1.5)-F12 MTTs (CFC-12 MTTs using EPM (1.5)), (c) EPM (2.2), DM & EMM MTTs vs. EPM (1.5)-<sup>3</sup>H MTTs. F11, F12 and F113 are short for CFC-11, CFC-12 and CFC-113. The shaded fields correspond to water samples from the UG (orange), West (light blue) and East bank (blue) of the 'East main canal' of MG, and DG (purple).

1090

1095

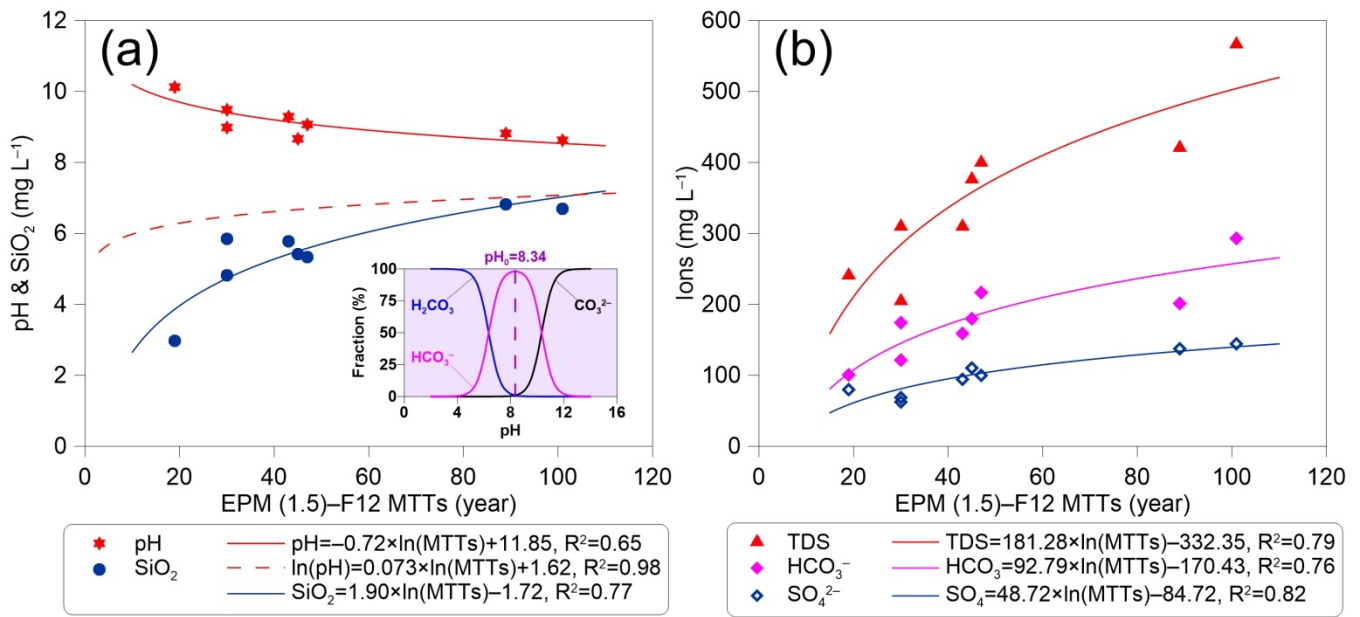


**Figure 1012.** (a) pH & silica (SiO<sub>2</sub>) and (b) ions including sulfate (SO<sub>4</sub><sup>2-</sup>), bicarbonate (HCO<sub>3</sub><sup>-</sup>), and total dissolved solids (TDS) vs. EPM (1.5)-F12 MTTs (CFC-12 MTTs using EPM (1.5)). The dashed red line in (a) is from Morgenstern et al. (2015).

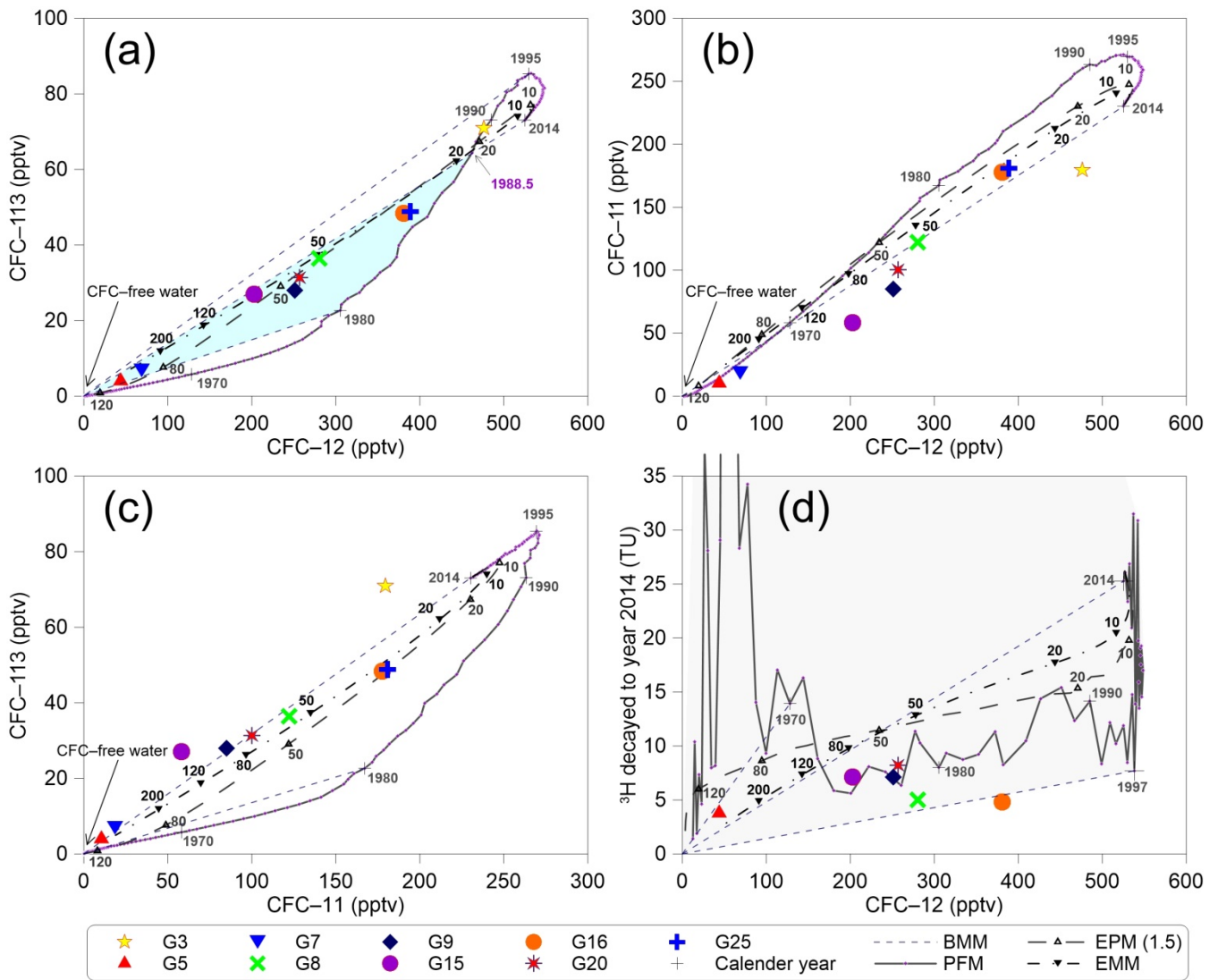


**Figure 11.** Plots showing relationships of (a) CFC-113 vs. CFC-12 (b) CFC-11 vs. CFC-12, (c) CFC-113 vs. CFC-11, and (d)  $^3\text{H}$  activity (TU) in Urumqi precipitation decayed to 2014 vs. CFC-12 in pptv for Northern Hemisphere air. The data are compared to four hypothetical mixing models. The solid lines correspond to the piston flow model (PFM) and the short-dashed lines show the binary mixing model (BMM). The number referenced to the EPM (1.5) and EMM lines are mean transit times. The '+' denotes selected apparent ages. The shaded regions in (a) indicate no post-1988.5 waters mixing and in (d) indicate concentrations that could arise due to mixing water of different ages.

1105